Function of Hypoxia Inducible Factor HIF1α in Dendritic Cells and Macrophages

Inaugural-Dissertation

Zur Erlangung des Doktorgrades
der Mathematisch-Naturwissenschaftlichen Fakultät
der Heinrich-Heine-Universität Düsseldorf

Vorgelegt von

Theresa Köhler

aus Cottbus

Düsseldorf, Juni 2012

aus dem Leibniz-Institut für umweltmedizinische Forschung
an der Heinrich-Heine-Universität Düsseldorf

Gedruckt mit der Genehmigung der Mathematisch-Naturwissenschaftlichen Fakultät
der Heinrich-Heine-Universität Düsseldorf

Referentin: Prof. Dr. rer. nat. Irmgard Förster
Koreferent: Prof. Dr. Johannes H. Hegemann

Tag der mündlichen Prüfung: 27.06.2012

Table of contents

Index of figures

Table of abbreviations

ARNT	Arylhdrocarbon receptor nucleus translocator
ATP	Adenosine triphosphate
BMDC	Bone marrow derived DC
BMMΦ	Bone marrow derived MΦ
bp	basepair
BSA	Bovine serum albumin
CD	Cluster of differentiation
CFU	Colony forming units
CHS	Contact hypersensitivity
CMFDA	5-chloromethylfluorescein diacetate
CMTMR	5-(and-6)-(((4-Chloromethyl) Benzoyl) Amino) Tetramethylrhodamine
CLR	C-type lectin receptor
CTL	Cytotoxic T lymphocyte
DAMP	Danger associated molecular pattern
DC	Dendritic cell
ddH_2O	Double distilled water
DNA	Desoxyribonucleic acid
DNFB	Dinitrofluorobenzene
d	Day
EDTA	Ethylenediaminetetraacetic acid
EGFP	Enhanced green fluorescent protein
EHEC	Enteropathogenic *E. coli*
ELISA	Enzyme-linked immunosorbent assay
GM-CSF	Granulocyte and macrophage colony stimulating factor
EPEC	Enterohaemorrhagic *E. coli*
ER	Endoplasmatic reticulum
ERK	Extracellular signal-regulated kinase
FACS	Fluorescence activated cell sorting
FCS	Fetal calf serum
FITC	Fluorescein isothiocyanate
Fpr	Formylated peptide receptor
GAS	Group A streptococcus
GBS	Group B streptococcus
h	Hour
HIF	Hypoxia-Inducible Factor
HRE	Hypoxia responsive element
IFN	Interferon
IL	Interleukin
InlA	Internalin A
iNOS	Inducible NO synthase
i.v.	Intra venous
kb	Kilobasepair
kPa	Kilopascal
LEE	Locus of enterocyte effacement
LLO	Listeriolysin O
LN	Lymph node
LPS	Lipopolysaccharide

M	Molar
MACS	Magnetic Cell Separation
M-CSF	Macrophage colony stimulating factor
MFI	Mean fluorescence index
MHC I	Major histocompatibility complex class I
MHC II	Major histocompatibility complex class II
min	Minute
МΦ	Macrophage
NO	Nitric oxide
NLR	NOD-like receptor
NOD	Nucleotide-binding oligomerization domain
O_2	Oxygen
OVA	Ovalbumin
PAMP	Pathogen associated molecular pattern
PBS	Phosphate buffered saline
PCR	Polymerase chain reaction
pDC	Plasmacytoid DC
PE	Phycoerythrin
PFA	Paraformaldehyde
PHD	Prolyl hydroxylases
PRR	Pattern recognition receptors
RNA	Ribonucleic acid
ROS	Reactive oxygen species
RLG	RIG-like receptor
RT-PCR	Reverse transcriptase PCR
SDS	Sodium dodecyl sulfate
sec	Second
SEM	Standard error of the mean
SSC	Saline sodium citrate
TAM	Tumor associated macrophage
Th	T helper
TLR	Toll-like receptor
TNF	Tumor necrose factor
TTSS III	Bacterial type III secretion system
TUNEL	TdT-mediated dUTP-biotin nick end labeling
V	Volt
VHL	Von Hippel-Lindau
VEGF	Vascular endothelial growth factor

1 INTRODUCTION

1.1 The Immune System

Organisms, from unicellular beings over plants to mammals, are frequently confronted with unknown substances and challenged by pathogens. As a system of defence, but also of tolerance, the immune system has developed a variety of mechanisms to cope with external challenges. One of the main aspects is recognition of pathogens and identification of danger signals. It is the role of the innate immune system to control the borders of the organism and to initiate an immune response in case of infections, or the presence of sterile danger signals. At the epithelial barriers of lung, skin and intestine, phagocytosing immune cells, like dendritic cells (DC) and macrophages (MΦ), patrol for incoming pathogens and other possibly harmful substances. They scan their surrounding area for conserved structures of the invaders, also known as pathogen associated molecular patterns (PAMPs) and danger associated molecular patterns (DAMPs), such as intracellular DNA, ATP and uric acid. These are recognized by specialized receptors, also known as pattern recognition receptors (PRR). Detection of PAMPs or DAMPs leads to the activation of immune cells by induction of signalling pathways in most cases by induction of NF-κB. Depending on the type of stimulation and the type of immune cell, specific effector mechanisms for initiation of the immune response will be turned on. This can be achieved via secretion of cytokines for communication with other cells or via production of chemokines to attract other cells, which are important for host defence. MΦ, for example, produce antimicrobial peptides, as well as reactive oxygen species (ROS) and nitric oxide (NO) after recognition of PAMPs and phagocytosis of pathogens. An additional mode of action is the expression of chemokine receptors on their cell surface, which enables the cells themselves to respond to chemotactic molecules and to migrate along a chemokine gradient through tissues and lymphatic vessels to the draining lymph nodes (LN). But not only chemokines, also integrins and adhesion molecules facilitate the migration of cells.

In the LN, the innate immune cells interact with cells from the adaptive immune system, such as T and B cells. DC present antigens to T cells, which is mediated by interaction of the major histocompatibility complex (MHC) and the T cell receptor. Under inflammatory conditions, these lymphocytes start to proliferate and are recruited by activation of chemokine receptors and by cytokine stimulation to the site

in infection. T and B cells can specifically act against invading pathogens. CD8 T cells, for example, become cytotoxic and eliminate virus-infected cells and B cells are able to produce pathogen-specific antibodies. Additionally, CD4-positive T helper cells play an important supporting and regulatory role in the adaptive immune system, as they are able to determine the cytokine milieu and thereby influence the differentiation and actions of nearby cells.

1.2 Dendritic cells

DC are professional antigen-presenting cells and play an indispensable role in connecting the innate immune system with the adaptive immune system. They are widely distributed throughout the whole body and possess the ability to take up antigens by phagocytosis or pinocytosis. DC can be classified into various subsets depending on origin, function and expression of distinct cell surface markers. Plasmacytoid DC (pDC) and Pre-conventional DC (Pre-cDC) both derive from a common DC precursor (CDP) and can be found circulating in the bloodstream. From there, the Pre-cDC give either rise to intestinal lamina propria DC or to resident conventional DC (cDC), which are located in lymphoid tissues, such as lymph nodes and spleen. pDC are also able to migrate into lymphoid tissues (Figure 1.1).

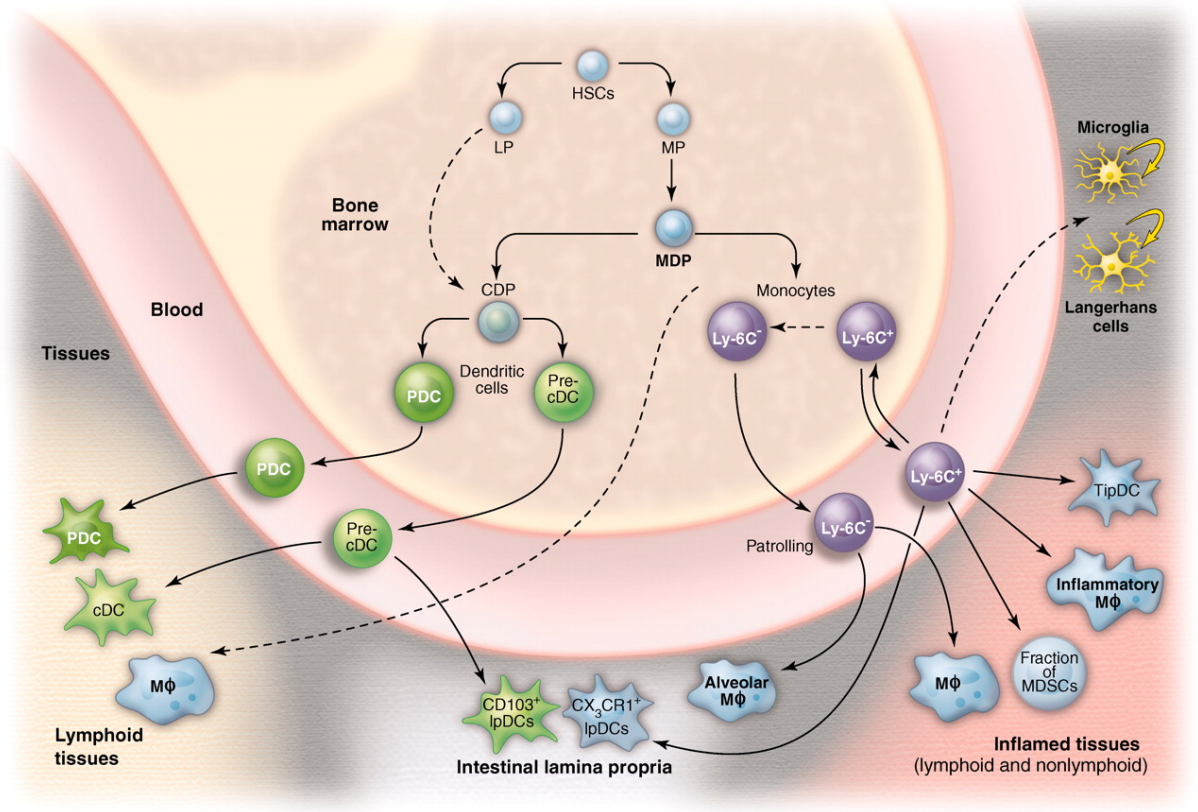

Figure 1.1 DC and MΦ differentiation. Myeloid cells, this includes DC and MΦ, are derived from one hematopoietic stem cell-derived progenitor in the bone marrow (HSC). A common precursor (MDP) gives rise to DC progenitors (CDP) and monocytes that can be divided into Ly-6C$^-$ and Ly-6C$^+$ subsets. These are released into the blood and develop, depending on which tissue they enter, to diverse types of MΦ, TNF- and iNOS-producing inflammatory DC (TipDC), or to the self-renewing microglia and Langerhans cells. The CDP divides into the pDC and the cDC lineage, which gives rise to CD8α$^-$ and CD8α$^+$ cells, which colonize lymphoid as well as non-lymphoid tissues (taken from Geissmann et al., 2010 [1]).

Migratory DC can be found in various organs like brain, kidney and liver, but predominantly in peripheral tissues such as lung, gut and skin. There, they patrol the borders for incoming pathogens and can also be found in peripheral draining LN [2-3]. Langerhans cells represent a special subset of peripheral DC in the epidermis. A characteristic feature is their capacity for self-renewal and the expression of Langerin [1, 4]. Immature DC take up antigens, such as viruses, bacteria, dead cell fragments or nanoparticles by phagocytosis [5]. The recognition of PAMPs and DAMPs activates the DC, which in turn develop a mature phenotype by upregulation of cell surface markers, such as MHC class II (MHCII) and the co-stimulatory molecules CD80 and CD86. Detection of pathogens, which have entered the organism, is regulated by a complex repertoire of PRR which differ among subtypes of DC and comprise C-type lectin receptors (CLR) [6], nucleotide binding and oligomerization domain (NOD)-like receptors (NLR) and retinoid acid-inducible gene (RIG)-like receptors (RLR) [7]. Besides, toll like receptors (TLR) represent a large family of

recognition receptors, which play an important role in sensing bacterial cell wall components like lipopolysaccharide (LPS) (TLR 4), but also intracellular nucleic acids (TLR 3, 7, 8, 9). Engagement of those receptors leads to the activation of NF-κB, either by signalling through TRIF (TLR 3), or by signalling through MyD88 (TLR 1, 2, 6, 7, 9), or by signalling through both molecules (TLR 4) [7]. Thereby, the transcription of genes, which encode for cell cycle regulators, anti-apoptotic molecules, anti-microbial peptides and, to a large part, for pro- and anti-inflammatory mediators, such as the cytokines interleukin (IL)-1β, IL-6, IL-10 and type I and type II interferons (IFN), is induced [8-9]. Activation of PRR leads to altered expression of chemokines and chemokine receptors by migratory DC. Migration from the peripheral tissue to the draining LN is coordinated by an interdependent apparatus of chemokines and adhesion molecules. Additionally, cells important for pathogen elimination and for maintenance of the tissue milieu are attracted from the blood to the site of inflammation. The chemokine CCL17, for example, is expressed by a subset of DC residing in peripheral tissues and attracts CCR4-expressing cells [10]. After uptake of antigens by phagocytosis and maturation, the expression of chemokine receptors enables DC to migrate themselves to remote organs, such as the draining LN. CCR7 with its ligands CCL19 and CCL21 is the predominant mediator of this process [11]. After entry into lymphoid tissues, DC present the processed antigen via MHCII to CD4-positive T cells. In concert with the co-stimulatory molecules CD80 and CD86, antigen-specific T cells respond by expansion and induction of effector functions (Figure 1.2) [12-13]. Antigen presentation via MHC II requires the endocytosis of exogenous antigens, which is followed by proteasomal degradation. Newly formed peptides are then loaded onto the MHCII molecule and transferred to the plasma membrane to be presented [14]. Specialized DC are able to cross-present exogenous antigens via MHC class I (MHCI) to CD8-positive T cells, either inducing tolerance or immunity to pathogens (Figure 1.2). Especially after activation of TLR3, TLR9 and RLR by viruses, the MHCI loading machinery is transferred to the endosomal compartments for peptide loading [15-16].

In contrast to activated DC, steady state immature DC are able to fulfil immunosuppressive functions by induction of regulatory T cells (Tregs), which themselves can counteract effector T cells (Figure 1.2) [17]. Additionally, it was

shown that resting DC were able to inhibit CD8-positive T cells by secretion of soluble suppressive molecules [18].

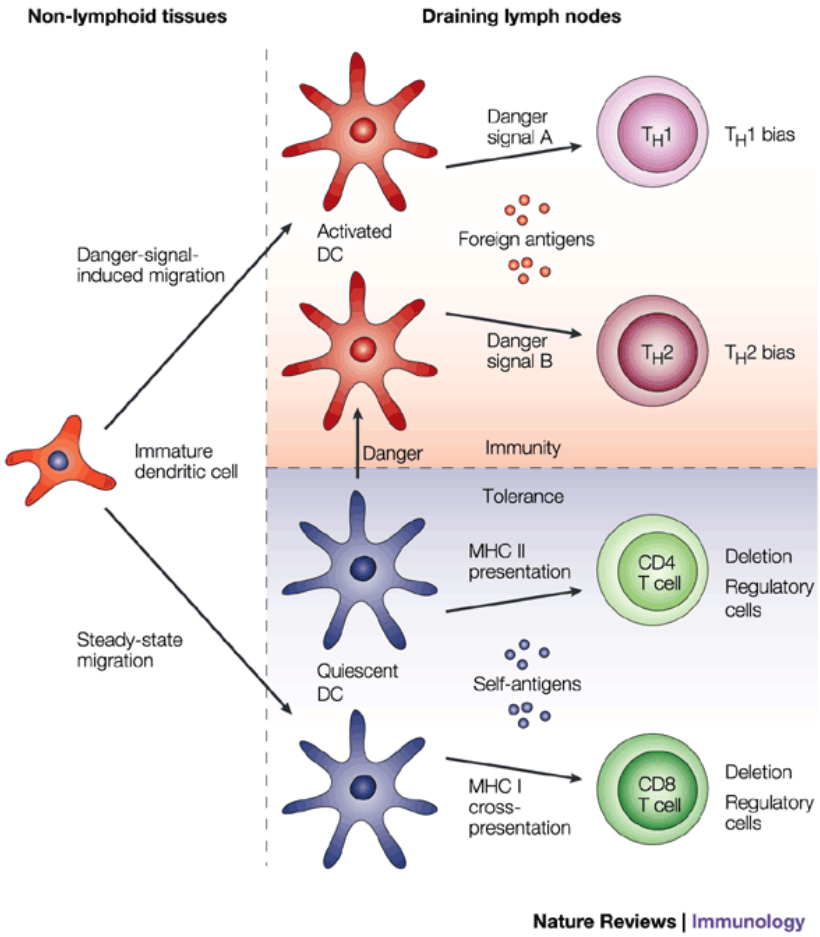

Figure 1.2 DC regulating immunity and tolerance. Depending on the stimulus, immature DC differentiate to activated, inflammatory DC or quiescent DC that determine the T cell's fate. The DC processing self-antigens can promote self-tolerance, either by antigen presentation via MHCII or cross-presentation via MHCI. PAMP or DAMP recognition leads to activation of DC, which, depending on the danger signal, induce Th1 or Th2 differentiation of CD4 T cells (taken from Shortman and Liu, 2002 [12]).

1.3 Macrophages

MΦ are innate immune cells that play a fundamental role in host defence and immune homeostasis. One of their main functions is phagocytosis and recognition of PAMPs and DAMPs. Like DC, they are derived from a hematopoietic stem cell-derived progenitor (HSC) in the bone marrow and, depending on the microenvironment, MΦ show diverse programs of differentiation and a wide spectrum of functions. Immature Ly-6C$^-$ and Ly-6C$^+$ monocytes, the precursors of MΦ, circulate in the blood stream and home to different organs to acquire a tissue-specific phenotype (Figure 1.1). Under the influence of the particular tissue environment, MΦ

display different functions in different organs and are even named tissue-specifically, such as the osteoclasts residing in the bone, the microglia in the brain and the Kupffer cells in the liver. In the spleen, they recycle dead cell material, as they phagocytose and clear old cell debris, senescent erythrocytes and cells, which have undergone apoptosis. Similar to DC, MΦ can respond to a variety of microbial stimuli by employment of a broad spectrum of PRR. Cytotoxic MΦ, whose microbicidal function is enhanced upon IFNγ and TNFα stimulation, are categorized as classically activated inflammatory M1 MΦ. Besides the production of pro-inflammatory cytokines, M1 MΦ secrete ROS, such as superoxide and peroxide, which is produced by the NADPH oxidase, a multicomponent enzyme complex [19], and NO to increase their killing capacity. Another type of MΦ is classified as alternatively activated M2 MΦ, which is induced upon IL-4 stimulation and can be identified by specific upregulation of the mannose receptor. These M2 MΦ are less microbicidal, display immunomodulatory functions and are indispensable for wound healing. Tumour-associated MΦ (TAMs) are known for their immuno-suppressive functions and produce high levels of IL-10. It is assumed that the hypoxic tumour environment leads to the de-activation of the classical M1 MΦ program and rather favours induction of pro-angiogenic and tolerogenic polarization of these MΦ. An important feature of all types of MΦ is their functional plasticity. As the role of a specific MΦ is mainly determined by its microenvironment, there is always the possibility of switching the polarization [20-23].

1.4 Infections

Humans and animals are frequently exposed to pathogens. An infection occurs, when the host cannot prevent colonization with the harmful microorganism, which can be viral, bacterial, fungal or parasitic. The invading pathogen enters the organism via inhalation, via the nutrition or via the skin, where it encounters the host defence system at the epithelial barriers. PRR-possessing cells, which include keratinocytes, alveolar or intestinal epithelial cells, but also patrolling DC or tissue-resident MΦ recognize the PAMPs of the pathogens. An immune response is initiated by the secretion of cytokines and chemokines to attract microbicidal neutrophils and the highly specialized adaptive T and B lymphocytes. But pathogens have evolved sophisticated methods to evade the host immune system and different types of

bacteria have developed different approaches to avoid the actions of the innate or the adaptive immune system and to successfully counteract them. The complex interplay between pathogen and host is a constantly evolving process, since both sides steadily adapt to new mechanisms of either host defence or immune evasion of the pathogen.

A characteristic feature of an infection is the dramatic decrease of tissue oxygen content, as the demand for oxygen rises by replicating pathogens and incoming host immune cells. Tissue-resident DC and invading MΦ encounter the problem of low oxygen supply or even anoxia and thus need to adapt their metabolism. Hypoxia can decisively influence the clearance of pathogens. Infection of human fallopian tube cells with *Chlamydia trachomatis*, e.g., revealed that low oxygen conditions reduce the antibacterial properties of IFN-γ by reduction of expression of the anti-inflammatory tryptophan-degrading enzyme indoleamine 2, 3-dioxygenase (IDO) [24]. In contrast, another study showed that hypoxia is able to enhance DC and MΦ actions for an improved defence against *Leishmania amazonensis* [25].

In this study, three models of bacterial infections were investigated. Three different types of bacteria were chosen, each colonizing different tissues and each making use of distinct mechanisms to invade the host organism. The common feature of these infection models is the generation of hypoxic conditions at the site of infection. *Staphylococcus aureus* (*S. aureus*), *Listeria monocytogenes* (*L. monocytogenes*) and *Citrobacter rodentium* (*C. rodentium*) are facultative anaerobe bacteria, which use oxygen for respiration, and have evolved alternative methods for ATP production in the absence of oxygen [26-28]. Additionally, the host immune response against the *S. aureus*, *L. monocytogenes* and *C. rodentium* is initiated, to a large part, by phagocytosing innate immune cells, such as DC and MΦ. In the following, the bacterial strains and their strategies for host colonization and immune evasion will be described in more detail.

1.4.1 *Staphylococcus aureus*

S. aureus is a gram-positive, skin-colonizing pathogen, which is also capable of invasion of inner organs for soft tissue infection. There, it can cause systemic infections such as endocarditis, meningitis, pneumonia and sepsis. Understanding the molecular mechanisms of *S. aureus* for a more efficient and better clearance of

this pathogen has recently become of high importance, since extremely virulent methicillin-resistant strains of *S. aureus* have become a huge health problem in hospitals and sanitary facilities and cause a high mortality rate amongst elderly and immuno-compromised patients [29-31]. *S. aureus* activates the innate immune system by TLR2 stimulation through bacterial lipoproteins and lipoteichoic acid, but also by TLR9 stimulation. Peptidoglycan, a prominent cell wall component of gram-positive bacteria and among these also *S. aureus*, plays an important role in DC activation via NOD2 and TLR2 and following induction of a Th1 and Th17 response [31-33]. One of the main virulence factors of *S. aureus*, the α-hemolysin pore-forming toxin, also acts in a NOD2-dependent way, when inducing cytokine responses [34]. To increase the resistance to antimicrobial products such as cathelicidins, β-defensin and fatty acids *S. aureus* strategically utilizes the iron-responsive surface determinant A (IsdA) protein [35]. The support of T cells is indispensable for bacterial clearance [29]. Antigen-presenting cells and T cells can be directly activated by secreted superantigens, the staphylococcal enterotoxins (SE), which differ between the serotypes of *S. aureus*. These are usually encoded by genes on plasmids, bacteriophages or pathogenicity islands. Superantigens are highly reactive, as they connect the MHC complex to the T cell receptor and induce T cell proliferation and strong cytokine production [36].

The recruitment of neutrophils to infected areas is induced by activation of the inflammasome in DC and MΦ [37]. The inflammasome is a multiprotein complex, which responds to multiple stimuli by induction of caspase-1, which subsequently, cleaves pro-IL-1β and pro-IL-18 [38]. The activation of the inflammasome is a tightly controlled process, which requires two distinct signals for production of IL-1β and IL-18. One signal, often provided by TLR stimulation, is needed for production of the pro-forms of IL-1β and IL-18, whereas the other signal, for example provided by the release of bacterial toxins, leads to assembly of the inflammasome complex and caspase-1-dependent cleavage of pro-IL-1β and pro-IL-18 [39]. It was shown that activation of the NLRP3-inflammasome by *S. aureus*-derived peptidoglycan is indispensable for production of IL-1β, the key molecule in host defence against *S. aureus* [40]. Formylated peptides are a special characteristic of bacteria, which start protein synthesis with a formylated methionine, in contrast to eukaryotes, which start translation with an unmodified methionine. Formyl peptide receptors (Fpr) belong to the group of seven-transmembrane G-protein coupled receptors and are expressed

by innate immune cells, but also by non-hematopoietic cells. Activation of Fpr by formylated peptides from *S. aureus* induces chemotaxis, phagocytosis and ROS production in neutrophils and monocytes [8].

1.4.2 *Listeria monocytogenes*

Listeria monocytogenes is an intracellular, gram-positive bacterium, which can induce gastroenteritis in humans after being taken up with food, but also severe meningitis and sepsis in immuno-compromised patients. Listeria enter non-phagocytic cells through binding of internalin A (InlA) to the receptor E-cadherin on host cells, which facilitates the entry of bacteria into the cytosol. Intestinal epithelial cells, and also DC and MΦ phagocytose invading Listeria, which soon escape from the acidic vesicles by pH-dependent pore-forming listeriolysin O (LLO) to start replication in the cytosol. After cytosolic replication, *Listeria monocytogenes* recruits the host cell actin machinery to induce bacterial motility for intracellular spreading to adjacent cells [41]. Recognition of Listeria is mediated, to a large part, by TLR, mainly TLR2, but also by TLR5, which recognizes flagellin, and TLR9 binding to CpG motifs in bacterial DNA. NLR play also an important role in recognition of intracellular *L. monocytogenes,* especially NOD2 and NLRP3, a central component of the inflammasome [42]. The innate immune system plays an indispensable role in the defence against *L. monocytogenes* and in the fast activation of the adaptive immune system. It was shown that IL-18, a pro-inflammatory cytokine, is crucial for IFN-γ production by NK cells, and thereby activates TNF-secreting MΦ as an initial step for host defence [43]. MΦ, which have internalized Listeria, produce CCL2 to attract circulating monocytes, which express CCR2 on their surface. These are then able to differentiate into TipDC, which produce TNF and iNOS to enhance bacterial killing [44]. In addition, the adaptive immune system is important, as antigen-presentation via MHCI is necessary to activate cytotoxic CD8-positive cells and the MHCII pathway is needed to initiate a strong CD4 T cell response for an efficient clearance of *L. monocytogenes* [45]. Another more recently discovered mechanism to control Listeria infection is autophagy. Originally, autophagy was found to be a system for maintenance of cell viability by organelle recycling and repair, but lately it was also linked to the defence against intracellular pathogens such as *L. monocytogenes*. Autophagy was shown to directly target intracellular microbes and to capture these in so called

autophagosomes. These fuse with lysosomal organelles to autolysosomes, in which the degradation of the pathogen takes place [46]. Although Listeria have evolved a variety of mechanisms to escape autophagy, such as the actin-based motility for spreading to adjacent cells and the employment of the phospholipases C, which are able to rupture the phagosomal membrane, it is still of need to further investigate the interactions of Listeria with the process called autophagy [47].

1.4.3 *Citrobacter rodentium*

Enteropathogenic *Escherichia coli* (EPEC) and enterohaemorrhagic *E. coli* (EHEC) can cause life threatening colitis in humans. Both colonize the gut via attaching to epithelial cells, inductions of effacing (A/E) lesions and final destruction of the gastrointestinal microvilli. However, these bacteria are poorly pathogenic to mice and to better study the mechanisms of A/E lesion-inducing microorganisms, a murine model of *Citrobacter rodentium* infection was introduced. *C. rodentium* is a gram-negative and non-motile bacterium, which induces thickening of the colon and diarrhoea in mice [48]. To induce A/E lesions EPEC, EHEC and *C. rodentium* employ genes located on a pathogenicity island, termed the locus of enterocyte effacement (LEE). LEE encodes genes for transcriptional regulators, structural components and effector proteins of the bacterial type III secretion system (TTSS). This secretion apparatus is able to inject effector proteins and virulence factors directly into the host cell via a needle complex. The TTSS from *Salmonella typhimurium*, *Burkholderia pseudomallei*, *E. coli*, *Shigella flexneri* and *Pseudomonas aeruginosa* has been shown to activate the NLRC4-inflammasome [49], which is closely related to the NLRP3-inflammasome [39], although there is no data for *C. rodentium*, yet. Genes for adhesion to the outer membrane of host cells, intimin and its receptor Tir, are also located on LEE. A/E lesion-inducing pathogens integrate Tir into the host epithelial cell membrane to establish an efficient pathogen-host connection by binding via intemin. The innate immune phase during an infection with *C. rodentium* is marked mainly by production of antimicrobial peptides and NO by epithelial cells, and the influx of DC, neutrophils and MΦ [50]. TLR signalling plays an important role for induction of host defence, which was shown by infection of MyD88-deficient mice, which, subsequently, led to an increased bacterial load in the colon [51]. Recently, NLR were proposed to mediate control of *C. rodentium* by induction of innate Th17

cells [52]. Commensal microbiota also seem to importantly contribute to both, resistance and tolerance, to *C. rodentium* infections [53]. Additionally, IL-22 was reported to be essential for the induction of the Regenerative (Reg) family of antimicrobial proteins, which represent a special secreted subgroup of C-type lectins [54], during an infection with *C. rodentium*. This was illustrated by the fact that mice with a deficiency for IL-22 showed higher bacterial burden and mortality due to downregulation of Reg proteins. The adaptive immune phase is marked by a pronounced influx of B cells, which secrete *C. rodentium*-specific antibodies, into the infected gut. T cells also invade the colon for production of IFNγ and TNFα to further enhance antimicrobial actions of epithelial gut cells [55].

1.5 Hypoxia

Most organisms depend on oxygen, as it is mandatory for ATP production by aerobic respiration. The lower terrestrial atmosphere, in which all oxygen-breathing species live in, consists of 78% nitrogen, 21% oxygen and small amounts of other gases. Mammals take up this gas mixture by pulmonary respiration. Oxygen concentrations in the body are much lower and vary between tissues depending on the blood supply and on the health status of the organ. The blood is a relatively highly oxygenated compartment of the body with an oxygen content of around 10%, whereas tissues in pathologic conditions can reach oxygen levels lower than 1% (Figure 1.3) [56].

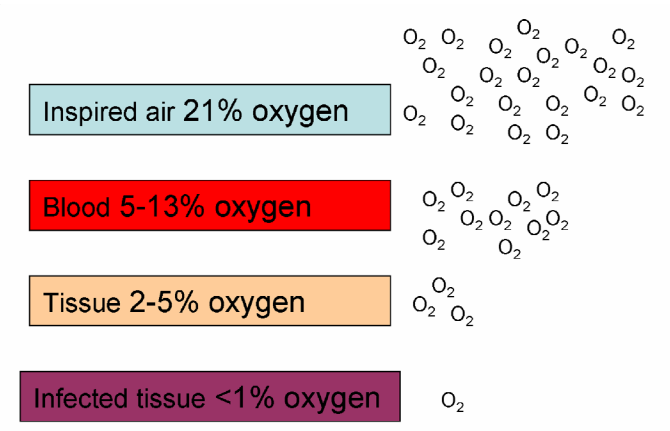

Figure 1.3 Oxygen concentrations inside the body. The oxygen concentration of inspired air is 21%. The oxygen concentration decreases to 5-13% in alveoli and blood circulation. In normal perfused tissues there is an oxygen concentration of 2-5% that can drop below 1% in the case of an infection (modified from Sitkovsky and Lukashev, 2005 [57]).

Hypoxia is a key feature of stem cell maintenance, proliferation and growth and can be found under normal non-pathologic circumstances, for example, in the skin and in the gut [58-60]. Further, hypoxic conditions serve as developmental stimuli during embryogenesis, for example, for placental morphogenesis and development of the vascular system and the heart [61-62]. Stem cell maintenance is preserved in hypoxic niches of the bone marrow, which provide an optimal environment for haematopoietic stem cell differentiation, because of the low ROS production [63].

Hypoxia is also an essential feature of cancer, inflammation and infection. Uncontrolled proliferation of cells and migration of immune cells to the inflamed tissues leads in most cases to an excess of oxygen-consuming cells and thus to a critical shortage of oxygen. Additional invasion of oxygen-consuming pathogens increases the deprivation of oxygen. The impact of low oxygen tensions on the functions and interactions of cells in the affected tissue is immense. The very efficient energy supply by oxidative phosphorylation is shut down and transcription of genes important for anaerobic glycolysis, which provides immediate but few ATP molecules, is turned on. Induction of angiogenesis by upregulation of vascular endothelial growth factor (VEGF) and erythropoesis are further mechanisms for improvement of tissue perfusion and oxygen delivery [57].

Immune cells are rapidly recruited to pathological tissues and thus are severely affected by shortage of oxygen. Different cell types reveal different behaviours in response to hypoxia. As T cells seem to shut down many effector functions, such as cytokine production and proliferation, MΦ rather upregulate secretion of TNF, IL-1 and expression of CD11b and CD18 [57]. Since the absence of oxygen can be fatal for cells, they have developed a sophisticated sensory system, which responds reliably to changes in oxygen concentration. The family of Hypoxia-Inducible Factors (HIF), which includes HIF1α, HIF1β, HIF2α, HIF2β and HIF3α [64], is well known for its management of cell responses to low oxygen [61]. Extracellular adenosine, which accumulates in hypoxic environments, has also been reported to act immuno-modulating on certain cell types under hypoxic conditions, for example, on T cells, which respond with immunosuppression [57, 65]. Other reports propose a leading role for NF-κB in controlling cellular reactions to hypoxia [66].

1.6 HIF1α

HIF1α is probably the best characterized transcription factor of the family of HIFs and is expressed constitutively in all mammalian cells. To ensure the activation of HIF1α only under hypoxic conditions, the stability of HIF1α is tightly controlled by prolyl hydroxylases (PHD) in normoxia. The PHD are activated by oxygen, but also by iron, and transfer hydroxyl groups to the proline residues 402 and 564 of HIF1α. This enables the von Hippel-Lindau tumour suppressor protein (VHL) to induce ubiquitinylation of HIF1α at short sequences of conserved residues [67], which marks HIF1α for proteasomal degradation. An additional point of control is exerted by the factor inhibiting HIF (FIH), which induces hydroxylation of an asparagine residue of HIF1α and thereby blocks its binding to the p300-CREB-binding protein (CBP), a co-activator of HIF1α. The reduced activity of the PHD in hypoxia leads to the accumulation of HIF1α, whose expression is further enhanced by the activation of NF-κB. After translocation into the nucleus and dimerization with HIF1β, also known as arylhdrocarbon receptor nuclear translocator (ARNT), the complex can bind to hypoxia-responsive elements (HRE) via its basic helix-loop-helix motives (Figure 1.4) [56-57].

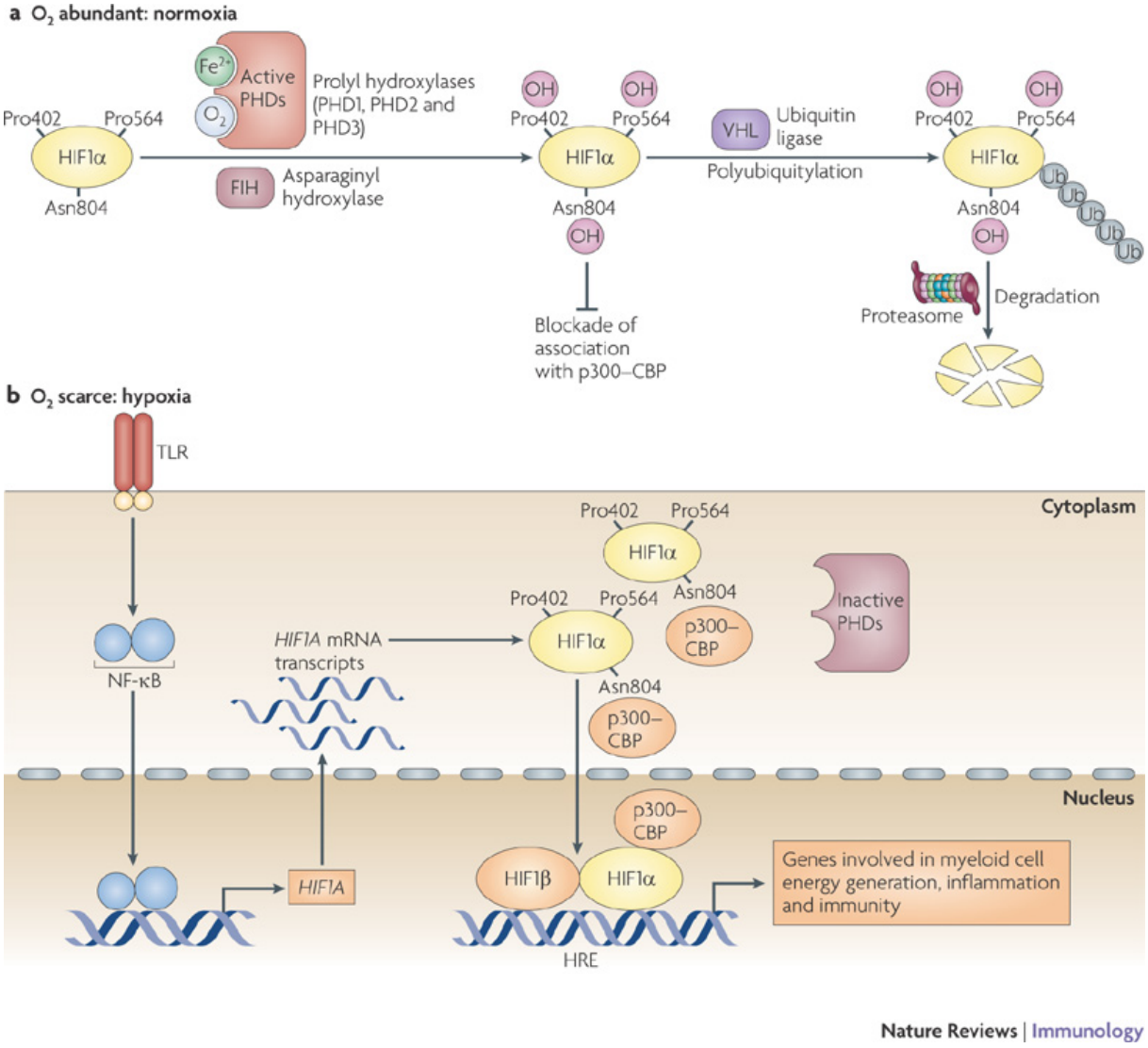

Figure 1.4 Stabilization of HIF1α. a In normoxia, HIF1α is hydroxylated by PHD, polyubiquitinated by VHL and rapidly degraded by the proteasome. **b** Under hypoxic conditions the PHD are inactive and HIF1α is upregulated through NF-κB. After translocation to the nucleus, it binds to HIF1β. There, the heterodimeric helix-loop-helix transcriptional regulator binds to HRE to induce expression of genes involved in energy metabolism and host defence (taken from Nizet and Johnson, 2009 [56]).

Binding of HIF1α to target promoters leads to the transcription of glycolytic enzymes and genes involved in erythropoiesis and angiogenesis, such as VEGF [56-57].

Because immune cells are frequently confronted with hypoxia, HIF1α plays a central role in function and survival of these cells. Several studies, in which HIF1α was silenced or cell type-specifically deleted, provided new insights about HIF1α as the key regulator in responses to hypoxia. HIF1α-deficient T cells displayed increased pro-inflammatory cytokine production and stronger proliferation, which resulted in enhanced survival of mice in a sepsis model [68]. Furthermore, a decisive role of HIF1α in regulation of T cell differentiation was described recently [69]. It was shown that under hypoxic, but also under normoxic conditions, HIF1α can directly induce

gene transcription of RORγt, which is a master regulator of the inflammatory Th17 cells. Concurrently, HIF1α targets Foxp3, the key transcription factor in the anti-inflammatory regulatory T (Treg) cell lineage, for proteasomal degradation [70-71]. Thereby, HIF1α remarkably shifts the T cell polarization from a regulatory type to an inflammatory type.

Mice with a deletion of HIF1α in myeloid cells showed amelioration of symptoms in the experimental settings of arthritis and skin irritation [72], and thereby revealed the importance of this transcription factor in innate immunity. Furthermore, in infection studies, HIF1α-deficient MΦ and neutrophils showed an impaired ability to kill bacteria highlighting the function of HIF1α to induce expression of anti-microbial peptides, such as cathelicidins and the granule proteases cathepsin G [72-73]. In addition, HIF activity was reported to increase phagocytosis and to promote NO production through inducible NO synthase (iNOS) in phagocytes (Figure 1.5) [56, 73].

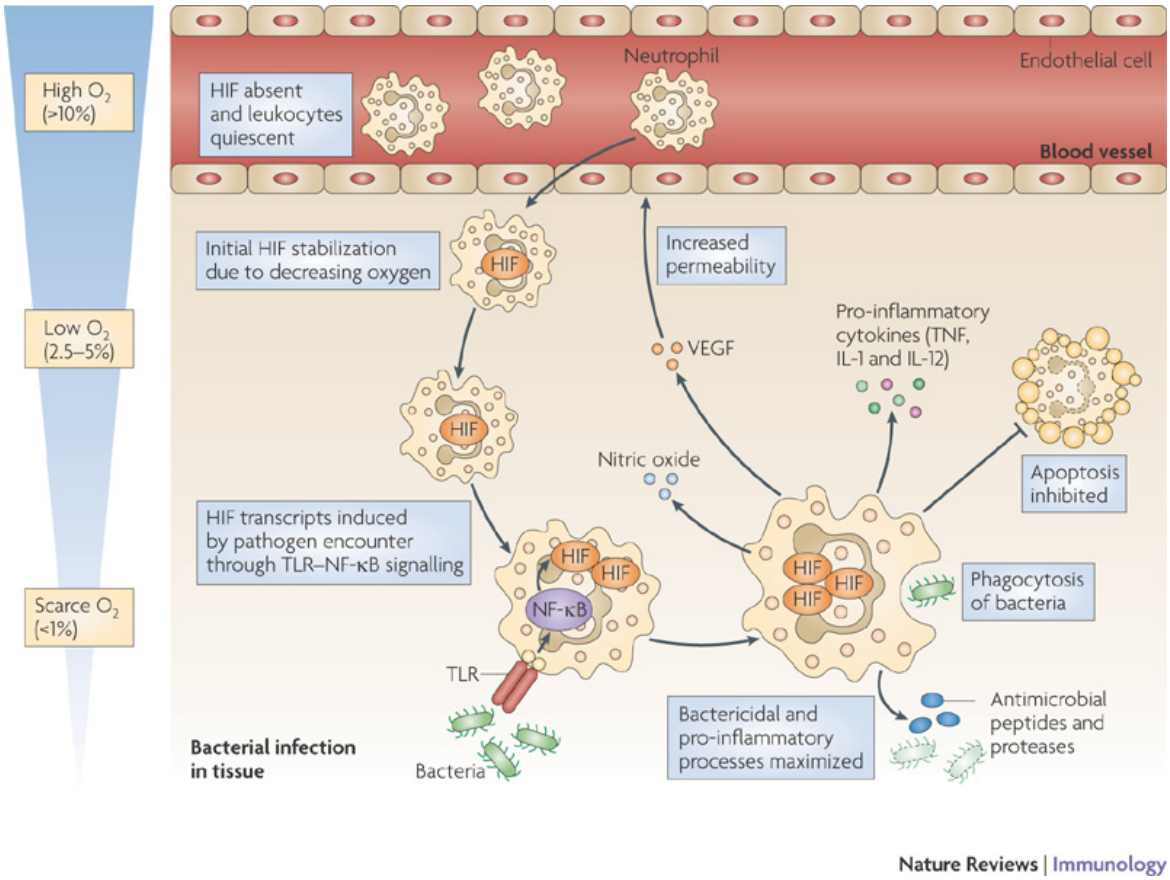

Figure 1.5 Role of HIF1α in immunity. Myeloid cells, such as monocytes, neutrophils and DC, have low levels of HIF1α in an environment containing moderate concentrations of oxygen. Upon entry into low oxygen-diffused tissues, HIF1α is stabilized and reaches high levels in areas with extremely low oxygen conditions. Maximal accumulation of HIF1α is induced by additional TLR stimulation, which is the case during an infection. In response, HIF1α leads to the secretion of NO and antimicrobial peptides and proteases, enhances phagocytosis and upregulates expression of VEGF and pro-inflammatory cytokines (taken from Nizet and Johnson, 2009 [56]).

HIF1α is not only stabilized by low oxygen concentration, but also by products derived from bacteria. *Chlamydia pneumonia,* a bacterium infecting respiratory airways, interferes with HIF1α in the early phase of an infection by stabilization of this transcription factor, whereas degradation of HIF1α is induced in the late phase [74]. Additionally, ROS was shown to interfere with HIF1α in several ways [75]. One publication has revealed stabilization of HIF1α by ROS through signalling of the adenosine monophosphate-activated protein kinase (AMPK) [76]. It will be interesting to detect further molecules interacting with HIF1α, either being upstream or downstream of the HIF transcription cascade.

1.7 HIF1α-conditional mutant mice

The role of HIF1α has been investigated in T cells and myeloid cells, but so far, there is no data on the function of HIF1α in DC. To directly study the role of HIF1α in DC and MΦ, HIF1α^{flox} mice [72] were crossed with different mouse strains expressing the Cre-recombinase under control of lineage-specific promoters. Cre-loxP recombination is a molecular tool, adopted from the bacteriophage P1, and allows "switching on" and "switching off" of genes containing loxP-sites. These loxP-sites are targeted by the Cre-recombinase, which is usually expressed under control of a cell type-specific promoter, a tissue-specific promoter or a promoter of a temporally-expressed gene. The Cre-recombinase catalyzes the DNA recombination between the loxP-sites, which leads to excision of the DNA [77]. CD11cCre mice have previously been shown to efficiently delete loxP-flanked target genes in the vast majority of DC [78], since CD11c represents the major surface marker for the DC lineage. A new Cre-expressing mouse line (CCL17Cre), in which Cre is expressed under control of the *ccl17* promoter, was also employed in this study. As shown previously, the inflammatory chemokine CCL17 can be induced by TLR stimulation and attracts CCR4-expressing cells which can be T cells, MΦ, basophiles and Langerhans cells [10]. It is expressed by a subset of CD11b^{+} myeloid DC residing in LN and peripheral organs, such as skin and gut [10, 79]. As these tissues are known to contain low concentrations of oxygen [59-60], it is of special interest to investigate HIF1α in CCL17-positive DC.

To further analyze the function of HIF1α in granulocytes and MΦ, HIF1α^{flox} mice were crossed with LysMCre mice [80]. Thereby, mice with a specific deletion of HIF1α in

myeloid cells, such as neutrophils, eosinophils, basophils and MΦ were generated. These innate immune cells are known to invade inflamed tissues and, therefore are often exposed to frequently changing oxygen concentrations.
The application of the Cre-loxP system enables the examination of the functional properties of *ex vivo* generated BM-derived cells, but also the analysis of mice with a cell-type specific deletion of HIF1α in certain disease models *in vivo*.

1.8 Aim of the work

In science, hypoxia has quite recently begun to attract the attention of researchers. Most *in vitro* or *ex vivo* experiments are still conducted under normoxic conditions, which do not resemble physiological environments. Especially under pathologic conditions, hypoxia is a prominent parameter and should be considered in studies dealing with cancer, allergies, inflammation and infection.
It was previously shown that deficiency of HIF1α in myeloid cells strongly inhibits the functions of MΦ, such as bacterial killing and invasion into inflamed tissues [72]. In this study, the role of HIF1α in DC was to be addressed, as they are, just like MΦ, potent inducers of immune reactions and professional antigen-presenting cells. Therefore, one of the goals set in this work, is to analyze the influence of hypoxic conditions on differentiation and function of DC and MΦ, since phagocytes are frequently exposed to low oxygen conditions.
The role of HIF1α in hypoxia-induced changes was addressed by employment of different mouse strains, each with a deficiency of HIF1α in a specific cell type. *In vitro* generated DC from mice with a deficiency of HIF1α in DC, and from mice with a deficiency in the CCL17-positive subset of DC were analyzed, especially focussing on their maturation after PRR recognition, migratory processes and bacterial killing. These bone marrow-derived DC (BMDC) were compared with *in vitro* generated MΦ from mice deficient for HIF1α in myeloid cells. *In vivo* mouse models of skin inflammation and bacterial infections were used to provoke situations of extreme hypoxia *in vivo*. A superficial infection model with *S. aureus* was employed for induction of hypoxic conditions in the skin, and thus to activate Langerhans cells and dermal DC for a closer observation of their behaviour under hypoxic conditions after deletion of HIF1α. Additionally, a model of systemic Listeria-infection was analyzed, because the cytosol of phagocytic innate immune cells represents the main niche for

the replication and immune evasion of *L. monocytogenes* [41-42, 81]. Furthermore, conditional mutant mice were infected with *C. rodentium* to provoke a hypoxic infection of the gut and to analyze the migration of HIF1α-deficient DC and the capacity of MΦ and neutrophils with HIF1α-deficiency to kill bacteria. By use of *in vitro* assays, as well as of *in vivo* models of diseases, the goal of this thesis was to study the effect of ablation of HIF1α regarding key characteristics of DC and MΦ. Finally, a detailed discrimination and definition of the different functions of HIF1α in DC and MΦ should be worked out in this study.

2 MATERIAL AND METHODS

2.1 Material

2.1.1 Equipment

Equipment	Manufacturer
HERA Cell 150 Hypoxic Incubator	Thermo Scientific, Bonn
Flow Cytometer FACSCalibur	BD Bioscience, Heidelberg
Flow Cytometer FACSCanto	BD Bioscience, Heidelberg
Flow Cytometer FACS Aria	BD Bioscience, Heidelberg
ELISA Reader	Biotek, Bad Friedrichshall
ULTRA-TURRAX	IKA, Staufen
Neubauer Hemocytometer	Brand, Wertheim
Sterile bench HERAsafe	Thermo Scientific, Bonn
Pico 17 centrifuge	Thermo Scientific, Bonn
Biofuge fresco	Thermo Scientific, Bonn
Centrifuge 5415D	Eppendorf, Hamburg
Hereaus Multifuge	Thermo Scientific, Bonn
Microscope Eclipse E100	Nikon, Düsseldorf
Balance 440-35N	Kern, Balingen-Frommern
Pipettes	Eppendorf, Hamburg
Incubator Shaker Innova 4200	New Brunswick Scientific, Edison, USA
Electrophoresis Subcell GT	BioRad, München
Electrophoresis Power pac 300	BioRad, München
Rotor-Gene 3000 cycler	QIAGEN, Hilden
MACS Separator	Miltenyi Biotec, Bergisch Gladbach
T1 Thermocycler	Biometra, Göttingen
Cryostat	Leica, Nussloch
Anoxomat	MART Microbiology, Drachten, Netherlands
AxioCamMR3	Zeiss, Göttingen
Observer D1	Zeiss, Göttingen

2.1.2 Laboratory Items

Item	Manufacturer
Plastic ware	Eppendorf, Hamburg Sarstedt, Nürnberg Greiner Bio-One, Solingen Costar, Cambridge, USA BD Bioscience, Heidelberg
Needles Microlance	BD Bioscience, Heidelberg
Tegaderm® 1624W	3M Medica, Neuss
Southern blot membrane	Pall Corperation, Dreieich
ImmEdge Pen	Vector Lab. Inc., Burlingame, USA
MACS LS Columns	Miltenyi Biotec, Bergisch Gladbach
Colombian sheep blood (COS) plates	Biomerieux, Nürtingen

2.1.3 Kits

Kit	Manufacturer
ATP Bioluminescence Assay Kit CLSII	Roche Diagnostics, Mannheim
ELISA DuoSet Development kits	R&D Systems, Wiesbaden
Ready-SET-Go! Kit	eBioscience, Frankfurt
Plasmid Midi Kit	QIAGEN, Hilden
Pan T Cell Isolation Kit II	Miltenyi Biotec, Bergisch Gladbach
Gel DNA Recovery Kit	Zymo Research, Freiburg
Ladderman labeling Kit	Takara, Shiga, Japan
RNeasy mini Kit	Qiagen, Hilden
PeqGOLD Total RNA Kit	Fermentas, St.Leon-Rot
Absolute SYBR-green ROX	Thermo Scientific, Schwerte
In Situ Cell Death Detection Kit	Roche Diagnostics, Mannheim
H&E stain	Sigma-Aldrich, München

2.1.4 Media and Buffer

Solution/Buffer/agent	Composition
PBS	13.7 mM NaCl 2.7 mM KCl 80.9 mM Na_2HPO_4 1.5 mM KH_2PO_4 pH 7.4
Ultra Pure 10x TAE buffer (Invitrogen, Darmstadt)	0.4 M Tris 10 mM EDTA
Washing buffer (ELISA)	0.05% Tween 20 in PBS
Blocking buffer (ELISA)	1% (w/v) BSA in PBS
Trypan blue (Sigma-Aldrich, München)	0.25% in PBS
Southern blot washing buffer	0.1 M Tris, 1 M NaCl, pH 7
Southern blot hybridization washing buffer 1	2 x SSC, 0.1% SDS
Southern blot hybridization washing buffer 2	0.2 x SSC, 0.1% SDS
Complete RPMI 1640 (Invitrogen, Karlsruhe)	10% FCS (PAN Biotech, Aidenbach) 1% L-glutamine (Invitrogen, Karlsruhe) 1% Penicillin-streptomycin, (Invitrogen, Karlsruhe) β-mercaptoethanol (Sigma-Aldrich, München)
MACS buffer	PBS, 1% FCS, 2mM EDTA
Anaesthesia agent	Xylapan 0.25 ml (20 mg/ml) (Vetoquinol, Ravensburg) Narketan 0.5 ml (100 mg/ml) (Vetoquinol, Ravensburg) 0.9% NaCl ad 5 ml

2.1.5 Chemicals and Enzymes

Chemical/Enzyme	Manufacturer
Collagenase D	Roche, Mannheim
DNaseI	Roche, Mannheim
Dinitrofluorobenzene (DNFB)	Sigma-Aldrich, München
LPS *E.coli* 0111:B4	Sigma-Aldrich, München
Peroxidase substrate (TMB Plus)	Kem-En-Tec, Köln
Schwefelsäure (H_2SO_4)	Merck, Darmstadt
EcoRI	Fermentas, St.Leon-Rot
PstI	Fermentas, St.Leon-Rot
Paraformaldehyde	Merck, Darmstadt
Agarose	Roth, Karlsruhe
LB-broth, high salt	BD Biosciences, Heidelberg
Bacto agar	BD Biosciences, Heidelberg
Ampicillin	Sigma-Aldrich, München
NaCl	Roth, Karlsruhe
KCl	Merck, Darmstadt
Na_2HPO_4	Sigma-Aldrich, München
KH_2PO_4	Sigma-Aldrich, München
Tris	Roth, Karlsruhe
SDS	Sigma-Aldrich, München
Saponine	Sigma-Aldrich, München
CellTracker Probes	Invitrogen, Karlsruhe
CpG	Eurofins MWG Operon, Ebersberg
Tween	Roth, Karlsruhe
BSA	Serva, Heidelberg
Ligase	Fermentas, St.Leon-Rot
Acetone	Sigma-Aldrich, München
Olive oil	Sigma-Aldrich, München
Dibutylphtalate	Sigma-Aldrich, München
FITC	Sigma-Aldrich, München
EDTA	Invitrogen, Karlsruhe
Cryo medium	HistoService Jung, Nussloch
Mowiol	Roth, Karlsruhe
Gentamycin	Invitrogen, Karlsruhe
GolgiStop	BD Biosciences, Heidelberg

2.1.6 Primer

Primer	Forward	Reverse	application
HIF1α cloning	GACAGCTCTCCTTGATAAAGCTT	CTGTCATGTGGAAGAATCGAGA	Probe cloning
HIF1α probe	CGGTGTGTATCATTCTATAG	CTGACATCAATACCTTCCCAC	Southern blot
β-actin	TGACAGGATGCAGAAGGAGA	CGCTCAGGAAGGAGCAATG	qRT-PCR
IL-12p40	ATCCAGCCCAAGAAAGAA	CTACGAGGAACTCACCTGTC	qRT-PCR

	AA		
p19	AGTTCGTGCGATCCCGGAGA	CCAGGCATCGCGCACATCCA	qRT-PCR
IL-12p35	CCATCAGCAGATCATTCTAGACAA	CGCCATTATGATTCAGAGACTG	qRT-PCR
NLRP3	CCCTTGGAGACACAGGACTC	GAGGCTGCAGTTGTCTAATTCC	qRT-PCR
Fpr1	TGTCCAGAGCTGTTGGAAAG	TCATGAGGTTCACTGCAGACTT	qRT-PCR
LC3	CATGAGCGAGTTGGTCAAGA	CCATGCTGTGCTGGTTGA	qRT-PCR
IDO	GGGCTTTGCTCTACCACATC	AAGGACCCAGGGGCTGTAT	qRT-PCR
iNOS	GGCAGCCTGTGAGACCTTTG	GAAGCGTTTCGGGATCTGAA	qRT-PCR
Cramp	TTCTTAGGCCTCGCTAAGACTG	TTGATCCCGGTGAAAAAGTC	qRT-PCR
HIF2α	GGTTAAGGAACCCAGGTGCT	GGGATTTCTCCTTCCTCAGC	qRT-PCR
IL-22	GTGGGATCCCTGATGGCTGTCCTGCAG	AGCGAATTCTCGCTCAGACTGCAAGCA T	qRT-PCR

All primers were designed with help of the RocheProbeLibrary and ordered at Eurofins MWG Operon, Ebersberg.

2.1.7 Antibodies

Specificity	Clone	Application	Manufacturer
MHC II	M5/114.15.2	FACS	eBioscience, Frankfurt
CD11c	N418	FACS	eBioscience, Frankfurt
CD80	16-10A1	FACS	eBioscience, Frankfurt
CD86	PO3.1	FACS	eBioscience, Frankfurt
CD3	145-2C11	FACS	eBioscience, Frankfurt
CCR7	4B12	FACS	eBioscience, Frankfurt
CD11c	HL3	FACS	BD Biosciences, Heidelberg
CD73	TY/23	FACS	BD Biosciences, Heidelberg
CCR5	C34-3448	FACS	BD Biosciences, Heidelberg
CD8	53-5.8	FACS	BD Biosciences, Heidelberg
CXCR4	247506	FACS	R&D Systems, Wiesbaden
CD69	H1.2F3	FACS	eBioscience, Frankfurt
F4/80	BM8	FACS	eBioscience, Frankfurt
Gr1	RB6-8C5	FACS	eBioscience, Frankfurt
CD11b	M1/70	FACS	Bio Legend, Uithoorn, Netherlands
CD4	RM4-5	FACS	Bio Legend, Uithoorn, Netherlands
IL-12p40	C15.6	FACS	BD Biosciences, Heidelberg
MHCII	MaP.DM1	Epidermal sheets	BD Biosciences, Heidelberg
Anti Rabbit texas red		Epidermal sheets	Invitrogen, Karlsruhe

CD11c MicroBeads	N418	MACS	Miltenyi Biotec, Bergisch Gladbach
Streptavidin -PE		FACS	BD Biosciences, Heidelberg

2.1.8 Bacteria

Strain	Growth medium	Origin
Staphylococccus aureus K57 (Isolate from a patient)	LB	Walter Däubener, Düsseldorf
Listeria monocytogenes ATCC wildtype strain 43251	BHI	Stephanie Scheu, Düsseldorf
Streptococcus agalactiae (GBS) (Isolate from a patient)	DMEM 10% FCS	Walter Däubener, Düsseldorf
Streptococcus pyogenes (GAS) (Isolate from a patient)	DMEM 10% FCS	Walter Däubener, Düsseldorf
Escherichia coli DH5α competent cell	LB	Invitrogen, Karlsruhe
Citrobacter rodentium DBS100 ICC180 [48]	LB kanamycin	Matthias Lochner, Hannover

2.1.9 Software

Program	Producer
AxioVision Rel. 4.6	Zeiss, Göttingen
Gen5	Biotek, Bad Friedrichshall
FlowJow 7.5	TreeStar, Ashland, USA
GraphPad Prism 4	GraphPad, La Jolla, USA
Rotor-Gene 6	QIAGEN, Hilden
FluorChem 8900	Protein Simple, Santa Clara, USA

2.2 Animals

2.2.1 Mice

CCL17Cre mice were generated by insertion of CreNLS [82] and a neomycin cassette flanked by FRT-recombination sites in the second exon of the *ccl17* gene. Homologously recombined embryonic stem cell clones (E14.1) were detected by southern blot. The neomycin resistance cassette was removed from the targeted *ccl17* locus by FLP recombinase expression *in vitro*. After germline transmission,

mice were backcrossed to the C57BL/6J background for more than 8 generations [83-84].

Cell-specific inactivation of HIF1α was achieved by cross-breeding CD11cCre [78], CCL17Cre [84] and LysMCre [80] transgenic mice with HIF1α^{flox} mice [72]. These mice are designated as cHIF1α^{CD11c}, cHIF1α^{CCL17} and cHIF1α^{LysM}, respectively in the following part of this thesis. As control mice HIF1α^{flox} littermates were used. CCL17/EGFP mice [79] and RA/EG reporter mice [85] were described previously. All mice were bread under pathogen-free conditions in the animal facility of the IUF. For infection studies the mice were transferred to a S2 area in the animal facility of the University of Düsseldorf. Animal experiments were performed with permission of the government of North Rhine-Westphalia.

2.3 Methods

2.3.1 Cloning of a HIF1α-specific DNA probe

A 2.1 kb fragment was amplified from HIF1α^{flox} DNA, detected via gel electrophoresis and cut out of the gel for DNA isolation. Eluation of the specific PCR fragment was performed using the Gel DNA Recovery Kit. After A-tailing with 1µl 2mM dATP (Fermentas, St.Leon-Rot) for 30 min at 70°C the eluate was ligated overnight at 16°C into the pGem T easy vector (Promega, Mannheim). To amplify the plasmid, it was transformed into DH5α library competent cells, an avirulent *E. coli*-strain. These were plated on LB agar containing ampicillin and 10 colonies were picked for overnight culture and plasmid purification. Digestion with *EcoRI* revealed two colonies, which had incorporated the plasmid with the insert. These amplified fragments were sequenced (GATC, Konstanz) and, based on these results, a 227 bp HIF1α probe was designed and generated by subcloning (Figure 2.1).

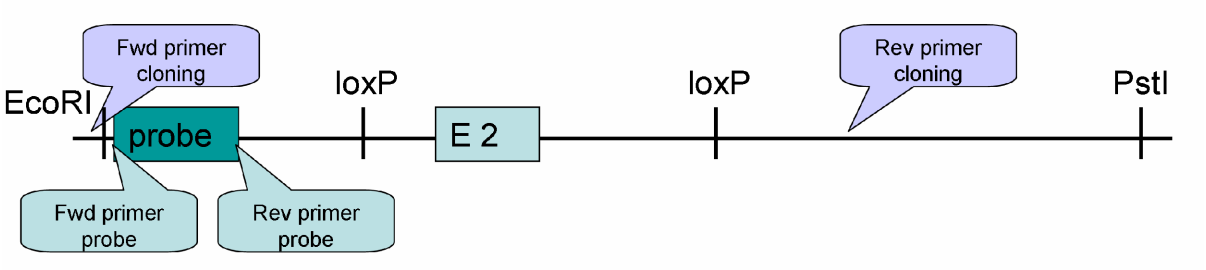

Figure 2.1 Generation of a HIF1α-specific DNA probe. The probe was generated to bind with high affinity to a 2.1 kb fragment after treatment of genomic DNA with restriction enzymes EcoRI and PstI. By cre recombination at loxP sites a fragment of 0.6 kb was removed.

2.3.2 Southern blot

To analyze the deletion efficiency of the Cre-recombinase in the different mouse strains, a 227 bp HIF1α 3´flanking probe (Figure 2.1), which detected a 2.1 kb fragment of the HIF1α gene spanning exon 2, which is flanked by loxP sites, was cloned. After Cre-mediated excision, a 1.5 kb fragment was detected. Genomic DNA was digested with *Eco*RI and *Pst*I and run on a 0.8% agarose gel at 30V overnight. After a short treatment of the gel with 0.25 N HCL and 0.4 N NaOH, the DNA was blotted on a nitrocellulose membrane for 14 hours. Then the membrane was washed for 15 min with Tris/NaCl buffer and baked at 80°C for 1 hour. Prior to the hybridization step, the membrane was incubated with salmon sperm DNA for 1 hour to block unspecific binding. The probe was labeled with the radioactive isotope 32p by use of the Ladderman labeling kit and hybridized to the membrane-bound DNA overnight at 60°C. On the next day, the membrane was washed in southern blot hybridization washing buffer 1 and 2 and the bands were detected on a phospho imager screen. For calculation of the deletion efficiency, the intensity of the bands was quantified using the FluorChem 8900 software. The local background intensity was subtracted from the intensity of the specific bands and the ratio of the normalized band intensities of the floxed and deleted band was calculated.

2.3.3 Generation and *in vitro* stimulation of BMDC and BMMΦ

BM cells were plated at a concentration of 5x 10^5 cells/ml in complete RPMI 1640 (see Material, 2.1.3 Media and Buffer). For differentiation to BMDC, 2% supernatant of GM-CSF transfected X63Ag8-653-cells [86] was added and for differentiation to BMMΦ, 10% M-CSF from the L929 cell line was added. BM cells

were cultured either under normoxic (21% O_2) or hypoxic (1% O_2) conditions. On day 3, cells were fed with the same medium and harvested on day 6. For *in vitro* stimulation, cells were plated at 1x 10^6 cells/ml onto 6-well plates and stimulated with 1 µg/ml LPS for 16-20 h.

Hypoxic conditions were obtained by culturing the cells in the presence of 1% O_2/ 5% CO_2/ 94 % N_2 in an incubator with adjustable O_2 concentration. For the period of BMDC/BMMΦ generation, LPS or bacterial stimulation, as well as *in vitro* migration assays, cells were kept in the hypoxic incubator. To prevent reoxygenation, cells were rapidly treated under normoxic conditions for feeding on d3 and kept on ice under normoxic conditions for all staining and centrifugation procedures. In some experiments, cells were fed with medium equilibrated under hypoxic conditions for 24 hrs before use and were immediately fixed in 1% PFA prior to surface marker staining to prevent reoxygenation.

2.3.4 Magnetic Cell Separation (MACS)

MACS is a method for enrichment and purification of specific cell types from a mixture of different cells. BMDC were directly labeled with CD11c MicroBeads, a magnetically labeled CD11c-specific monoclonal antibody, and stained for 15 min at 4°C. For isolation of untouched T cells, spleen cells were negatively selected by application of a biotin-labeled antibody cocktail from the Pan T Cell Isolation Kit, which depletes all cells except T cells. After additional incubation with anti-biotin MicroBeads for 15 min at 4 °C, magnetically labeled cells were retained in the LS columns by the magnetic field of the MACS separator and unlabeled cells were collected in the flow-through. Positively selected cells could be recovered from the column by washing with MACS buffer in the absence of the magnetic field. In all steps MACS buffer was used for incubation and eluation.

2.3.5 Cell sorting

To isolate CCL17-positive DC for determination of Cre-mediated deletion efficiency, BMDC were generated from cHIF1α^{CCL17} mice crossed to CCL17/EGFP reporter mice. Cells from these mice express Cre on one allele of CCL17 and EGFP on the other allele. Induction of CCL17 by TLR stimulation leads to the expression of Cre

and EGFP. As EGFP is expressed instead of CCL17, this mouse represents a perfect tool for determination of Cre activity in CCL17-expressing cells [79]. After overnight stimulation of BMDC with 1 µg/ml LPS, DC expressing EGFP under the control of *ccl17* were sorted with a purity of more than 95% using a FACS Aria sorter.

2.3.6 Fluorescence activated cell sorting (FACS)

Flow cytometry is used for qualitative and quantitative analysis of cell populations in a mixture of diverse cell types. The cells to be analyzed are marked with antibodies coupled to fluorescent molecules. In the cytometer the cells are separated and the fluorochromes are activated by laser light, which leads to fluorescence emission of different wave lengths depending on the fluorochrome. The photomultiplier is also capable for detection of size and granularity of the cells.

Cells were stained with the appropriate antibody in PBS on ice for 15 min and analyzed with a FACSCalibur or a FACSCanto flow cytometer. Data were analyzed with FlowJo software. For intracellular staining, cells were pre-incubated with GolgiStop for 4 hours at 37°C, fixed and permeabilized in PBS containing 1% FCS and 0.1% saponine before staining.

2.3.7 ATP measurement

BMDC or BMMΦ were harvested on day 6 and adjusted to 5x 10^7 cells/ml in PBS. Intracellular ATP was quantified with the ATP Bioluminescence Assay Kit CLSII according to the manufacturers instructions (Roche Diagnostics, Mannheim).

2.3.8 ELISA

Cell culture supernatants were analyzed for IL-1β, IL-10, IL-6, IL-22, IL-23, TNFα, CCL17 and CCL22 using ELISA DuoSet Development kits; IL-12p70 was detected with the Ready-SET-Go! Kit. For all analyses, 96-well flat-bottom Microplates (Greiner Bio-One, Solingen) were used. For calculation of concentrations, the program Gen5 (Biotek, Bad Friedrichshall) was applied.

2.3.9 cDNA synthesis

BMDC or BMMΦ were stimulated or not with 1 µg/ml LPS for 3 h. RNA from *ex vivo* generated cells or from organ tissue was isolated using the RNeasy mini kit or the PeqGOLD Total RNA Kit. First-strand cDNA was synthesized as follows:

1 µg RNA in 10 µl RNAse-free H_2O
2 µl oligo(dT) (1 µg/ml)

→ 10 min 70°C → 4°C

10 µl RNAse-free H_2O
8 µl 5x RT-buffer
4 µl dNTP (10 mM)
4 µl DTT (100 mM)
1 µl RiboLock (40 U/µl)
1 µl Revert Aid reverse transcriptase (200 U/µl)

→ 60 min 42°C → 10 min 70°C → 4°C

All substances were obtained from Fermentas, St.Leon-Rot.

2.3.10 Quantitative Real-time PCR (qRT-PCR)

For quantitative analysis of gene expression the following mix was prepared:

7.5 µl Absolute SYBR-green ROX mix
0.2 µl forward primer (10 nM/ml)
0.2 µl reverse primer (10 nM/ml)
2.1 µl ddH_2O
1 µl 1:5 diluted cDNA

PCR products were amplified using a Rotor-Gene 3000 cycler with use of following program:

95°C 10 min Hold
95°C 20 sec Cycling 40x
60°C 20 sec
Melt curve 50°C - 99°C

RNA expression levels were normalized to β-actin and displayed as fold-change relative to normoxic, unstimulated $HIF1\alpha^{flox}$ cells used as calibrator (set to 1) using the comparative CT Method (ΔΔCT Method) according to the ABI User bulletin #2 :

ΔCT = CT gene of interest – CT housekeeping gene
ΔΔCT = ΔCT experimental group – ΔCT control
Ratio = $2^{-\Delta\Delta CT}$

2.3.11 *In vitro* migration assay

Migration of BMDC was assessed using Transwell Chambers (8.0 µm pore diameter) (Costar, Cambridge, USA). The lower wells contained 700 µl of RPMI/0.5% FCS as control, or RPMI/0.5% FCS containing 200 ng/ml recombinant mouse CCL19/MIP-3β or 200 ng/ml recombinant mouse CXCL12/SDF-1α (both R&D Systems, Wiesbaden). 2x 10^5 cells in 300 µl medium were added to the upper chambers and incubated at 37 °C either under normoxic or under hypoxic conditions. After 4 h, the cells in the lower chamber were counted microscopically and the proportion of $CD11c^+$ $MHCII^+$ cells in the BMDC culture, which was applied in the experiment, as well as the proportion of migrated $CD11c^+$ cells, was assessed by FACS analysis.

2.3.12 *In vivo* migration of BMDC

BMDC were labeled in serum-free RPMI with CellTracker Probes for Long-Term Tracing of Living Cells. BMDC to be labeled green were incubated for 30 min with 10 µM 5-chloromethylfluorescein diacetate (CMFDA) and BMDC to be labeled red with 20 µM 5-(and-6)-(((4-Chloromethyl) Benzoyl) Amino) Tetramethylrhodamine (CMTMR). After a washing step, they were incubated additional 30 min at 37°C in complete RPMI medium. Green labeled BMDC were mixed in equal amounts with red labeled BMDC. In independent experiments, groups of BMDC to be compared were labeled with one or the other fluorescent marker to exclude dye-specific influences. 2x 10^6 cells were injected into the footpad of C57BL/6 mice. 24 h later, popliteal LN were dissected and analyzed by flow cytometry.

2.3.13 Cytotoxic T lymphocyte (CTL) assay

Mice were subcutaneously immunized with 50 µl PBS containing 300 µg Ovalbumin (OVA) and 5 nmol CpG or only with 300 µg OVA (Sigma-Aldrich, München). At day 7, spleen cells from mice of the same strain were loaded with the OVA peptide SIINFEKL (200 µM) or not and labeled differentially with CellTracker Probes. Green CMFDA labeled (8 µM) SIINFEKL cells were mixed in equal amounts with red CMTMR labeled (15 µM) unloaded cells and mice were i.v. injected with 200 µl PBS containing 1x 10^7 cells. After 4 hours, spleens of mice were dissected and screened

via FACS analysis for CellTracker labeled cells. Specific killing was calculated as follows: % specific killing = [1 − (% CMFDA / % CMTMR)] × 100.

2.3.14 Contact hypersensitivity (CHS)

CHS was induced by application of 100 µl 0.5% dinitrofluorobenzene (DNFB) in acetone/olive oil (4:1) on the shaved back of mice after anaesthetisia with isoflurane. On day 5 after sensitization, mice were challenged on the ears with 0.3% DNFB and swelling of ears was measured after 24 hours with a micrometer gauge. Mice, which had been challenged without prior sensitization, as well as mice, which had received no treatment at all, served as negative controls.

2.3.15 FITC-induced cell migration

To investigate the ability of dermal DC and Langerhans cells to migrate upon an irritant stimulus, mice were anaesthetized with isoflurane, and 200 µl of 0.5% fluorescein isothiocyanate (FITC) in 1:1 acetone/dibutylphtalate was applied on the shaved back. Activated dermal DC and Langerhans cells, which had taken up FITC and had migrated, could be quantified in skin draining brachial LN after 24 hours or 3 days by flow cytometric detection of $CD11c^{+}$ $MHCII^{hi}$ FITC-positive cells.

2.3.16 Preparation of epidermal sheets

To monitor migration of Langerhans cells *ex vivo*, mice were challenged with 20 µl 0.5% DNFB in acetone/olive oil (4:1) on the right ear for 4 hours. The left ear was treated with acetone/olive oil (4:1) only and served as control. Both ears were dissected and split into two halves, so that each side was incubated with the dermal side towards the complete RPMI medium in the culture dish to allow DC to migrate out of the tissue. Both ear halves were incubated for 48 hours either in a normoxic or in a hypoxic incubator. After change of the medium into PBS containing 20 mM EDTA and 2 hours incubation at 37°C, the epidermis was separated from the dermis and fixed in ice-cold acetone for 20 min. After rehydration in PBS, the epidermal sheets were blocked in 5% BSA/PBS. This was followed by staining with a monoclonal antibody specific for MHCII for 2 hours, three steps of PBS washing and the second

anti-rabbit antibody coupled to Texas Red. The epidermal sheets were mounted with mowiol, microscopically analyzed and the emigration of the Langerhans cells was quantified by manual counting of the remaining MHCII-positive cells in the epidermis. For detection of apoptosis, a TUNEL assay was conducted on epidermal sheets with the *In Situ* Cell Death Detection Kit (Roche Diagnostics, Mannheim) according to the manufacturers instructions. Here, a DNAse-treated epidermal sheet served as positive control.

2.3.17 *In vitro* killing assay of bacteria

BMDC or BMMΦ were adjusted to 1x 10^6 cells/ml in complete RPMI 1640 without antibiotics. Bacteria were grown in appropriate media as indicated above (2.1.7 Bacteria) and concentration was controlled photometrically at O.D. 600 nm. Bacteria were adjusted to 1x 10^9 cells/ml in antibiotic-free RPMI and BMDC or BMMΦ were infected with bacteria at a ratio of 1:100 (BMDC/ BMMΦ: bacteria) and incubated at 37°C either under normoxic, under hypoxic or under anoxic conditions for 1 hour. For incubation under anoxic conditions, six-well-plates containing the infected cells were placed in anaerobic jars, which were evacuated with the use of an anoxomat. Evacuated air was replaced with a standard anaerobic gas mixture composed of 80% N_2, 10% H_2, and 10% CO_2 (standard anaerobic recipe). Since, the anoxomat cannot completely eliminate all oxygen, a remainder of 0.1 -0.2% oxygen was left inside the incubation jars. First, it was only possible to work with anoxia. During the study, a pre-programmed recipe for a gas mixture containing 1% oxygen was purchased for the anoxomat. Thus, some experiments were conducted under anoxic and some were conducted under hypoxic conditions. After 60 min, 100 µg/ml gentamycin was added to the infected BMDC or BMMΦ to kill extracellular bacteria, and cells were incubated under the same conditions as before for either 1 hour or overnight. Immediately after that period, culture dishes were kept on ice and cells were scraped off the bottom and washed twice with PBS. Cells were always controlled microscopically for viability during co-culturing and, finally, stained with trypan blue to determine living cells. Alive cells were counted, and the cell number was adjusted to 10^5 cells/ml in PBS and plated in different concentrations on agar plates. For *E. coli*, LB plates and for *S. aureus*, *L. monocytogenes*, GAS and GBS, COS plates were used and incubated overnight at 37°C for enumeration of colony forming units (CFU).

2.3.18 *In vivo* infection with *S. aureus*

Mice were anaesthetized with 100 µl of Xylapan/Narketan in 0.9% NaCl and tape stripped on the shaved back with Tegaderm 3M patches 4 times to irritate the epidermal layer of the skin. A patch (1x1 cm) soaked with 10^7 CFU of *S. aureus* in PBS was applied dorsally and sealed with air- but not water-permeable Tegaderm 3M tape. Control mice were treated with a patch soaked with PBS. On day 4, the mice were dissected and skin-draining brachial LN were taken for FACS analysis. The infected skin was split into three parts to investigate bacterial burden, for RNA isolation and for histological examinations. For enumeration of CFU of *S. aureus*, skin was mechanically homogenized with an ULTRA-TURRAX disperser, diluted and plated in different concentrations on COS plates for 37°C incubation overnight. For histology, skin samples were embedded in cryo medium and cut into 12 µm thick slices at a temperature of -20°C using a cryostat microtome. After acetone fixation, tissue sections were stained with hematoxylin&eosin (H&E) for analysis of epidermal thickening after *S. aureus* infection.

2.3.19 H&E staining

H&E staining of tissue slides allows the differentiation between tissue structures and the precise examination of the tissue morphology. Therefore, it is a widely used diagnostic tool for detection of pathologic structures and alterations of tissues. Hemalum, a mixture of hematoxylin and alum, stains the nuclei of the cells, whereas eosin stains eosinophilic structures, such as the cytoplasm. Tissue sections of *S. aureus*-infected skin and uninfected skin were stained using following protocol:

- 2 min rehydration in ddH_20
- 3-10 min hematoxylin
- Rinse in tap water
- 5 sec 1% HCl/ 70% ethanol
- Rinse again in tap water and blue at least for 10 min
- 30 sec alcoholic eosin
- 2x 3 min 70% EtOH
- 5 sec 95% EtOH
- 2x 5 sec 100% EtOH
- 5 min xylole
- Mount with Euparal (Roth, Karlsruhe)

2.3.20 *In vivo* infection with *L. monocytogenes*

Mice are almost resistant to oral infection with *L. monocytogenes*, as only few bacteria are able to cross the intestinal barrier due to an amino acid change in the murine E-cadherin receptor, which prevents binding to Listeria InlA and thus the entry of Listeria to the cytosol of non-phagocytosing cells [41]. Therefore, 200 µl PBS containing 10^4 CFU of *L. monocytogenes* were administered intravenously and mice were analyzed 2 or 4 days after infection. In this model, the bacteria mainly invade liver and spleen, where they induce apoptosis in T lymphocytes. To enumerate bacterial burden, the liver, as well as half of the spleen, were homogenized with an ULTRA-TURRAX disperser and the suspension was diluted in different concentrations and plated on COS plates for 37°C incubation overnight. The other half of the spleen was weighed and a single cell suspension in PBS was generated with a microstrainer for FACS analysis.

2.3.21 *In vivo* infection with *C. rodentium*

Mice were infected orally by use of a gavage needle with 200 µl PBS containing 10^7-10^{14} CFU of *C. rodentium* (kanamycin-resistant) to induce an infection of the gastrointestinal tract. Mice were monitored by regular controls of body weight. Stool samples were controlled regularly for CFU of *C. rodentium*. Clearance of bacteria, usually took 30 to 40 days. The stool was homogenized in PBS and plated on LB plates containing kanamycin.

2.3.22 Statistical analysis

Statistical analysis of the data was performed using the Student's *t* test. All data are presented as mean ± SEM. p-values < 0.05 were depicted as (*) or (#), p< 0.01 as (**) or (##), and p< 0,001 as (***) or (###) as indicated in the figure legends.

3 RESULTS

3.1 Analysis of HIF1α deletion in DC

3.1.1 Cloning of a DNA probe to target the HIF1α gene

To determine the specific deletion efficiency of the Cre-recombinase in cells from cHIF1α^{CCL17} and cHIF1α^{CD11c} mice, a specific DNA probe (Figure 2.1) was generated to target a sequence of the HIF1α gene containing the loxP sites and exon 2. To identify the precise position of the loxP sites in the floxed allele, a 1.6 kb fragment was amplified. By sequencing of the PCR product, it was possible to locate the exon 2, which encodes the DNA binding helix-loop-helix motif, and the loxP sites on the gene. For efficient discrimination between HIF1α-deleted and HIF1α-undeleted fragments, I screened for restriction sites in the sequenced PCR product. EcoRI and PstI were chosen, as digestion of murine genomic DNA with these restriction enzymes produced a DNA fragment of 2.1 kb on the floxed allele and a 1.5 kb fragment after Cre-mediated excision (Figure 3.1). To target the locus, a 227 bp probe for southern blot was designed. This DNA fragment was amplified by PCR and ligated into the pGEM T easy Vector and transformed into DH5α *E. coli*. The plasmid containing the probe was amplified by bacterial replication, purified and the probe was excised from the vector for further use.

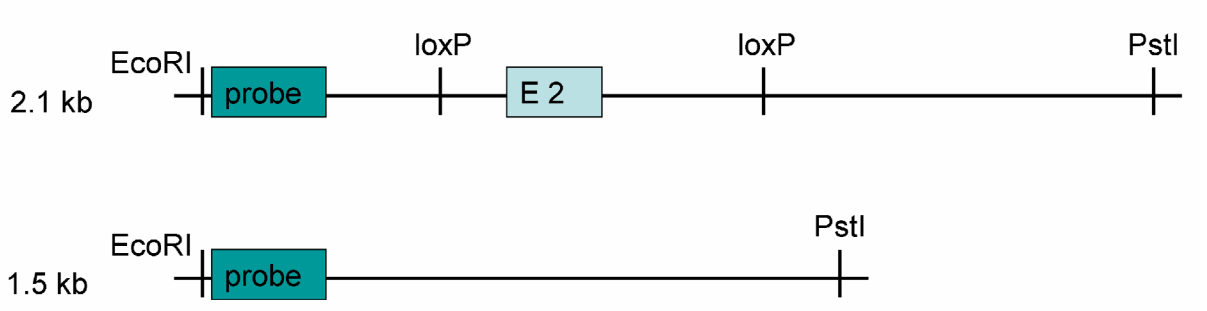

Figure 3.1 Strategic approach for detection of Cre-mediated excision. The probe was generated to bind with high affinity to a 2.1 kb strand on the floxed allele of HIF1α. After Cre-mediated excision of a 0.6 kb fragment, the probe detects a 1.5 kb fragment.

3.1.2 Conditional deletion of HIF1α in DC

To analyze the role of HIF1α in DC, two mouse models with a specific conditional deletion for HIF1α were established. By crossing HIF1α^{flox} mice [72] to CCL17Cre mice, deletion of HIF1α in all cells expressing the chemokine CCL17 was achieved. This chemokine is almost exclusively produced by DC located in peripheral organs. To generate the CCL17Cre strain, the Cre-recombinase was inserted into the second exon of the *ccl17* gene (Figure 3.2A). To extend the deletion of HIF1α to all DC of the organism including pDC and various organ-specific subsets of cDC, HIF1α^{flox} mice were crossed to CD11cCre mice. For determination of the deletion efficiency of Cre-recombination in either mouse strain, a specific probe, which binds to a specific fragment of the *HIF1*α gene was used (see above and Figure 3.1) for southern blot analysis. In whole BMDC cultures, which usually contain 70% DC, I detected a deletion of 40% in cells derived from cHIF1α^{CCL17} mice and 73% deletion in cells from cHIF1α^{CD11c} mice. After MACS purification of DC from cHIF1α^{CD11c} BMDC cultures, I was able to show that in pure DC there is almost a complete deletion of the functional *HIF1*α gene with a Cre-recombinase efficiency of 93% in DC from cHIF1α^{CD11c} mice. FACS sorting of cHIF1α^{CCL17} BMDC expressing eGFP under the control of *ccl17* even revealed a deletion efficiency of 95%.

Unexpectedly, Cre-mediated deletion of HIF1α was also detected in 30% of MACS purified T cells from cHIF1α^{CD11c} spleen, whereas there was no deletion detectable in T cells of HIF1α^{flox} and cHIF1α^{CCL17} mice (Figure 3.2B). Certain subsets of CD8 T cells, which were brought into association with specific regulatory functions, have been reported to be positive for CD11c [87]. To further analyze Cre-induced recombination in T cells of CD11cCre mice, the CD11cCre line was bred to RA/EG mice [85]. This EGFP reporter line can be used to monitor Cre-mediated deletion and the deletion efficiency in different cell types. When crossing Cre-expressing mice to RA/EG mice, Cre induces excision of intervening genomic sequences. Thereby, the TK promoter moves directly in front of an EGFP cassette, which allows expression of EGFP [85]. Employment of RA/EG mice revealed that Cre-mediated deletion in CD11cCre mice affects both, CD4$^+$ and CD8$^+$ T cells, to a large extent (Figure 3.2C). From this analysis, it can be concluded that both knockout lines are suitable to study the role of HIF1α in BMDC. In *in vivo* studies, it has to be considered, however, that there is a deletion of HIF1α not only in DC, but also in a substantial proportion of T cells.

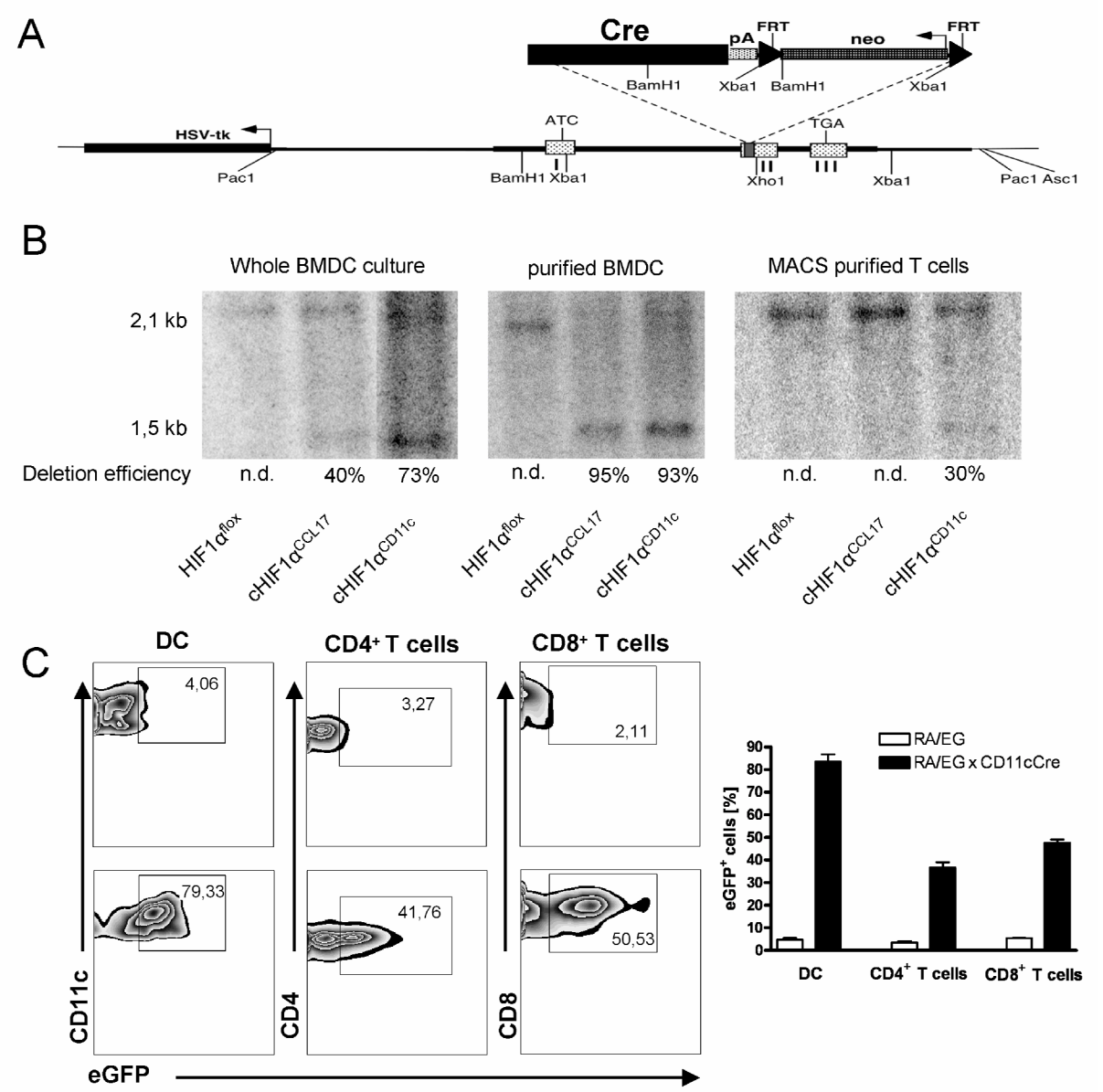

Figure 3.2 Conditional knockout of HIF1α. A Targeting strategy for integration of Cre in the second exon of the ccl17 gene. **B** Efficiency of HIF1α deletion was tested by Southern blot. A ^{32}P-labeled HIF1α probe was hybridized to DNA from whole BMDC cultures, as well as to FACS sorted CCL17-positive cells from BMDC of CCL17/EGFP reporter [79] x cHIF1α^{CCL17} mice, and MACS purified CD11c-positive cells from cHIF1α^{CD11c} BMDC. MACS sorted CD3-positive T cells were also analyzed for HIF1α deletion. Fragments with the size of 2.1 kb represent intact HIF1α, whereas the 1.5 kb band indicates Cre-mediated deletion. Data are representative of 2 or 3 experiments, except for analysis of FACS-sorted cells, which was only conducted once. **C** FACS analysis of spleen cells from RA/EG and RA/EG x CD11cCre mice. DC were identified as CD11c^{hi} MHCII^{+} cells and for analysis of T cells gates were set on CD3^{+} CD4^{+} or CD3^{+} CD8^{+} cells. The bar graph on the right depicts mean values +SEM of two RA/EG and four RA/EG x CD11cCre mice.

3.2 Analysis of BMDC generated in a hypoxic milieu

3.2.1 Hypoxia leads to reduced cell growth and enhanced maturation

To study the effects of hypoxia on wild-type DC and on HIF1α-deficient DC, primary cells were taken from the bone marrow of HIF1α^{flox}, cHIF1α^{CCL17} and cHIF1α^{CD11c} mice and differentiated into BMDC by stimulation with GM-CSF. For generation of normoxic and hypoxic BMDC, primary bone marrow cells were cultured for 6 days either in 21% oxygen or in a hypoxic incubator containing 1% oxygen. Counting of total cells after 6 days revealed a statistically significant decrease of cells of all three mouse strains grown under hypoxic conditions compared to normoxia (Figure 3.3A). This effect might be due to reduced cell proliferation and/or survival resulting from changes in cell metabolism and function due to the lack of oxygen. Deficiency of HIF1α led to further growth retardation under oxygen deprived conditions (Figure 3.3A). Interestingly, whereas in normoxia around 65% of total cells in the culture were positive for CD11c, up to 75% CD11c-positive cells in hypoxic cultures of HIF1α^{flox} bone marrow could be detected. This increase was not observed in cells derived from cHIF1α^{CCL17} and cHIF1α^{CD11c} bone marrow (Figure 3.3A). The growth retardation, as well as the inhibition of CD11c upregulation in HIF1α-deficient BMDC under hypoxic conditions, can, at least in part, be explained by failure of these cells to maintain their energy metabolism and ATP production in hypoxia (Figure 3.3B). The ecto-nucleotidase CD73, which cleaves extracellular ATP to adenosine, is a known target of HIF1α [88]. It was found to be expressed at low levels on the surface of BMDC and was upregulated in hypoxia in a HIF1α-dependent manner. FACS analysis showed an increase of the mean fluorescence intensity (MFI) after hypoxic treatment only in HIF1α^{flox} cells (Figure 3.3C). To evaluate the differention status of the BMDC generated under normoxic or hypoxic conditions, maturation markers on the cell surface were analyzed by FACS. MHCII and the costimulatory molecule CD86 were strongly upregulated, whereas expression of CD80 was only slightly increased on BMDC grown in the hypoxic incubator (Figure 3.3D). These data show that conditions of low oxygen remarkably enhance the maturation of BMDC in a HIF1α-independent manner, whereas the production of ATP and the upregulation of CD73 were inhibited in hypoxic HIF1α-deficient BMDC.

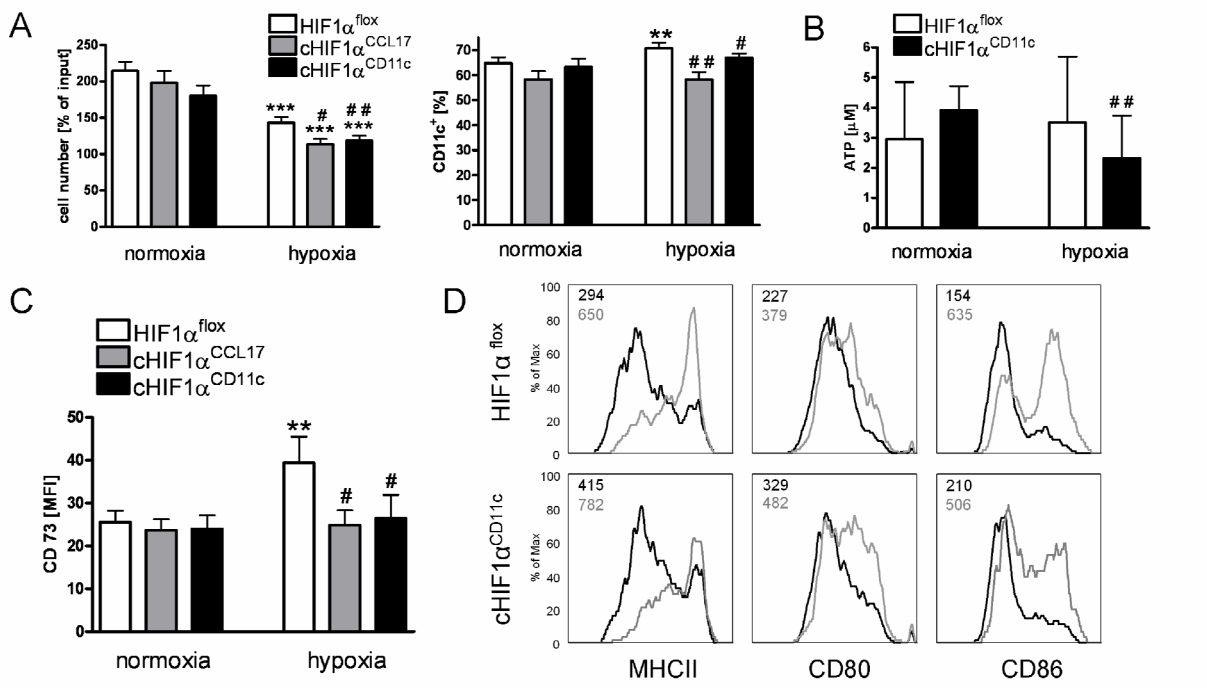

Figure 3.3 Reduced growth and enhanced maturation of BMDC under hypoxia. BMDC of HIF1α^{flox}, cHIF1α^{CCL17}and cHIF1α^{CD11c} mice were cultured with GM-CSF at 21% or 1% O_2. **A** On day 6, cells were counted and the % increase over input cells was calculated. The percentage of DC in BM cultures was assessed by CD11c staining. Results are depicted as mean +SEM of at least 15 independent experiments, (n = 11-51). **B** Intracellular ATP was measured after cell lysis using a luciferase-based assay. Results are depicted as mean +SEM of at least 9 independent experiments, (n = 9). **C** MFI of CD73 staining on gated CD11c-positive BMDC grown under normoxic or hypoxic conditions. Results are depicted as mean +SEM of at least 10 independent experiments, (n = 10-15). **D** Hypoxic BMDC (gray lines) and normoxic BMDC (black lines) were analyzed by FACS. Histograms depict expression of MHCII, CD80 and CD86 on gated CD11c-positive BMDC. Numbers in the histograms indicate the MFI. Results are representative data of at least three independent experiments. *, $p < 0.05$; **, $p < 0.01$; ***, $p < 0.001$, hypoxic versus normoxic cells. #, $p < 0.05$; ##, $p < 0.01$; ###, $p < 0.001$, HIF1α-deficient BMDC versus HIF1α^{flox} controls.

3.2.2 Altered production of cytokines in hypoxia

Communication between cells may take place via cell-cell contacts or via secretion of soluble messengers such as cytokines, which can induce differentiation of cells and are able to change their behavior [13]. Therefore, the ability of HIF1α-proficient and HIF1α-deficient BMDC to produce cytokines in a normoxic or hypoxic environment was tested. Interestingly, secretion of the proinflammatory cytokines IL-12p70 and IL-6 and the anti-inflammatory cytokine IL-10 was significantly reduced in hypoxia compared with normoxia in cells of all three mouse strains, whereas the proinflammatory cytokine IL-23 was only marginally suppressed. TNFα and IL-1β were detected in lower amounts, only in the supernatants of hypoxic HIF1α^{flox} and hypoxic cHIF1α^{CD11c} BMDC, but not in cHIF1α^{CCL17} BMDC (Figure 3.4A). Though IL-22 is known to be mainly made by T cells [89], one publication has reported the IL-

23-dependent production of IL-22 in BMDC [55]. Therefore, I also analyzed the expression of IL-22 in normoxic and hypoxic BMDC. Surprisingly, IL-22 could be detected in supernatants of HIF1α^{flox} BMDC generated in 1% oxygen. This effect seems to be, at least in part, mediated by HIF1α, as the ability of BMDC to produce large amounts of IL-22 under hypoxia negatively correlated with the efficiency of HIF1α-deletion in cHIF1α^{CCL17} versus cHIF1α^{CD11c} mice (Figure 3.4A). Since IL-12 and IL-23 are structurally related cytokines, the regulation of the common subunit p40 in hypoxia was investigated. Intracellular IL-12p40 cytokine staining was conducted and measured by FACS analysis. BMDC, which had only been incubated with an antibody against CD11c, but not against IL-12p40, served as negative control. The reduced expression of IL-12p40 in hypoxia was confirmed. This effect appears to be dependent on HIF1α, as cHIF1α^{CD11c} BMDC showed only a marginal reduction of IL-12p40 expression under hypoxic conditions (Figure 3.4B left and right). In line with these results, also BMDC from cHIF1α^{CCL17} mice showed a slight reduction of IL-12p40 in hypoxia (Figure 3.4B right). p40 heterodimerizes with IL-12p35 to the biologically active IL-12p70, whereas IL-23 represents a heterodimer of p40 and p19. The mRNA levels of p40, p35 and p19 were examined by quantitative Real-Time PCR in HIF1α^{flox} and cHIF1α^{CD11c} BMDC (Figure 3.4C). The expression of p40 mRNA was unaltered in cHIF1α^{CD11c} BMDC compared with controls. The expression of p35, however, was reduced in BMDC from both mouse strains generated in hypoxic conditions, which correlates with the reduced production of IL-12p70 protein. In contrast to IL-23 protein, the expression of IL-23p19 mRNA was strongly enhanced under hypoxic conditions (Figure 3.4C). Taken together, the investigations on cytokine expression by BMDC in an oxygen-deprived environment revealed the inhibition of a wide range of cytokines in hypoxia, which was not due to a general shutdown of protein secretion, as evident by the induction of IL-22 under hypoxic conditions. I could show for the first time that IL-22 production is enhanced in hypoxic BMDC, which was, to a large part, dependent on HIF1α.

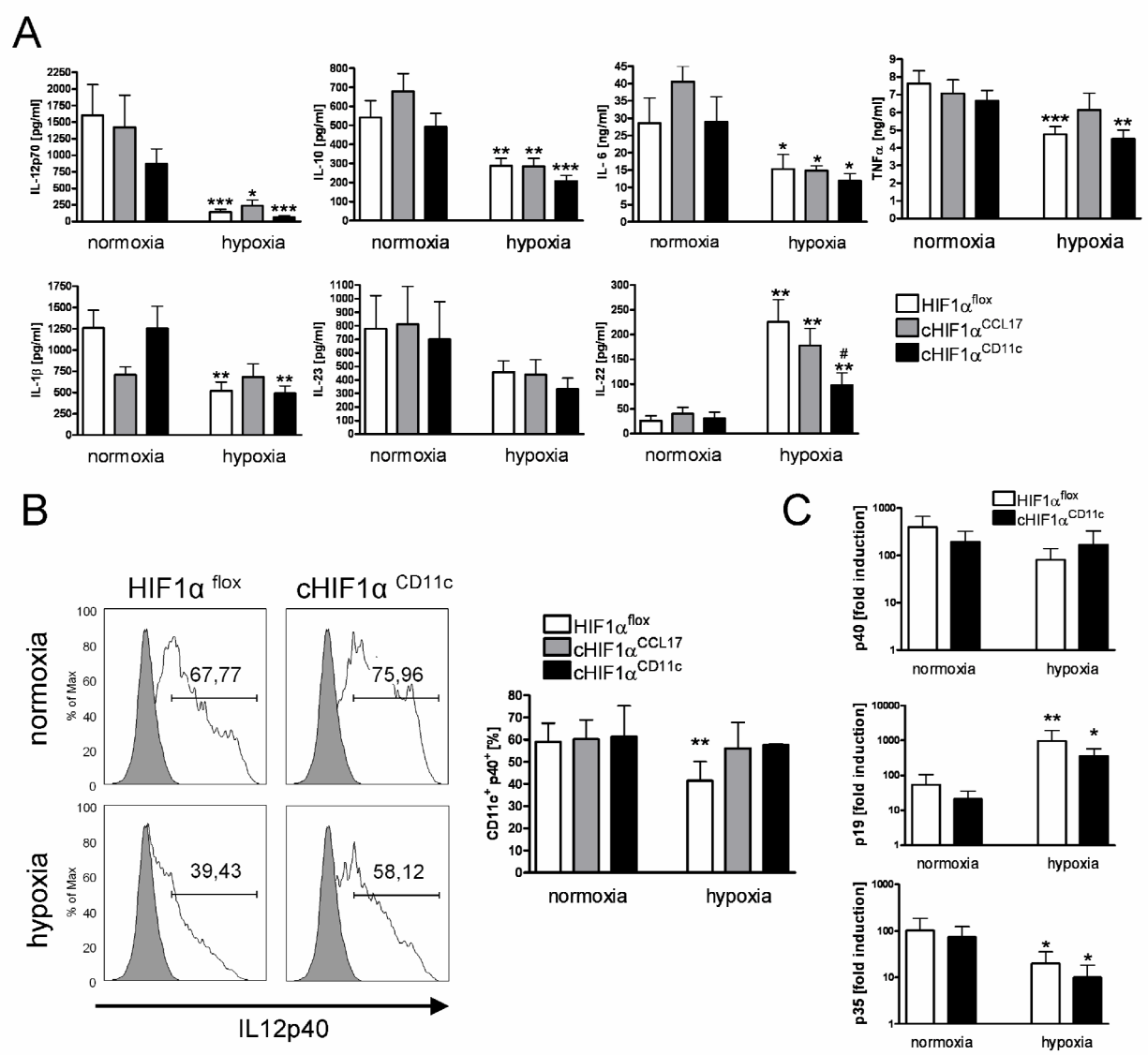

Figure 3.4 Altered production of cytokines in hypoxia. BMDC of HIF1α^{flox}, cHIF1α^{CCL17} and cHIF1α^{CD11c} mice were cultured with GM-CSF at 21% or 1% O_2. **A** and **B** On day 6, BMDC were stimulated with LPS for 16-20 h. **A** Cytokine concentrations in culture supernatants were measured by ELISA. Results are depicted as mean +SEM of at least 4 independent experiments, (n = 4-24). **B** Intracellular cytokine staining for IL-12p40 on gated CD11c-positive BMDC. The proportion of IL-12p40-positive cells was determined in comparison to the negative control (gray shaded histogram) as indicated. To generate a negative control, BMDC were stained only for CD11c. FACS plots shown are representative data of at least 6 independent experiments. Bar graphs depicted on the right show mean values +SEM of all experiments performed, (n = 2-6). **C** RNA was isolated 3 h after LPS stimulation and expression of p40, p19, and p35 was determined by relative quantification. Expression levels of unstimulated normoxic HIF1α^{flox} cells were set to 1. Results are depicted as mean + SEM of at least 3 independent experiments, (n = 4-6). *, $p < 0.05$; **, $p < 0.01$; ***, $p < 0.001$ hypoxic versus normoxic cells. #, $p < 0.05$; ##, $p < 0.01$; ###, $p < 0.001$, HIF1α-deficient BMDC versus HIF1α^{flox} controls.

3.2.3 Regulation of chemokines and chemokine receptors under hypoxic conditions

Immune cells are known to precisely orchestrate their expression of chemokine receptors and their production of chemokines depending on cell type, location and

environmental conditions, such as inflammation or oxygen deprivation [90-92]. After receipt of danger signals or microbial stimuli, peripheral DC upregulate their chemokine receptors CCR7 and CXCR4 on their surface for migration from inflammatory sites to the draining LN [11, 93]. To investigate, if hypoxia and deficiency of HIF1α alter the expression of CCR7, CXCR4 and CCR5 on BMDC, FACS analysis was performed using isotypes as negative controls for each staining (Figure 3.5A left). Bar graphs summarize all experiments conducted (Figure 3.5A right). Expression of CCR7 was clearly enhanced, when cells were grown under hypoxic conditions compared with normoxic cells. This upregulation was not detectable in HIF1α-deficient BMDC. Only marginal amounts of CXCR4 were detectable in normoxia, whereas there was a slight increase of this chemokine receptor on hypoxic HIF1α^{flox} BMDC, which was not found on HIF1α-deficient BMDC. CCR5, which is involved in the recruitment of immature DC from the blood to inflamed tissues, was barely detectable and not significantly altered by hypoxia or by deletion of HIF1α (Figure 3.5A). It was shown recently that the chemokine CCL17 is indispensable for emigration of cutaneous DC from the skin to the draining LN [10], which could be also influenced by hypoxia. Therefore, I analyzed the impact of hypoxia on CCL17 secretion of BMDC and the closely related chemokine CCL22, which are both ligands for CCR4. In either case, hypoxia led to a statistically significant increase of cytokine expression independent of HIF1α (Figure 3.5B). Of note, the production of CCL17 in cHIF1α^{CCL17} BMDC was generally reduced compared with control BMDC, because integration of the Cre transgene led to heterozygosity of the *ccl17* gene and thus to a gene dosage effect for the production of CCL17 [10]. These results prove that conditions of low oxygen clearly influence the secretion of chemokines and chemokine receptor expression. Changes in expression of CCR7 and CXCR4, as well as of CCL17 and CCL22 might influence the migration of peripheral DC to the LN. However, CCR5 expression was not affected by hypoxia.

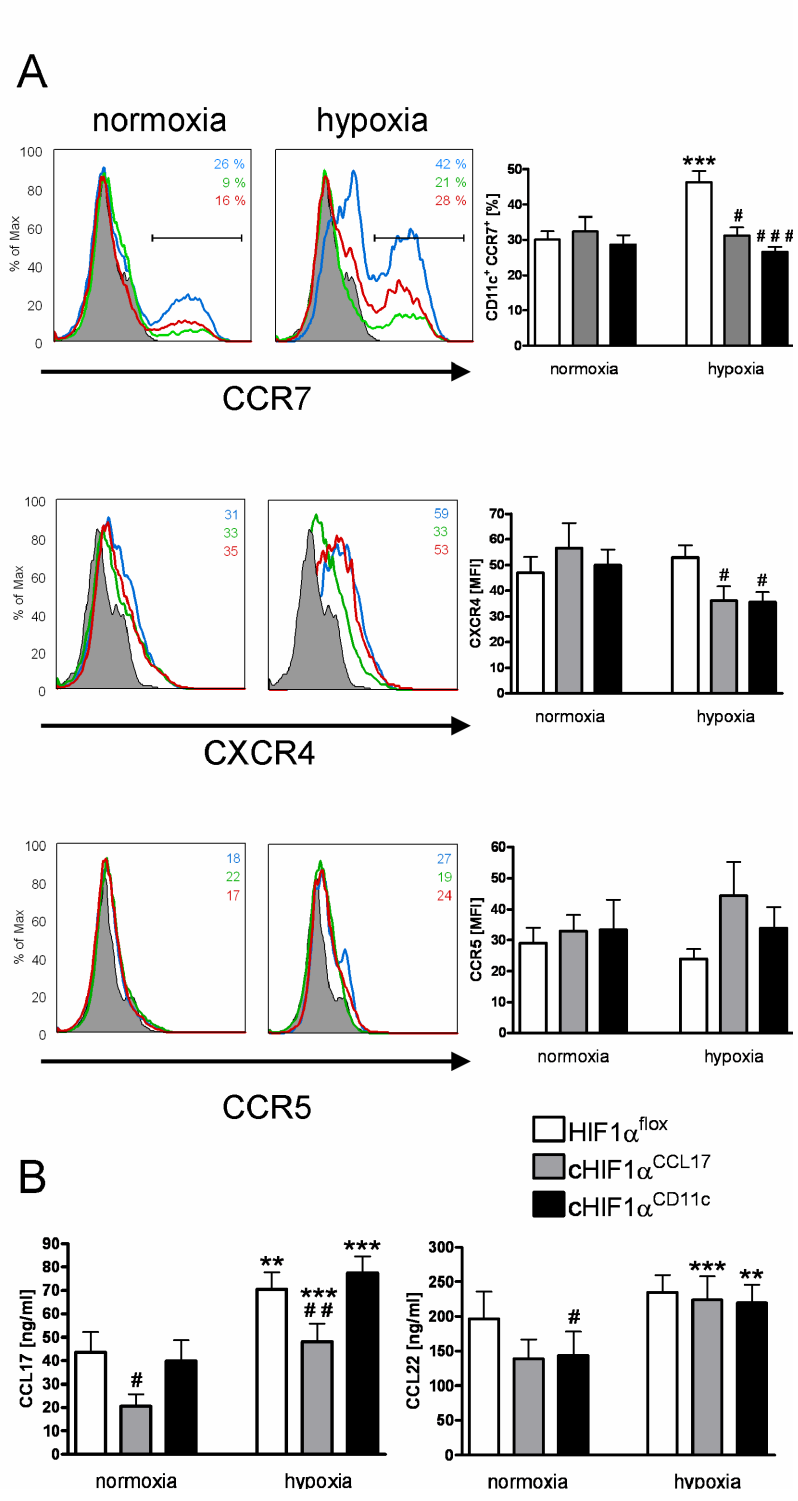

Figure 3.5 Regulation of chemokines and chemokine receptors under hypoxic conditions. BMDC of HIF1α^{flox}, cHIF1α^{CCL17} and cHIF1α^{CD11c} mice were cultured with GM-CSF at 21% or 1% O_2. **A** Gated CD11c-positive cells were stained with anti-CCR7, anti-CXCR4 or anti-CCR5. cHIF1α^{CD11c} BMDC (red lines) and cHIF1α^{CCL17}BMDC (green lines) were compared with HIF1α^{flox} BMDC (blue lines). The numbers in the representative histograms indicate percentage of CCR7-positive cells (upper panel), or the MFI of the CXCR4- and CCR5-staining (middle and lower panel). The isotype control staining is shown as a gray shaded histogram. Bar graphs on the right depict mean +SEM of at least 3 independent experiments, (n = 4-12). **B** Supernatants of LPS-stimulated cultures were tested for the presence of CCL17 and CCL22 by ELISA. Results are depicted as mean +SEM of at least 9 independent experiments, (n = 9-14). *, $p < 0.05$; **, $p < 0.01$; ***, $p < 0.001$ hypoxic versus normoxic cells. #, $p < 0.05$; ##, $p < 0.01$; ###, $p < 0.001$, HIF1α-deficient BMDC versus HIF1α^{flox} controls.

3.2.4 Hypoxia leads to increased migration of BMDC to CCL19 in a HIF1α-dependent manner

To further investigate the migratory behavior of DC, transwell experiments were conducted to evaluate the capacity of BMDC to migrate towards a chemokine gradient under normoxic versus hypoxic conditions in the absence or presence of HIF1α. In line with the results obtained from the surface expression studies of CCR7, BMDC showed enhanced migration towards CCL19 in hypoxia, which was dependent on HIF1α. Migration towards CXCL12, which binds to CXCR4, was neither affected by low oxygen pressure nor by presence or absence of HIF1α in BMDC (Figure 3.6A). To confirm the results obtained from *in vitro* experiments, *in vivo* studies were performed. 1:1 mixtures of differentially labelled BMDC were injected into footpads of mice. To compare the ability to migrate between normoxic and hypoxic HIF1α^{flox} BMDC, for example, normoxic cells were labeled with CMFDA, which emits green fluorescence, whereas hypoxic cells were labeled with CMTMR emitting red fluorescence (Figure 3.6C). These cells were mixed in equal amounts and injected into the footpads of C57BL/6 mice. In independent experiments, groups of BMDC to be compared were labeled with one or the other fluorescent marker to exclude dye-specific influences. After 24 hours, immigration into draining LN was analyzed by flow cytometry and the relative proportions of red or green labeled BMDC, which had reached the popliteal LN, were calculated (Figure 3.6B and C). HIF1α^{flox} and HIF1α-deficient BMDC grown in 21% oxygen migrated equally well to the draining LN (Figure 3.6B, upper panel left), whereas co-injection of HIF1α-deficient and HIF1α^{flox} BMDC generated under hypoxic conditions revealed a significantly reduced migration of cHIF1α^{CD11c} BMDC (Figure 3.6B, upper panel right). When comparing hypoxic HIF1α^{flox} BMDC with normoxic HIF1α^{flox} BMDC, a more than threefold increase of the migratory capacity could be detected, when cells were raised in an oxygen-low environment (Figure 3.6B, lower panel left). This effect was dependent on HIF1α, since this enhanced migration was not observed, when normoxic cHIF1α^{CD11c} BMDC were compared to hypoxic counterparts (Figure 3.6B, lower panel right). Thus, HIF1α appears to be required for the hypoxia-induced enhancement of the migratory capacity of BMDC towards CCL19 *in vitro* and *in vivo*.

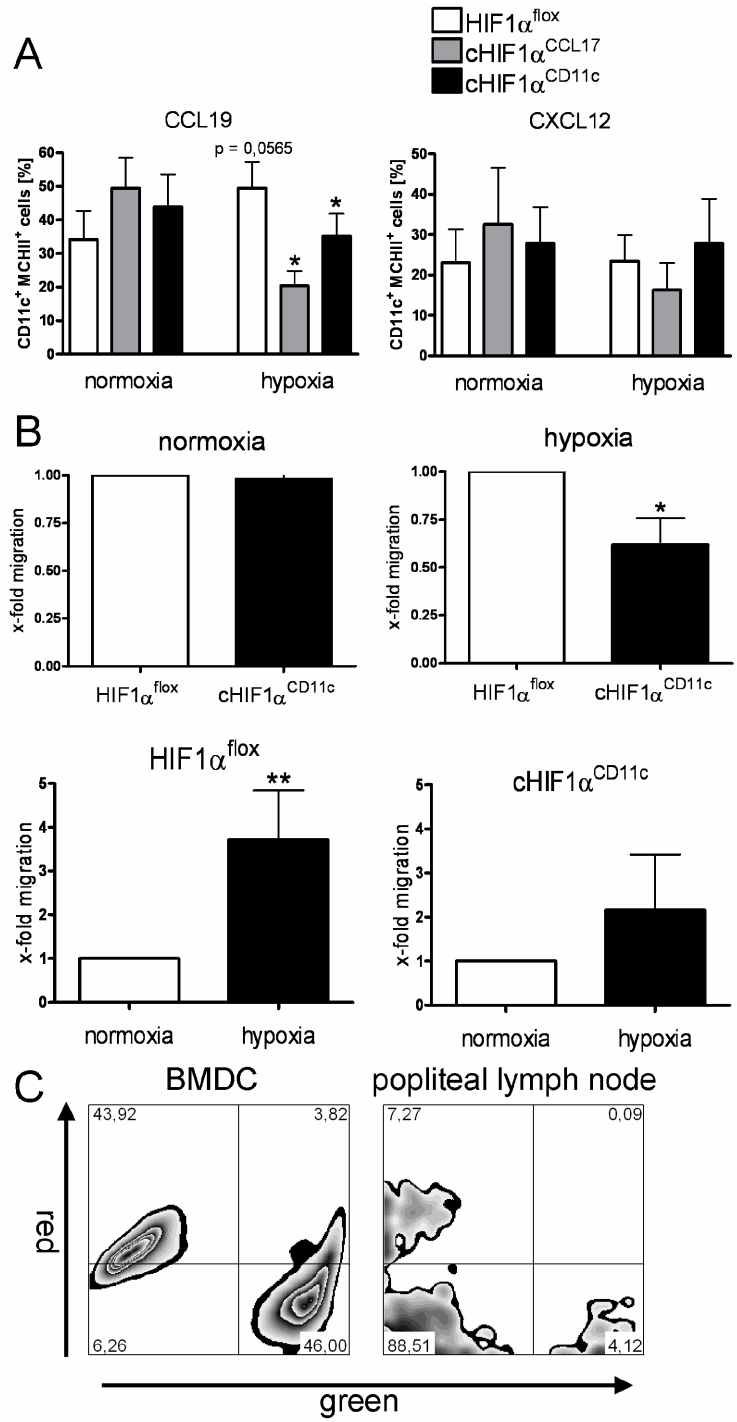

Figure 3.6 Enhanced migration of hypoxic BMDC is HIF1α-dependent. BMDC of HIF1α^{flox}, cHIF1α^{CCL17} and cHIF1α^{CD11c} mice were cultured with GM-CSF at 21% or 1% O_2. **A** Migration of BMDC towards the chemokines CCL19 and CXCL12 was examined in transwell chamber assays. Migrated cells were counted and stained with anti-CD11c and anti-MHCII to calculate the percentage of migrated DC. Results are depicted as mean +SEM of at least 3 independent experiments, (n = 3-6). **B** CMFDA-labeled (green) and CMTMR-labeled (red) BMDC were mixed in equal proportions and injected in the footpad. After 24 h, proportions of differentially labeled CD11c-positive BMDC in popliteal LN were analyzed by flow cytometry as indicated in **C** and the ratio of migrated HIF1α^{flox} BMDC (set to 1) compared to cHIF1α^{CD11c} BMDC was determined for cells grown either under normoxic (left, top) or under hypoxic conditions (left, bottom). In addition, the ratio of migrated normoxic BMDC (set to 1) compared to hypoxic BMDC was determined for HIF1α^{flox} BMDC (right, top), or for cHIF1α^{CD11c} BMDC (right, bottom). Results are depicted as mean +SEM of at least 5 independent experiments, (n = 5-7). *, $p < 0.05$; **, $p < 0.01$; ***, $p < 0.001$, HIF1α-deficient BMDC versus HIF1α^{flox} controls (**A** and **B** right, top) or hypoxic versus normoxic cells (**B** left, bottom).

3.2.5 Loss of HIF1α in cutaneous DC does not affect emigration from epidermis

After analysis of the migratory capacity of *in vitro* generated BMDC, the role of HIF1α in skin-resident DC was investigated. Therefore, 4 different assays were performed to test, if HIF1α has an influence on migration of DC to LN *in vivo*. In a cytotoxic T lymphocyte (CTL) assay, mice were subcutaneously immunized with OVA/CpG. In a similar model, activated CCL17-positive DC migrate after i.v. or intraperitoneal immunization to the draining LN to attract naive CTL for cross-priming via MHCI [94]. After 7 days, priming was measured by challenge with a 1:1 mixture of SIINFEKL (OVA peptide)-loaded and unloaded spleen cells, which were labeled differentially with the fluorescent dyes CMFDA and CMTMR. Specific killing of SIINFEKL-loaded cells was measured by FACS analysis and calculation of the proportions of the differentially labeled cells. No differences in induction of CTL, possibly mediated by equal migration and priming of DC from HIF1α^{flox}, cHIF1α^{CCL17} and cHIF1α^{CD11c} mice were detected (Figure 3.7A). Additionally, a model of contact hypersensitivity (CHS) was chosen, since Langerhans cells from the epidermis initiate an immune reaction against topically applied antigens by emigration to draining LN after epicutaneous stimulation with a contact sensitizer, such as DNFB. On d0, mice were sensitized on the shaved back with either DNFB or the control solution acetone/oil only. 5 days later, mice were challenged with DNFB on both sides of the ears. Control mice were treated identically with acetone/oil solution. Measurement of ear swelling revealed no statistical significant differences between HIF1α^{flox}, cHIF1α^{CCL17} and cHIF1α^{CD11c} mice, which had been sensitized and challenged (Figure 3.7B). These results implicate that the deficiency of HIF1α in DC does not impact the outcome of the CHS reaction. To directly track Langerhans cells after emigration from skin, fluorescein isothiocyanate (FITC) was applied on the shaved back of mice. The fluorescent FITC is taken up by the skin-resident DC and induces migration to skin-draining LN, where immigrated fluorescent Langerhans cells can be detected via FACS analysis. However, Langerhans cells from HIF1α^{flox}, cHIF1α^{CCL17} and cHIF1α^{CD11c} mice possessed the same ability to emigrate from the skin into the brachial LN after uptake of FITC (Figure 3.7C).

A potential concern regarding this experiment was that FITC might not induce an immune reaction strong enough to cause hypoxic conditions in skin. Therefore, the direct emigration of Langerhans cells was analyzed in another model. Here DNFB, which is a strong contact sensitizer, was applied on both sides of the ears of mice to

induce DC activation and emigration from the epidermis. After 4 hours, ears were removed, cultured under normoxic and hypoxic conditions for further 48 hours to allow Langerhans cells to migrate out of the epidermis. Then epidermal sheets were prepared and Langerhans cells were stained for MHCII and counted. As expected, DNFB induced emigration compared with the solvent. This occurred independently of HIF1α. In hypoxia, however, fewer cells could be detected in solvent-treated tissues (Figure 3.7D). To analyze whether this could be due to cell death, a TUNEL stain was conducted revealing that a major number of epidermal cells stained positive for TUNEL under hypoxia and thus had undergone apoptosis. Due to these results, it can be assumed, that hypoxia leads to cell death independently of HIF1α in this experimental setting, probably because the cells in the dense network of the epidermis are not able to adapt to the oxygen-deprived conditions (Figure 3.7E).

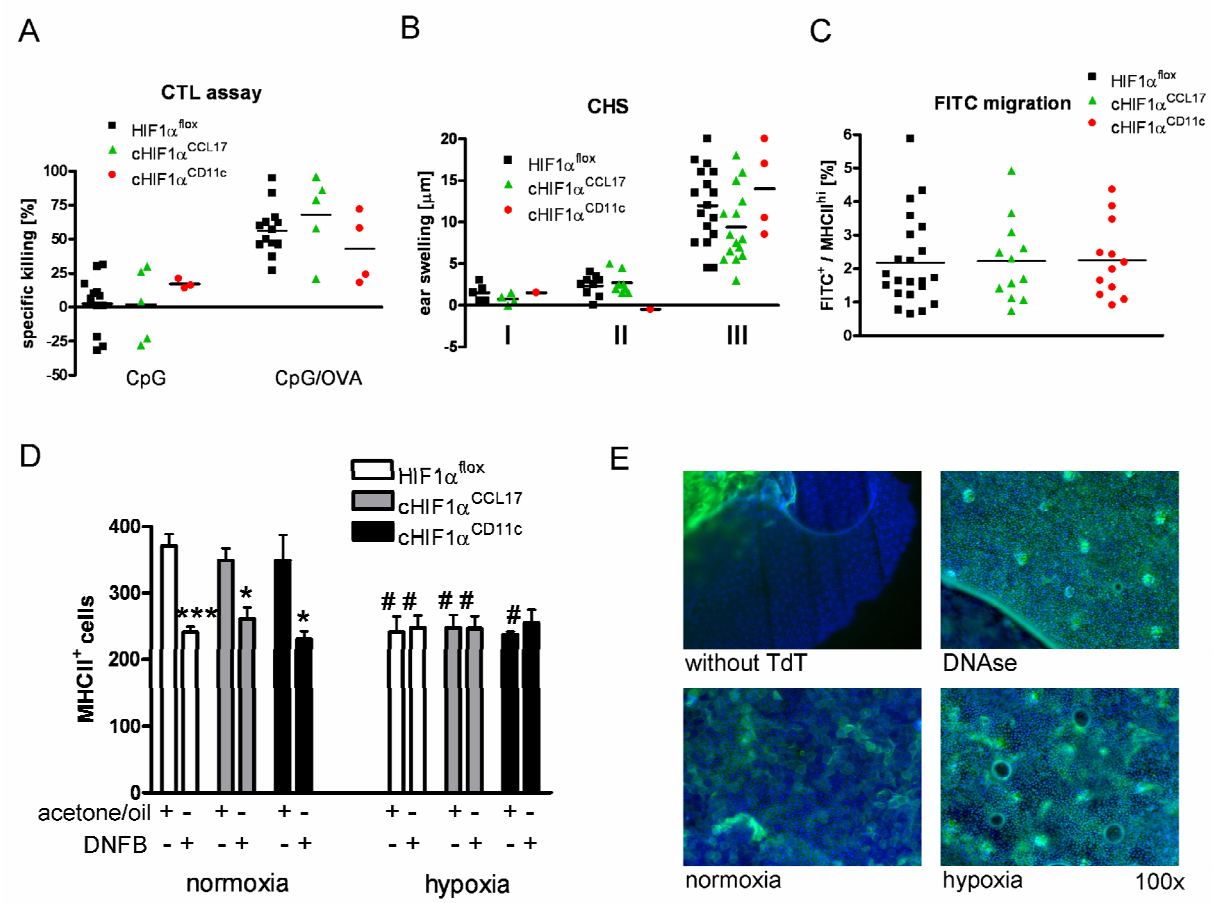

Figure 3.7 Loss of HIF1α in cutaneous DC does not affect emigration from epidermis. A To induce killing of SIINFEKL-loaded cells by cytotoxic T lymphocytes, mice were primed by subcutaneous injection of OVA/CpG. Specific killing was calculated by FACS analysis of previously injected differentially labeled cells from spleen. **B** CHS was induced by topical sensitization with DNFB and ear swelling was measured after DNFB challenge on the ear. Group I neither received priming nor challenge, whereas group II was challenged without previous priming. Group III was primed and challenged. **C** Migration was induced by dorsal FITC application and after 24 hours. Skin-derived DC were identified as $FITC^{+}/MHCII^{hi}$ cells in skin draining brachial LN by FACS analysis. Each dot/symbol represents one mouse and the mean for each group is depicted as a line. **D** Epidermal sheets were prepared and analyzed by counting $MHCII^{+}$ cells in an area of 0,3525 mm^2. *, $p < 0.05$; **, $p < 0.01$; ***, $p < 0.001$ hypoxic versus normoxic cells. #, $p < 0.05$; ##, $p < 0.01$; ###, $p < 0.001$, HIF1α-deficient BMDC versus $HIF1\alpha^{flox}$ controls. **E** Apoptosis induction on epidermal sheets was analyzed by TUNEL stain. A DNAse-treated epidermal sheet served as a positive control for TUNEL stain. The negative control was not treated with terminal deoxynucleotidyl transferase (TdT). Results are depicted as mean +SEM of at least 3 independent experiments, except for the TUNEL stain **(E)**, which was only conducted once.

3.3 Analysis of hypoxic BMMΦ

3.3.1 Upregulation of surface molecules in cHIF1α^{LysM} BMMΦ in hypoxia

To explore the role of HIF1α in MΦ, bone marrow derived macrophages (BMMΦ) were generated from HIF1α^{flox} and cHIF1α^{LysM} mice. The cHIF1α^{LysM} mouse was established by crossing of LysMCre mice with a targeted insertion of Cre in the M lysozyme locus [80] to HIF1αflox mice [72], thereby causing an efficient deletion of HIF1α in all myeloid cells, such as macrophages and granulocytes. Generation of BMMΦ under normoxic versus hypoxic conditions revealed a striking decrease of cell growth under conditions of low oxygen independent of HIF1α (Figure 3.8A). Since hypoxia can lead to growth reduction or reduced survival, ATP production of BMMΦ was investigated. Here, neither hypoxia nor the deletion of HIF1α had an influence on ATP supply (Figure 3.8B). In BMDC, hypoxia caused remarkable upregulation of cell surface maturation markers. Therefore, FACS analysis was performed to characterize hypoxic BMMΦ and to investigate the role of HIF1α concerning the expression of maturation and other surface markers. Interestingly, expression of CD86, a classical costimulatory molecule, was unchanged in hypoxic HIF1α^{flox} BMMΦ compared with normoxic HIF1α^{flox} BMMΦ, whereas cHIF1α^{LysM} BMMΦ revealed strong upregulation of CD86 in hypoxia indicating an activated phenotype (Figure 3.8C). Surprisingly, after stimulation with LPS the same effect was found for the surface expression of F4/80. An increase of F4/80 on the cell surface was only observed in hypoxic BMMΦ from cHIF1α^{LysM} mice (Figure 3.8C). F4/80 is a widely used marker for monocytes and mouse MΦ, belonging to the family of EGF-TM7 receptors, but so far the function of this molecule is still enigmatic [95]. Taken together, HIF1α does neither play a role in regulation of cell growth under hypoxic conditions, nor in ATP production of BMMΦ. However, HIF1α suppressed the upregulation of CD86 and F4/80 expression of HIF1α^{flox} BMMΦ in a low oxygen environment.

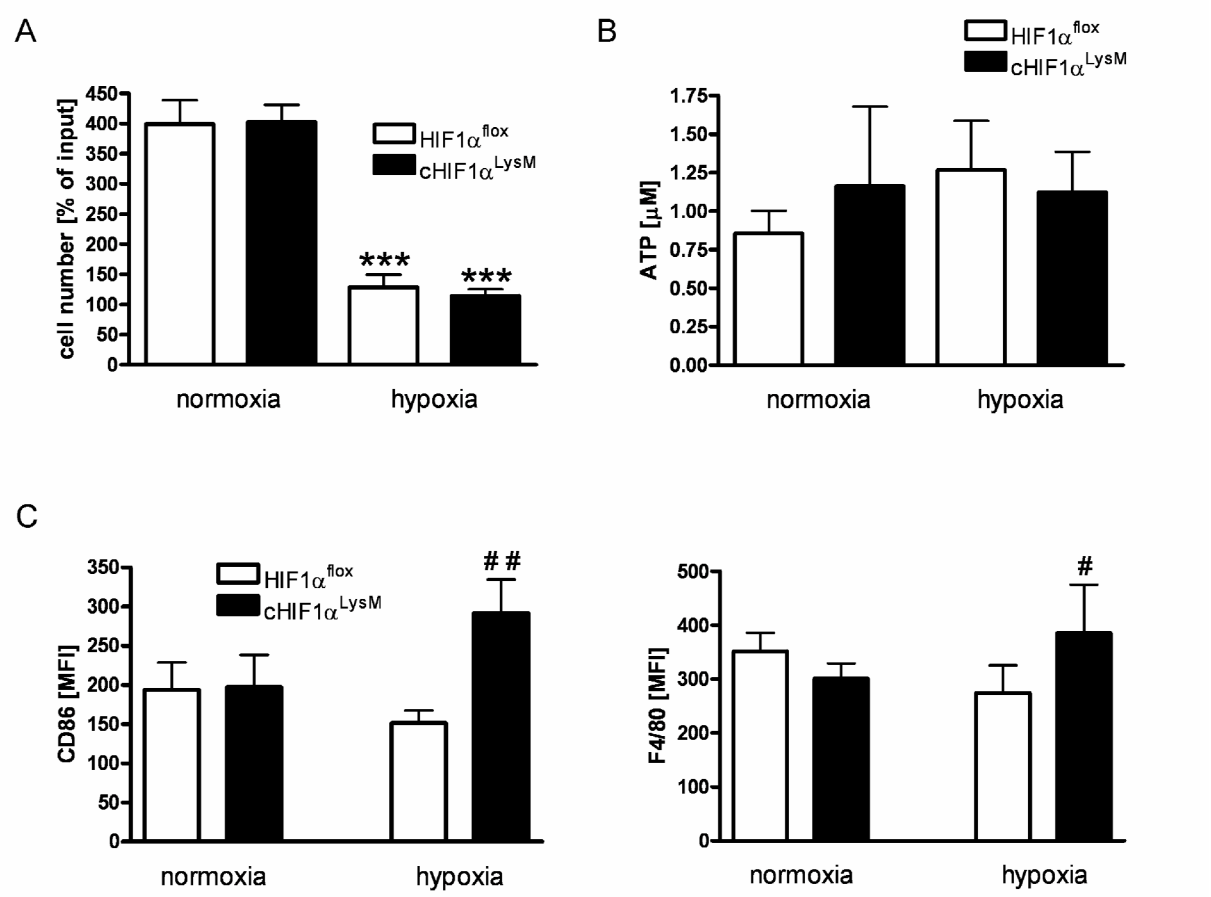

Figure 3.8 Cell growth/survival, ATP production and regulation of surface molecules in BMMΦ in hypoxia. BMMΦ of HIF1α^{flox} and cHIF1α^{LysM} mice were cultured with M-CSF at 21% or 1% O_2. **A** On day 6, cells were counted and the % increase over input cells was calculated. Results are depicted as mean +SEM of at least 6 independent experiments, (n = 11). **B** Intracellular ATP was measured in lysates of BMMΦ using a luciferase-based assay. Results are depicted as mean +SEM of at least 3 independent experiments, (n = 5). **C** MFI of CD86 (left) or F4/80 (right) staining on BMMΦ grown under normoxic or hypoxic conditions. Results are depicted as mean +SEM of at least 5 independent experiments, (n = 9). *, $p < 0.05$; **, $p < 0.01$; ***, $p < 0.001$, hypoxic versus normoxic cells. #, $p < 0.05$; ##, $p < 0.01$; ###, $p < 0.001$, HIF1α-deficient BMMΦ versus HIF1α^{flox} controls.

3.3.2 Cytokine expression of BMMΦ

Communication of MΦ with other immune but also with non-immune cells is, to a large part, orchestrated by recognition and secretion of cytokines. As these processes might be critically influenced by the tissue oxygen content, the secretion of cytokines was measured in cell culture supernatants of LPS stimulated BMMΦ. Comparison of the secretion of the pro-inflammatory cytokines IL-12p70 and TNFα revealed no differential regulation between normoxic and hypoxic HIF1α^{flox} BMMΦ. Astonishingly, cHIF1α^{LysM} BMMΦ, which have been grown under hypoxic conditions, showed enhanced levels of IL-12p70 and TNFα compared with normoxic cHIF1α^{LysM} BMMΦ and also compared with hypoxic

HIF1α^{flox} BMMΦ (Figure 3.9). IL-10 is one of the most important anti-inflammatory cytokines and LPS-induced IL-10 production of BMMΦ was affected by both, hypoxia and HIF1α-deficiency. BMMΦ, which had been generated in an oxygen low environment, produced significantly lower amounts of IL-10 than normoxic BMMΦ. Comparison of cHIF1α^{LysM} with HIF1α^{flox} BMMΦ displayed an additional reduction of IL-10 secretion in BMMΦ from cHIF1α^{LysM} mice, not only in hypoxia, but also under normoxic conditions (Figure 3.9). Interestingly, levels of IL-12p70 in general were much lower, whereas the levels of IL-10 were much higher compared to BMDC.
However, since expression of IL-23 was only detected in hypoxic HIF1α-deficient BMMΦ, I assume that HIF1α suppressed IL-23 production in hypoxic HIF1α-proficient BMMΦ. Compared with LPS-stimulated BMDC, which were shown to produce high levels of IL-22 under hypoxic conditions in a HIF1α-dependent manner, BMMΦ produce very low amounts of IL-22. Nevertheless, the production of this cytokine, which is implicated to play a relevant role in the course of infection [55, 96] was three- to sixfold higher, when BMMΦ were grown in an oxygen-deprived surrounding (Figure 3.9).

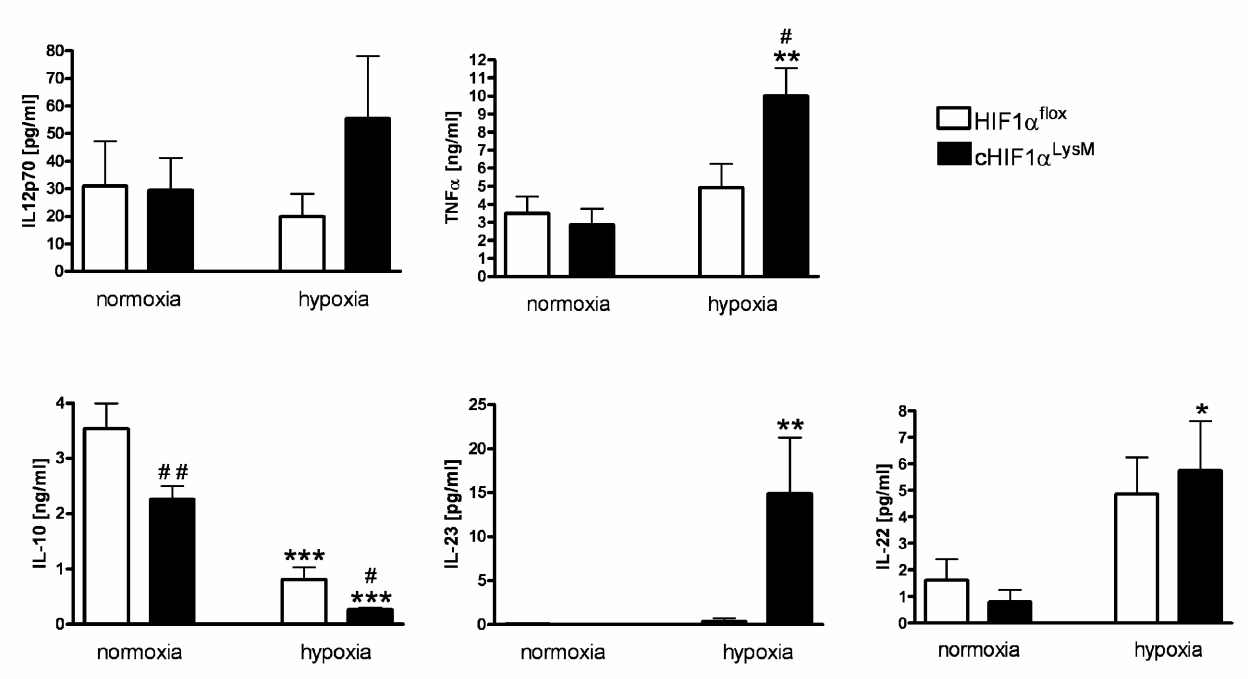

Figure 3.9 Cytokine expression of BMMΦ. BMMΦ of HIF1α^{flox} and cHIF1α^{LysM} mice were cultured with M-CSF at 21% or 1% O_2 and LPS-stimulated from d6 to d7. Cytokine secretion was measured with ELISA in cell culture supernatants. Results are depicted as mean +SEM of at least 3 independent experiments, (n = 5-7). *, $p < 0.05$; **, $p < 0.01$; ***, $p < 0.001$, hypoxic versus normoxic cells. #, $p < 0.05$; ##, $p < 0.01$; ###, $p < 0.001$, HIF1α-deficient BMMΦ versus HIF1α^{flox} controls.

3.3.3 Chemokine and chemokine receptor expression of BMMΦ

MΦ are very motile cells and are found in almost every tissue. They are attracted to sites of infection or inflammation by chemotaxis, following a gradient of chemokines. To respond to specific chemokines, MΦ express appropriate chemokine receptors on their surface, but they are also able to secrete chemokines themselves, which act as autocrine or paracrine ligands for chemokine receptors. CCR5 and CXCR4, both G-protein coupled receptors, are frequently implicated in HIV infection because of their function as co-receptors of CD4 during the entry of the virus [97]. To investigate their expression levels during hypoxia, the surface expression of these receptors was analyzed by flow cytometry. Interestingly, only a small proportion of BMMΦ expressed CCR5, whereas CXCR4 could be detected on all normoxic BMMΦ. Both receptors were significantly downregulated on BMMΦ of HIF1α^{flox} mice under hypoxic conditions. Interestingly, chemokine receptor expression on cHIF1α^{LysM} BMMΦ was regulated differently in hypoxia, as the reduction of CCR5-expressing BMMΦ could not be observed in the absence of HIF1α. In contrast, cell surface expression of CXCR4 was reduced on cHIF1α^{LysM} BMMΦ, as well as on HIF1α^{flox} BMMΦ in hypoxia (Figure 3.10A).

As BMDC strongly increase the secretion of the chemokines CCL17 and CCL22 under hypoxic conditions, I also addressed the regulation of these chemokines in hypoxic BMMΦ. Both were secreted by BMMΦ after LPS stimulation, but in much lower amounts compared with the secretion of these chemokines by BMDC. Nevertheless, the expression of CCL17 and CCL22 could be increased strongly in HIF1α^{flox} BMMΦ generated under oxygen deprived conditions. Hypoxic BMMΦ of cHIF1α^{LysM} mice failed to upregulate the expression of these chemokines, implicating that HIF1α regulates the expression of CCL17 and CCL22 under hypoxic conditions (Figure 3.10B). Taken together, examination of chemokine and chemokine receptor expression of normoxic versus hypoxic BMMΦ and HIF1α^{flox} versus cHIF1α^{LysM} BMMΦ revealed a great influence of hypoxia on MΦ. I could show that hypoxia induced the downregulation of the chemokine receptors CCR5 and CXCR4 on BMMΦ, whereas secretion of the chemokines CCL17 and CCL22 was increased in a HIF1α-dependent manner.

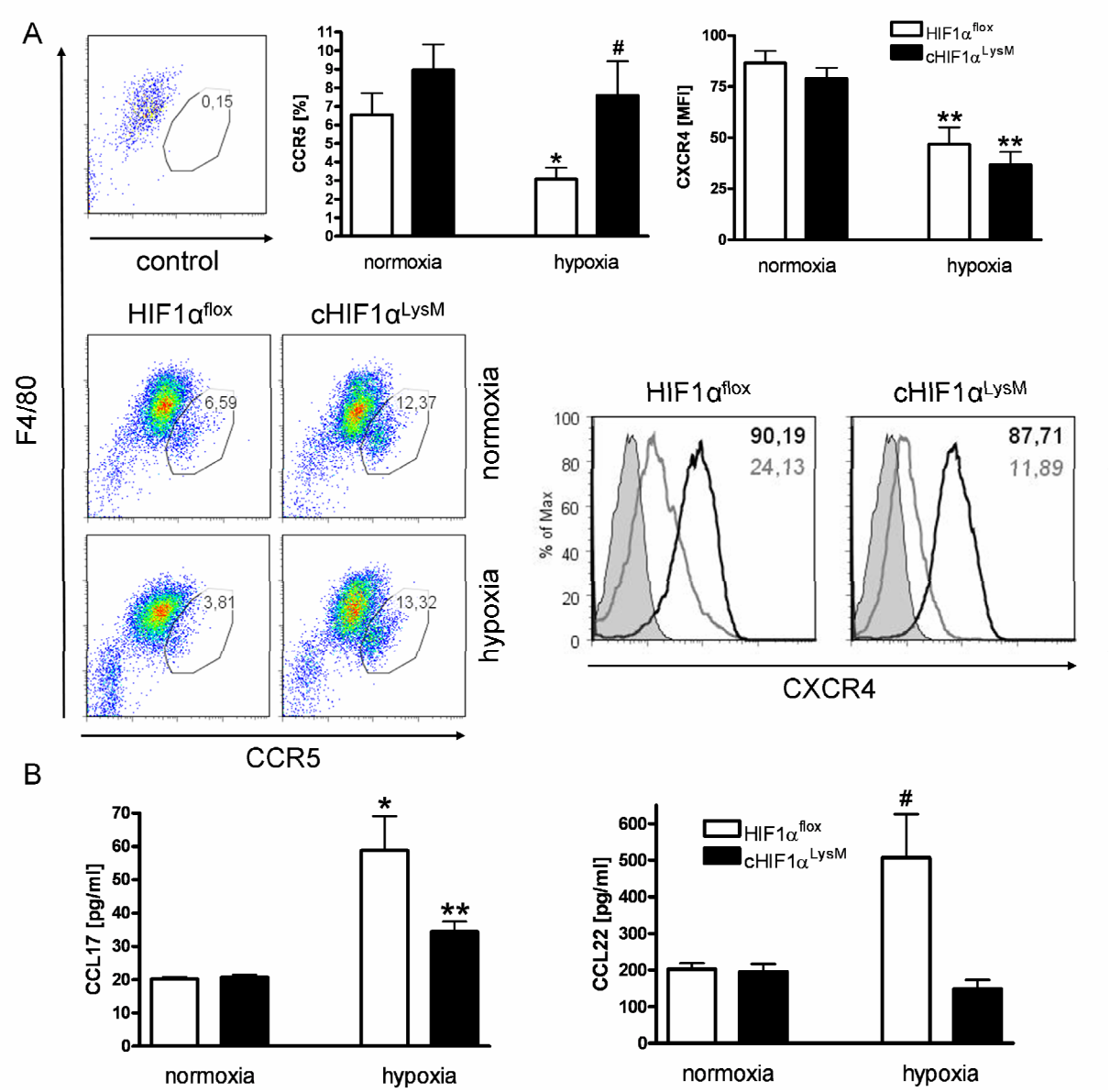

Figure 3.10 Chemokine and chemokine receptor expression of BMMΦ. BMMΦ of HIF1α^{flox} and cHIF1α^{LysM} mice were cultured with M-CSF at 21% or 1% O_2. **A** Chemokine receptor expression was measured by FACS analysis. Bar graphs are depicted as mean +SEM of at least 3 independent experiments. The gates in the representative dot plot (n = 6) for the CCR5 expression (left) are set according to the negative control (top, left), which was stained against F4/80, but not against CCR5. In the representative histogram of the CXCR4-staining (n = 8), BMMΦ generated under normoxic conditions (black lines) are compared with BMMΦ generated under hypoxic conditions (gray lines). The numbers in the representative histogram (right) indicate the MFI of the CXCR4-staining of normoxic (black) and hypoxic (gray) BMMΦ. The negative control, which was stained with an antibody against F4/80, but not against CXCR4, is shown as a gray shaded histogram. **B** Chemokine secretion was measured by ELISA in cell culture supernatants. Results are depicted as mean +SEM of at least 4 independent experiments, (n = 7). *, $p < 0.05$; **, $p < 0.01$; ***, $p < 0.001$, hypoxic versus normoxic cells. #, $p < 0.05$; ##, $p < 0.01$; ###, $p < 0.001$, HIF1α-deficient BMMΦ versus HIF1α^{flox} controls.

3.4 Role of HIF1α in different models of infection

3.4.1 *In vitro* kill assay of *Staphylococcus aureus*

Bacterial infections can cause a dramatic decrease of tissue oxygen concentration, since the demand for oxygen rises by invading pathogens and immigrating host immune cells. Tissue-resident DC and invading MΦ both react to low oxygen supply or even anoxia by adaptation of their metabolism. Under special circumstances *Staphylococcus aureus*, a commensal of skin and nose flora, can act as a high-risk pathogen, which induces cutaneous or systemic infections by activation of TLR2 and other PRR [30-31]. To analyze the role of HIF1α in cell survival and bacterial killing, BMDC and BMMΦ were challenged with *S. aureus* under normoxic and anoxic conditions. Due to the experimental setting, it was not possible to conduct the bacterial kill assay in 1% oxygen. Instead, anoxic conditions (0.2% oxygen) were achieved in anaerobic jars by the anoxomat. After 16 hours of co-culturing of BMDC with *S. aureus*, survival of BMDC and bacterial burden did not differ between normoxic and anoxic environments. In addition, comparing HIF1α-deficient BMDC with HIF1α-proficient BMDC under normoxic and under hypoxic conditions, the viability of BMDC and the intracellular survival of bacteria was unchanged. This indicates that HIF1α does not play a decisive role for cell survival and bacterial killing in this experimental setting (Figure 3.11A). In contrast, BMMΦ co-cultured with *S. aureus* under anoxic conditions showed a strong increase in cell survival compared with normoxic BMMΦ and deletion of HIF1α, surprisingly, appeared to even further enhance the percentage of surviving anoxic MΦ (Figure 3.11B upper panel). Focussing on bacterial killing of BMMΦ, in turn, revealed that neither the absence of oxygen, nor the deficiency of HIF1α influenced the clearance of *S. aureus* on a per cell basis (Figure 3.11B lower panel). These results clearly show that deprivation of oxygen differentially affects pathogen control in BMDC and BMMΦ. In BMMΦ, but not in BMDC, the absence of HIF1α strongly increased the survival of these phagocytes in anoxia after bacterial challenge.

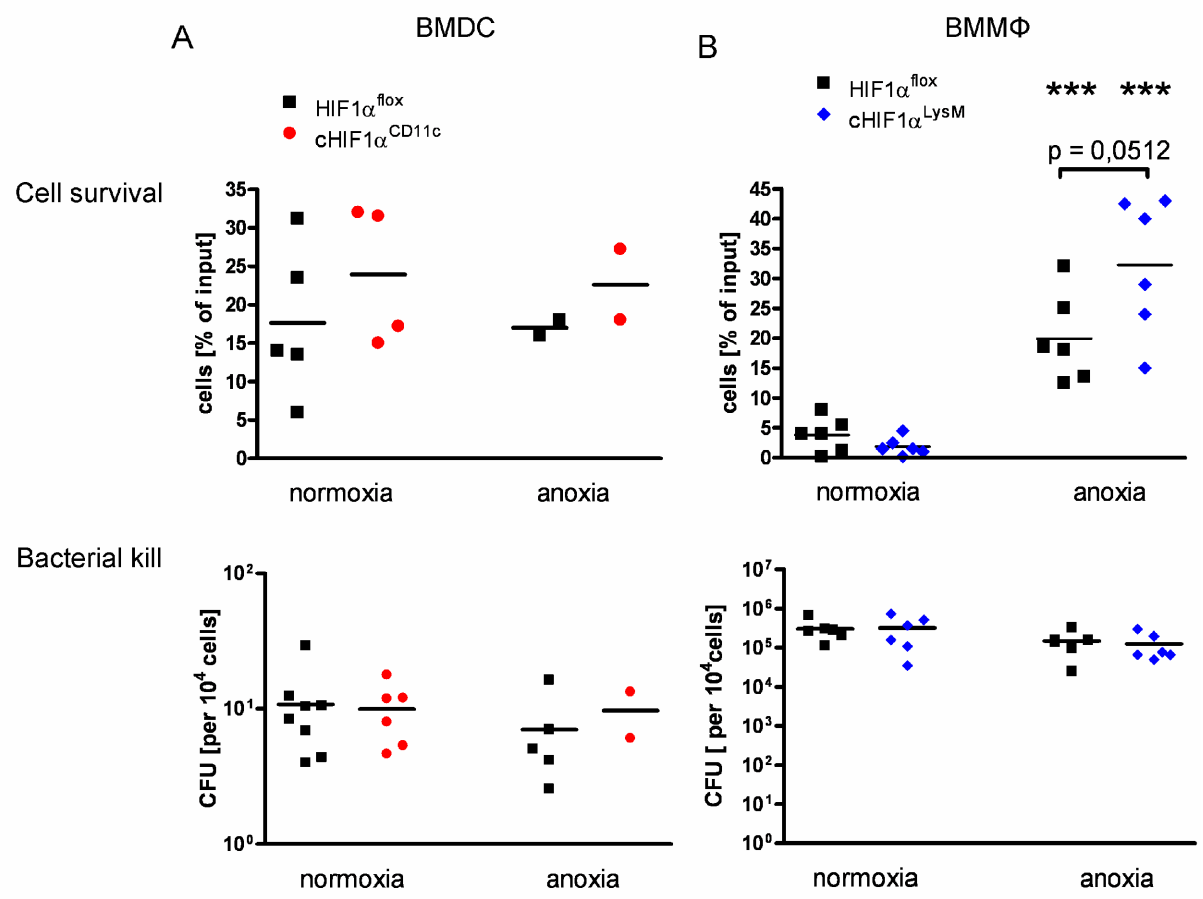

Figure 3.11 ***In vitro*** **kill of** ***Staphylococcus aureus*****.** BMDC of HIF1α^{flox} and cHIF1α^{CD11c} mice and BMMΦ of HIF1α^{flox} and cHIF1α^{LysM} mice were cultured at 21% O_2 or under anoxic conditions. After 16h co-culturing of BMDC (**A)** or BMMΦ (**B)** with *Staphylococcus aureus*, cells were counted and the pellet was plated on blood agar for determination of intracellular bacterial burden. *, $p < 0.05$; **, $p < 0.01$; ***, $p < 0.001$, hypoxic versus normoxic cells. Graphs depict data obtained from at least 2 **(A)** and 3 **(B)** experiments.

3.4.2 *In vivo* infection with *S. aureus*

Because of the differential response of normoxic and anoxic BMMΦ and BMDC from HIF1α^{flox} and HIF1α-deficient mice to *S. aureus in vitro*, an *in vivo* model of skin infections was investigated. *S. aureus* is a potent pathogen causing bacterial skin infections and can seriously threaten life by systemic dissemination to inner organs, such as kidney and spleen. Recently, the awareness of highly virulent antibiotic-resistant strains of *S. aureus* increased, since it has become a huge public health problem in hospitals [29, 98]. DC, especially CCL17-expressing peripheral DC, are thought to play an important role for initiation of cutaneous immune reactions [99]. MΦ and neutrophils, both deficient for HIF1α in cHIF1α^{LysM} mice, are involved in host defence against *S. aureus*, as MΦ secrete IL1-β upon phagocytosis of bacteria, which leads to recruitment of neutrophils to the site of infection [40]. To identify the

role of HIF1α in this process, mice of HIF1α^{flox}, cHIF1α^{CCL17}, cHIF1α^{CD11c} and cHIF1α^{LysM} were anesthetized, shaved on the back and tape stripped with tegaderm 3M tape to mechanically irritate the skin barrier for facilitation of bacterial host colonization. A patch soaked with either PBS as control, or *S. aureus* in PBS was applied onto the back skin and sealed with waterproof tape (Figure 3.12A). After 4 days, the back skin was removed, mechanically homogenized and examined for bacterial burden by plating the homogenate on blood agar plates. No significant differences in CFU were found, except a tendency of cHIF1α^{CD11c} mice to carry higher bacterial loads at the site of infection compared with HIF1α^{flox}, cHIF1α^{CCL17} and cHIF1α^{LysM} mice. Further, skin sections were stained with H&E and epidermal thickening was analyzed. Epidermal thickness was increased in all strains after topical application of *S. aureus* (Figure 3.12B). Since early after infection, Langerhans cells and dermal DC migrate from the skin into the skin draining LN, these LN were analyzed by flow cytometry. A strong increase of total cell numbers in the brachial LN could be detected after infection. Analysis of the distribution of different cell populations in these LN showed that CD11c^{+} MHCII^{+} DC were significantly increased in all mouse strains, except in cHIF1α^{LysM} mice after *S. aureus* challenge. I also detected an enhanced influx of CD11c-negative CD11b^{+} Gr1^{+} cells, probably representing monocytes or granulocytes, into the draining LN in response to the epicutaneous infection with *S. aureus* (Figure 3.12C). When testing skin samples for gene expression after bacterial stimulation, iNOS and IL-22 were strongly upregulated. Infected skin of cHIF1α^{CD11c} and cHIF1α^{LysM} mice showed slightly decreased IL-22 expression compared with HIF1α^{flox} mice, but this difference was not statistically significant (Figure 3.12D). In summary, the data show that, against all expectations, the deficiency of HIF1α in either DC or MΦ and neutrophils did not lead to major changes in the outcome of cutaneous *S. aureus* infections.

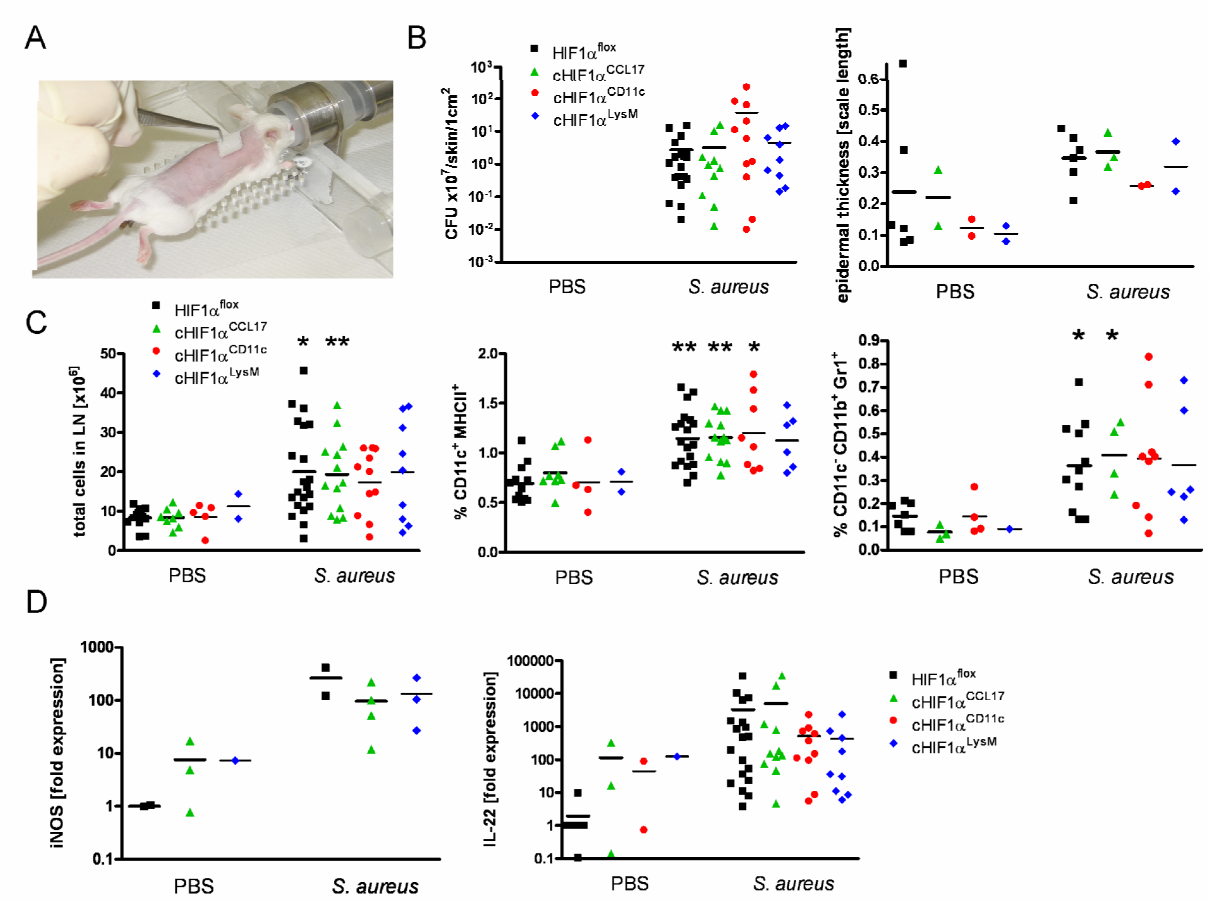

Figure 3.12 ***In vivo infections*** **with** ***Staphylococcus aureus*****. A** Mice were shaved, tape-stripped 4 times and infected epicutaneously with *S. aureus* by application of a bacteria-soaked patch on the back. **B** At d4 the dorsal skin was removed, homogenized and plated in different concentrations on agar plates for determination of bacterial burden. Epidermal thickness was measured with the FluorChem 8900 software after HE staining. **C** Total cells from brachial LN were counted. DC were identified as $CD11c^+$ $MHCII^+$ cells. To determine the percentage of granulocytes/neutrophils, a gate was set on $CD11c^-$ $CD11b^+$ $Gr1^+$ cells. **D** mRNA was isolated from skin samples and expression of iNOS and IL-22 was determined by relative quantification. Expression levels of uninfected normoxic $HIF1α^{flox}$ skin samples were set to 1. Each dot/symbol represents one mouse and the mean is also depicted for each group. *, $p < 0.05$; **, $p < 0.01$; ***, $p < 0.001$, infected versus uninfected mice. Graphs depict data obtained from at least 4 independent experiments, except for iNOS expression **(D)**, which was measured in 1 experiment only.

3.4.3 *In vitro* kill assay of *Listeria monocytogenes*

Listeria monocytogenes is an intracellular gram positive pathogen, which primarily invades spleen and liver of the host [43]. After phagocytosis of the bacteria by MΦ or DC, the Listeria escape from the phagosome to start replication in the cytosol. Spreading to adjacent cells is mediated by vacuole formation, which enables *L. monocytogenes* to infect other cells without contact to the extracellular space and, thereby, to minimize contact with the PRR of the host immune defence system. DC restrict the growth of *L. monocytogenes* by retaining these in MHCII containing compartments, whereas BMMΦ provide a significant niche for replication of these

bacteria [45]. In this thesis, the response of both, BMDC and BMMΦ, to *L. monocytogenes* after co-culture under normoxic and anoxic conditions was analyzed. In contrast to the experiments with *S. aureus*, in which around 20% of the infected BMDC survived the bacterial challenge, only a small fraction of BMDC survived overnight bacterial infection with no difference between normoxic and anoxic groups. The lack of HIF1α neither affected cell survival, nor the clearance of *L. monocytogenes* (Figure 3.13A). BMMΦ, on the other hand, had a higher chance to survive bacterial infection, when co-cultured in the absence of oxygen. HIF1α-deficient BMMΦ even showed increased resistance to *L. monocytogenes* compared with control BMMΦ in an anoxic environment (Figure 3.13B upper panel). Enhanced survival of anoxic BMMΦ was accompanied by improved clearance of bacteria in an oxygen-deprived milieu compared with a normoxic environment. Regarding the bacterial burden in infected BMMΦ, the presence of HIF1α favours clearance of *L. monocytogenes*, as BMMΦ from cHIF1α^{LysM} mice carried somewhat more bacteria than HIF1α^{flox} BMMΦ, when incubated in oxygen-free conditions (Figure 3.13B lower panel).

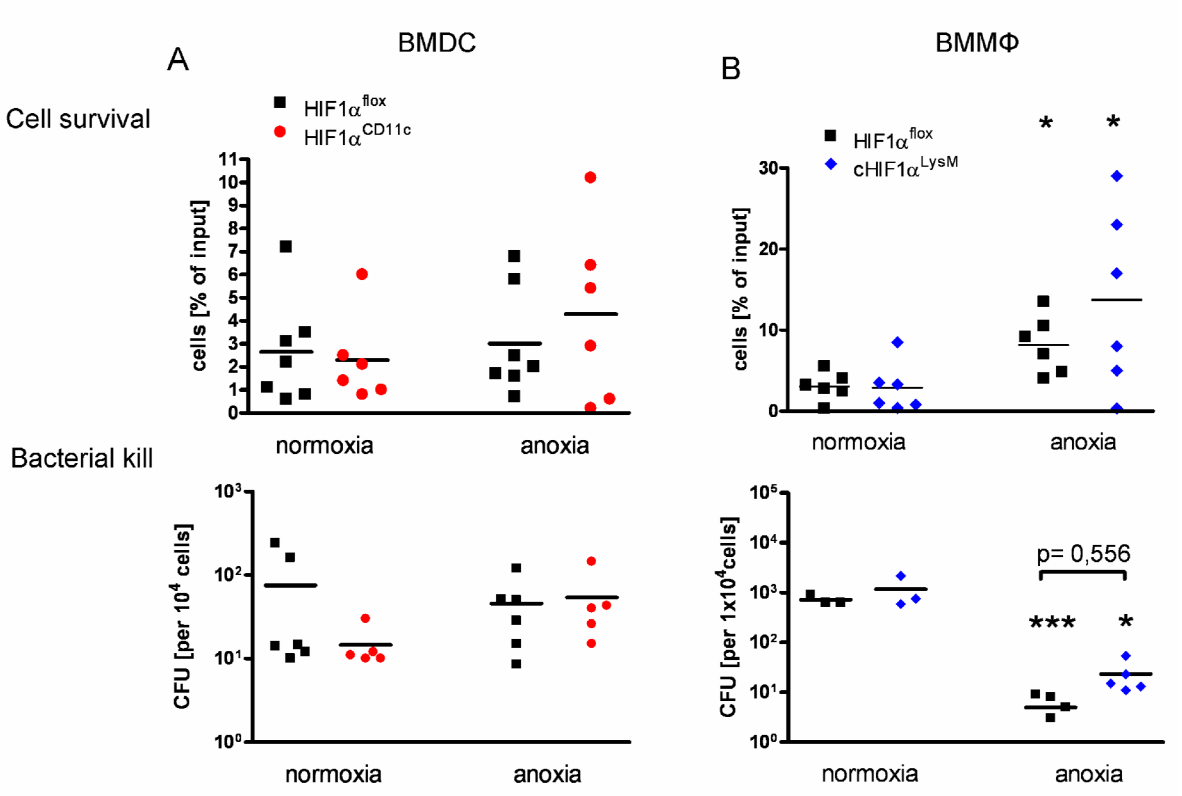

Figure 3.13 *In vitro* kill of *L. monocytogenes*. BMDC of HIF1α^{flox} and cHIF1α^{CD11c} mice and BMMΦ of HIF1α^{flox} and cHIF1α^{LysM} mice were cultured at 21% O_2 or under anoxic conditions. After 16h co-culturing of BMDC (**A)** or BMMΦ (**B)** with *Listeria monocytogenes*, cells were counted and the cell pellet was plated on blood agar for determination of intracellular bacterial burden. *, $p < 0.05$; **, $p < 0.01$; ***, $p < 0.001$, hypoxic versus normoxic cells. Graphs depict data obtained from 3 **(A)** and 2 **(B)** independent experiments.

3.4.4 *In vivo* infection with *L. monocytogenes*

Systemic infection with *L. monocytogenes* leads to a rapid apoptotic death of lymphocytes in the spleen of mice, probably induced by LLO [43]. Based on the strong influx of bacteria and immune cells into spleen and liver, serious hypoxic conditions can be assumed. Therefore, a systemic infection with *L. monocytogenes* represents an interesting model for examination of function and bactericidal capacity of DC and MΦ with a deletion of HIF1α. HIF1α^{flox}, cHIF1α^{CD11c} and cHIF1α^{LysM} mice were infected intravenously with *L. monocytogenes* or PBS and analyzed after 2 or 4 days. In all 3 strains, the spleen was enlarged and had gained weight at day 2, which was even more pronounced at day 4 (Figure 3.14A). Measurement of CFU in spleen and liver revealed a high bacterial burden after 2 days, which was further enhanced on day 4 (Figure 3.14A). But, neither in spleen weight, nor in bacterial colonization a difference between HIF1α^{flox} mice, HIF1α^{CD11c} and cHIF1α^{LysM} mice could be detected. FACS analysis of splenic single cell suspensions showed a strong upregulation of the activation marker CD69 on CD3$^+$ CD4$^+$ T cells of all mouse strains analyzed, peaking at day 2 after infection (Figure 3.14C). Examination of CD11c$^+$ MHCII$^+$ DC and CD11c$^-$ CD11b$^+$ F4/80$^+$ MΦ revealed a small increase in percentage of this cell population on day 2, without any effect induced by the lack of HIF1α in either cell type (Figure 3.14C). Interestingly, CD11c$^-$ CD11b$^+$ Gr1$^+$ cells, which characterize monocytes and granulocytes, were found to accumulate in spleen with peak levels on day 4 in all mouse strains, but only on day 4 after infection, significantly increased percentages of these cell types were found in cHIF1α^{LysM} mice compared with HIF1α^{flox} mice (Figure 3.14C). These examinations show that listeriosis seriously affects the physical health of mice by bacterial invasion of liver and spleen and change of cellular composition of the spleen, but a specific deletion of HIF1α in DC or MΦ and neutrophils does not lead to major changes in the outcome of listeriosis.

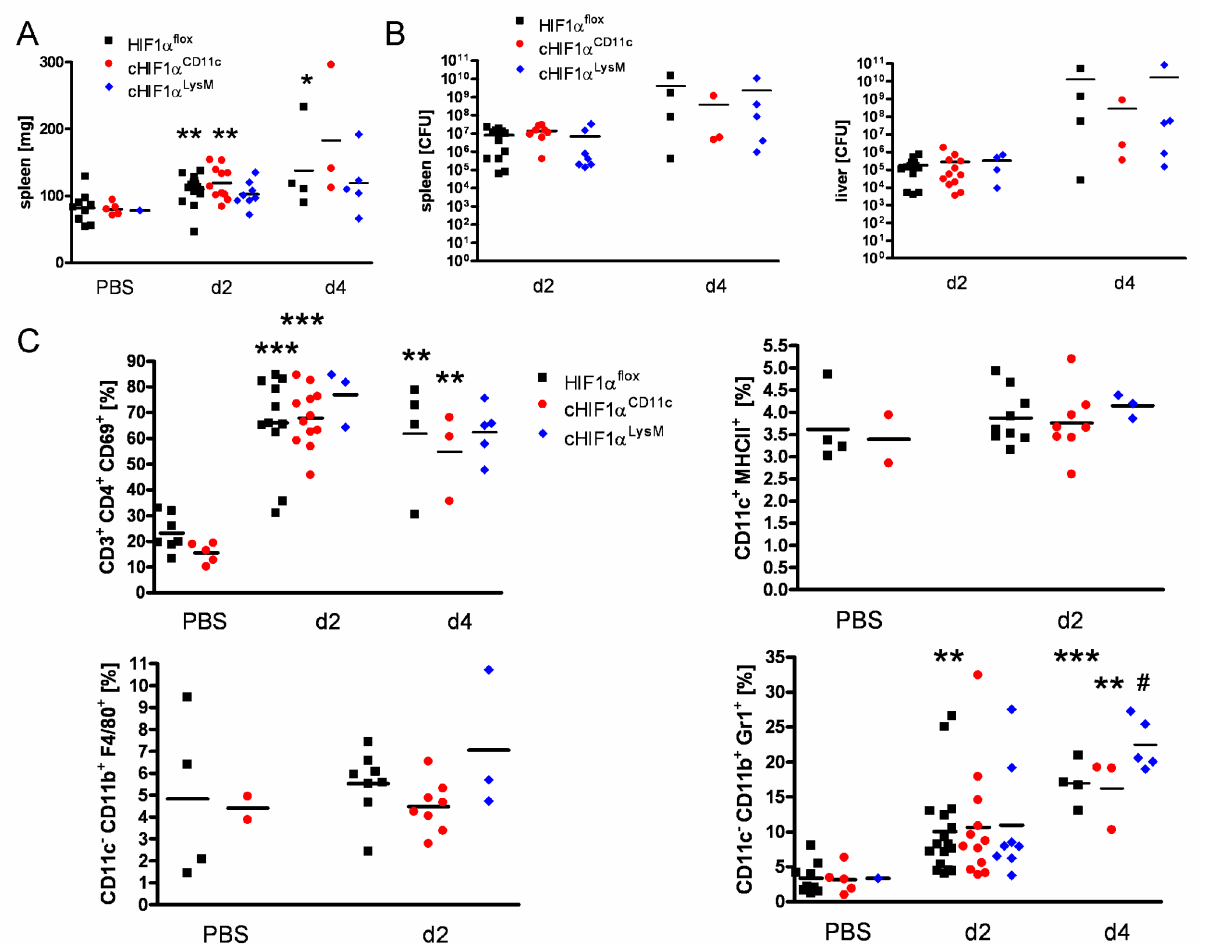

Figure 3.14 ***In vivo infections*** **with** ***Listeria monocytogenes*****. A** Mice were infected i.v. with Listeria and on d2 and d4 spleen weight was noted. **B** Spleen and liver were removed at indicated times, homogenized and plated on blood agar in different concentrations for determination of bacterial burden. **C** Splenic activated CD4 T cells were stained with $CD3^+$ $CD4^+$ $CD69^+$ (upper panel left), DC were identified as $CD11c^+$ $MHCII^+$ cells (upper panel right), and MΦ were identified as $CD11c^-$ $CD11b^+$ $F4/80^+$ cells (lower panel left). To determine the percentage of granulocytes/neutrophils, a gate was set on $CD11c^-$ $CD11b^+$ $Gr1^+$ cells (lower panel right). Each dot/symbol represents one mouse and the mean is also depicted for each group. *, $p < 0.05$; **, $p < 0.01$; ***, $p < 0.001$, infected versus uninfected mice. #, $p < 0.05$; ##, $p < 0.01$; ###, $p < 0.001$, HIF1α-deficient mice versus $HIF1α^{flox}$ controls. Graphs depict data obtained from 4 independent experiments.

3.4.5 *In vitro* kill assay of *Streptococcus pyogenes (group A)*

Streptococcus pyogenes, also known as group A *streptococcus* (GAS), is a prominent, worldwide-spread, gram-positive pathogen. GAS is the cause for many human diseases ranging from superficial skin infections to tonsillitis and severe pathologic conditions, such as toxic shock syndrome and sepsis. GAS has evolved multiple virulence factors to improve bacterial proliferation for invasion of inner organs and for evasion of the host immune defence. Degradation of IL-8, a phagocyte attracting chemokine, by the bacterial proteinase (*Spy*CEP) leads to the decrease of neutrophil and MΦ invasion [100]. GAS shows high resistance to

antimicrobial peptides, for example, by expression of the cysteine proteinase SpeB, which inactivates the human cathelicidin LL-37, which is closely related to the murine cathelicidin-related antimicrobial peptide (Cramp) [101]. Furthermore, β-hemolysins, such as the pore-forming streptolysin S, lead to direct phagocyte disruption [102]. It has been reported that HIF1α is induced directly upon *streptococcal* infection of myeloid cells, thereby leading to expression of antimicrobial effector molecules, such as cathelicidin, granule proteases, and NO [73]. To further examine, if HIF1α-deficiency influences the interaction between pathogen and host cell, BMDC and BMMΦ from HIF1α^{flox} and HIF1α-mutant mice were challenged with GAS. Since a newly purchased recipe allowed the generation of gas mixtures containing 1% oxygen by the anoxomat, the experiments were from now on conducted under hypoxic conditions instead of anoxia. Hypoxic conditions led to increased cell survival of HIF1α^{flox} BMDC after overnight co-culturing with GAS, which was not statistically significant, compared with normoxic conditions. This effect could not be seen in HIF1α-deficient hypoxic BMDC (Figure 3.15A upper panel). The bacterial burden, in contrast, was neither affected by the oxygen concentration, nor by the absence of HIF1α (Figure 3.15A lower panel). Regarding the cell survival and the capacity to kill GAS, no differences could be detected for hypoxic versus normoxic BMMΦ, nor could a regulatory function of HIF1α be observed (Figure 3.15B).

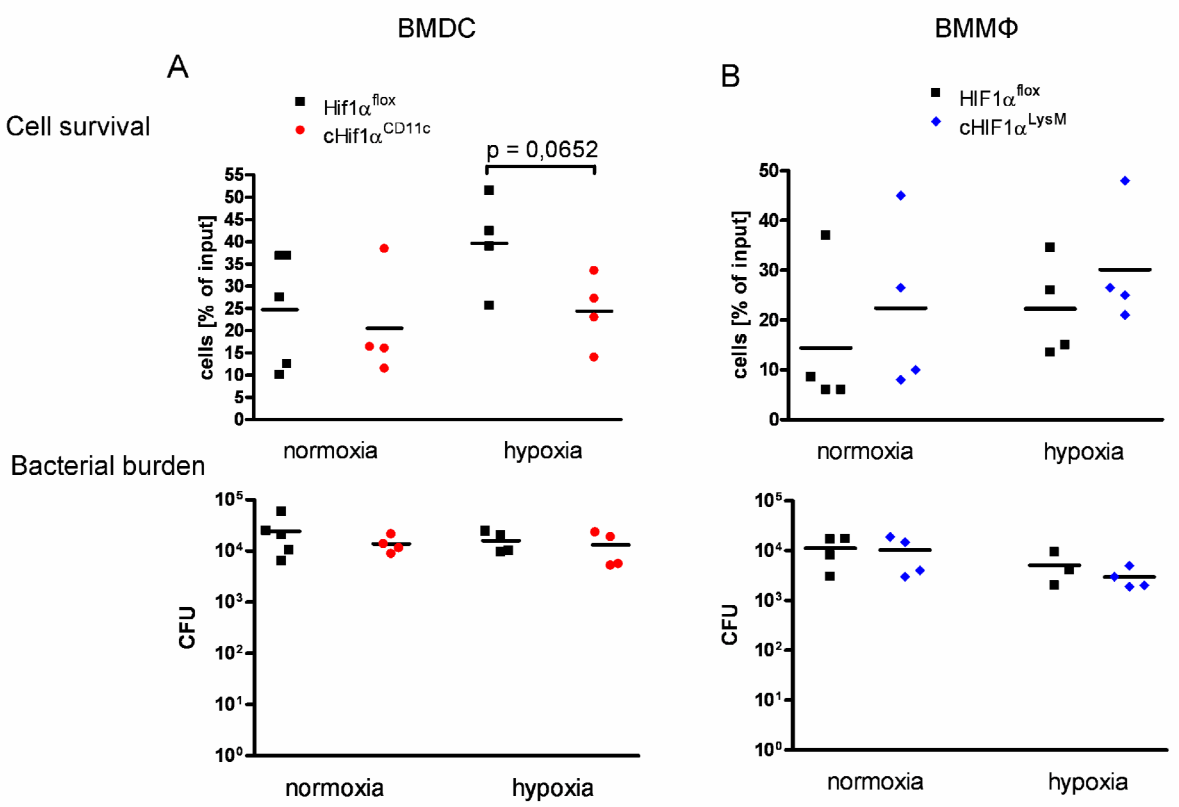

Figure 3.15 *In vitro* kill of *Streptococcus pyogenes* (GAS). BMDC of HIF1α^{flox} and cHIF1α^{CD11c} mice and BMMΦ of HIF1α^{flox} and cHIF1α^{LysM} mice were cultured at 21% O_2 or under hypoxic conditions. After 16h co-culturing of BMDC (**A)** or BMMΦ (**B)** with *Streptococcus pyogenes*, cells were counted and the pellet was plated on blood agar for determination of intracellular bacterial burden. Graphs depict data obtained from 2 independent experiments.

3.4.6 *In vitro* kill assay of *Streptococcus agalactiae (group B)*

Streptococcus agalactiae, also known as group B *streptococcus* (GBS), is, gram-positive, like GAS, and can be found in healthy human genital flora and in the gastrointestinal tract. As a pathogen, GBS can cause neonatal sepsis, meningitis and pneumonia. The surface-associated β-hemolysins with their cytolytic properties contribute to the virulence of GBS. Neutrophils and MΦ are the main cells to kill streptococci by lysis of bacteria in the phagolysosomes [103]. Interestingly, GBS is able to survive inside phagocytic vacuoles, as they show a strong resistance to the rapid release of ROS by MΦ and to the respiratory burst by neutrophils [103-104]. In an *in vitro* kill assay with GBS, I could demonstrate that BMDC strongly enhance their capacity to survive, when co-cultured with GBS in an oxygen-deprived environment. Clearance of GBS on a per cell basis was neither influenced by hypoxia, nor by absence of HIF1α (Figure 3.16A). BMMΦ also showed a slight increase of cell survival after GBS challenge in hypoxia compared with normoxia. This increase was most pronounced in cHIF1α^{LysM} BMMΦ. Just as in BMDC, no effects of oxygen

deprivation and HIF1α-deficiency could be observed in co-cultures of MΦ and GBS regarding bacterial burden (Figure 3.16B).

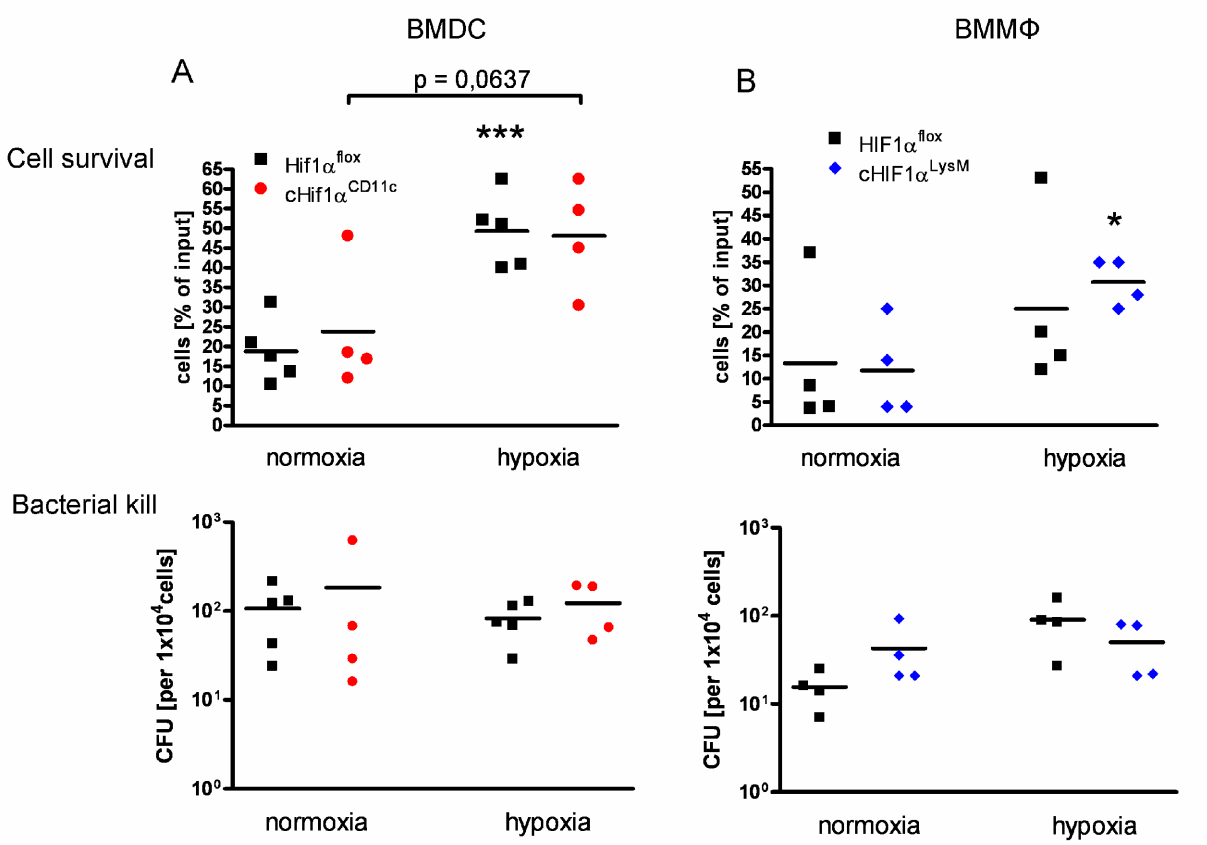

Figure 3.16 *In vitro* kill of *Streptococcus agalactiae* (GBS). BMDC of HIF1α^{flox} and cHIF1α^{CD11c} mice and BMMΦ of HIF1α^{flox} and cHIF1α^{LysM} mice were cultured at 21% O_2 or under hypoxic conditions. After 16h co-culturing of BMDC (**A)** or BMMΦ (**B)** with *Streptococcus agalactiae*, cells were counted and the pellet was plated on blood agar for determination of intracellular bacterial burden. *, $p < 0.05$; **, $p < 0.01$; ***, $p < 0.001$, hypoxic versus normoxic cells. Graphs depict data obtained from 2 independent experiments.

3.4.7 *In vitro* kill assay of *Escherichia coli*

Escherichia coli (*E. coli*) is a gram-negative commensal of our gastrointestinal tract. It can acquire severe pathogenicity, for example, after disruption of the intestinal barrier and subsequent invasion of the urinary tract and the peritonel cavity. *E. coli* bacteria have evolved various serotypes, which differ in their factors of virulence, such as the enterohemorrhaghic *E. coli* (EHEC), which produces Shiga-toxin and can cause hemorrhagic colitis (HC) or bloody diarrhea [105]. In this study, the ability of BMDC and BMMΦ to kill *E. coli* of the avirulent laboratory strain K12 was tested. BMDC co-cultured under oxygen-free conditions with *E. coli* showed increased survival rates compared with co-cultures in normoxia. This effect was independent of HIF1α

expression (Figure 3.17A upper panel). In contrast, bacterial killing in a hypoxic environment was dependent on HIF1α, since higher amounts of CFU were detected in cHIF1α^{CD11c} and cHIF1α^{CCL17} BMDC compared with BMDC from HIF1α^{flox} mice after 1 hour of co-culturing. At that time point, no differences in the viability of the BMDC were detected and therefore, the whole cell pellet was plated for bacterial enumeration without prior count of BMDC. In overnight cultures, however, which were carried out under anoxic conditions due to the experimental set up, it was not possible to see the same effect in anoxia (Figure 3.17A lower panel). Normoxic BMMΦ revealed a surprisingly low capacity to survive in co-cultures with *E. coli*, whereas anoxia was able to strongly improve the survival rates of BMMΦ with a slight tendency for HIF1α-deficient BMMΦ to survive better (Figure 3.17B upper panel). The clearance of *E. coli* in an oxygen-deprived environment turned out to be regulated, at least in part, by HIF1α, as in cHIF1α^{LysM} BMMΦ significantly more CFU were detected than in HIF1α-proficient counterparts (Figure 3.17B lower panel).

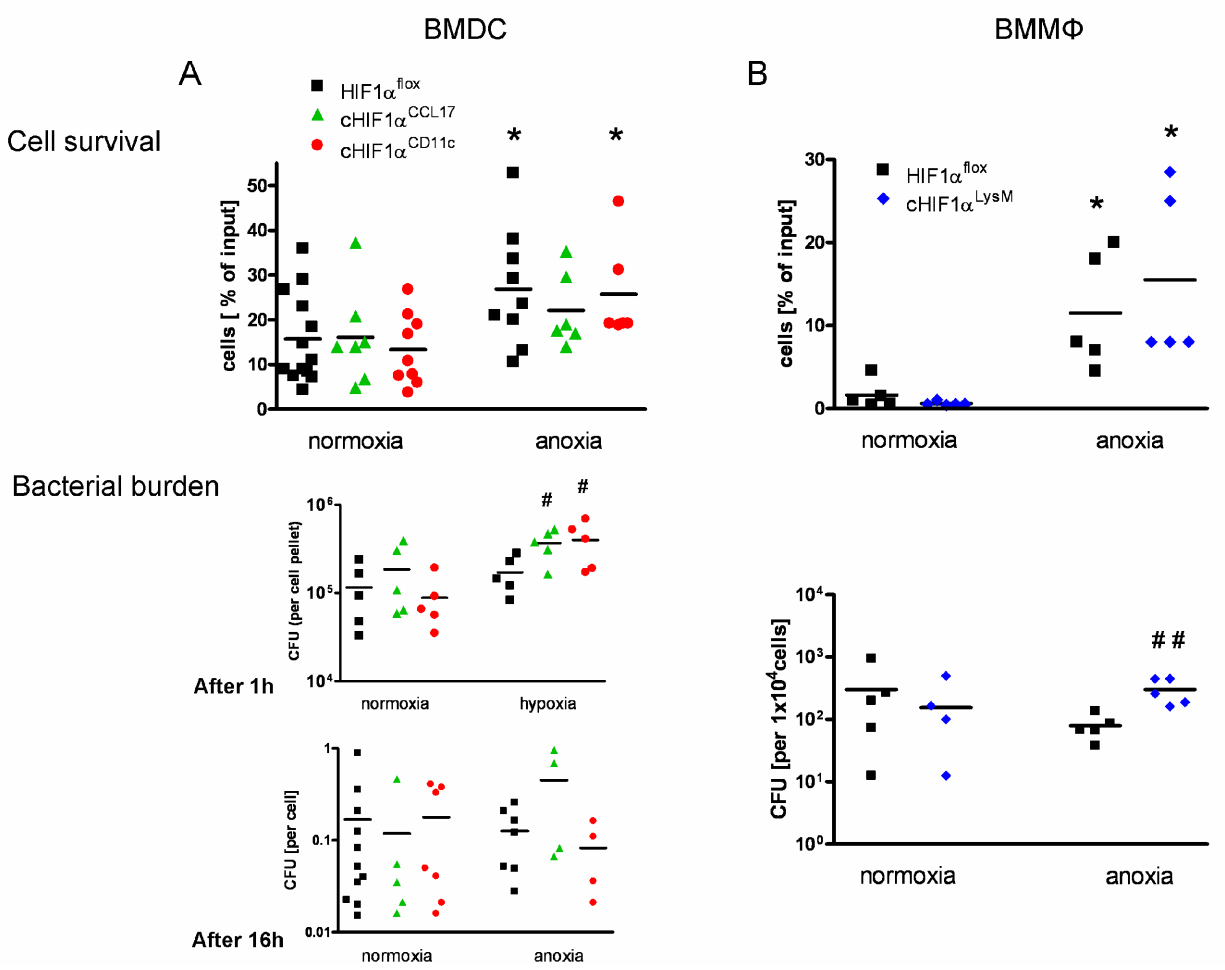

Figure 3.17 *In vitro* kill of *E. coli*. BMDC of HIF1α^{flox}, cHIF1α^{CCL17} and cHIF1α^{CD11c} mice and BMMΦ of HIF1α^{flox} and cHIF1α^{LysM} mice were cultured at 21% O_2 or under anoxic conditions; for the 1h time point under hypoxic (1% oxygen) conditions. After 16h co-culturing of BMDC (**A)** or BMMΦ (**B)** with *E. coli*, cells were counted and the pellet was plated on LB agar for determination of intracellular bacterial burden. For BMDC, the bacterial burden was also analyzed at the time point of 1h co-culturing without prior enumeration of viable cells **(A)**. *, $p < 0.05$; **, $p < 0.01$; ***, $p < 0.001$, hypoxic versus normoxic cells. #, $p < 0.05$; ##, $p < 0.01$; ###, $p < 0.001$, HIF1α-deficient mice versus HIF1α^{flox} controls. Graphs depict data obtained from at least 4 (**A)** and 2 **(B)** independent experiments.

3.4.8 *In vivo* infection with *Citrobacter rodentium*

Gastrointestinal diseases are, in the majority of cases, accompanied by hypoxic conditions and induction of HIF1α [106]. Inflammatory bowel disease goes along with an increase of cell metabolism and tissue remodelling, subsequently causing hypoxia in mucosa and epithelium [60]. Additionally, it is known that different types of *Enterobacteriaceae* can induce HIF1α in a hypoxia-independent way [107] and constitutive expression of HIF1α leads to an aggravation of DSS-induced colitis symptoms [108]. *C. rodentium* also induces colitis and is a suitable model organism to investigate attaching and effacing (A/E) bacterial pathogens in rodents, such as the enteropathogenic *Escherichia coli* (EPEC) and the enterohaemorrhagic *E. coli*

(EHEC), which can cause life threatening conditions in humans. Colitis caused by infection with *C. rodentium* is accompanied by strong infiltration of neutrophils and MΦ in the colonic mucosa, as well as by production of antimicrobial peptides and IL-22 by colonic epithelial cells [55, 109]. To investigate the role of HIF1α in DC and MΦ during *C. rodentium* infection, HIF1α^{flox}, cHIF1α^{CD11c} and cHIF1α^{LysM} mice were orally infected. This led to a mild reduction of weight during the first 5 days after infection without any differences between HIF1α^{flox} mice and mice with a cell type specific deletion of HIF1α. After this period, all mice continuously gained weight (Figure 3.18A upper panel and B upper panel). In the first infection experiment, when comparing HIF1α^{flox} with cHIF1α^{CD11c} mice, mice were infected with 1x 10^7 CFU of *C. rodentium*. The bacterial burden in the stool of mice reached its peak around d7 after infection and clearance of bacteria occurred at d20, independent of the mouse strain analyzed (Figure 3.18A lower panel). Because of only mild symptoms during the course of infection, HIF1α^{flox} and cHIF1α^{LysM} mice were infected with a high dose of *C. rodentium* (5x 10^{14} CFU) to induce more striking symptoms, such as a significant weight loss. However, no extreme weight changes were detected, but the high dose of bacteria caused a longer-lasting infection compared with the low dose, which was not cleared until d40. Mice with a deficiency of HIF1α in myeloid cells did not differ in disease symptoms during *Citrobacter rodentium* infection compared with HIF1α^{flox} mice (Figure 3.18B).

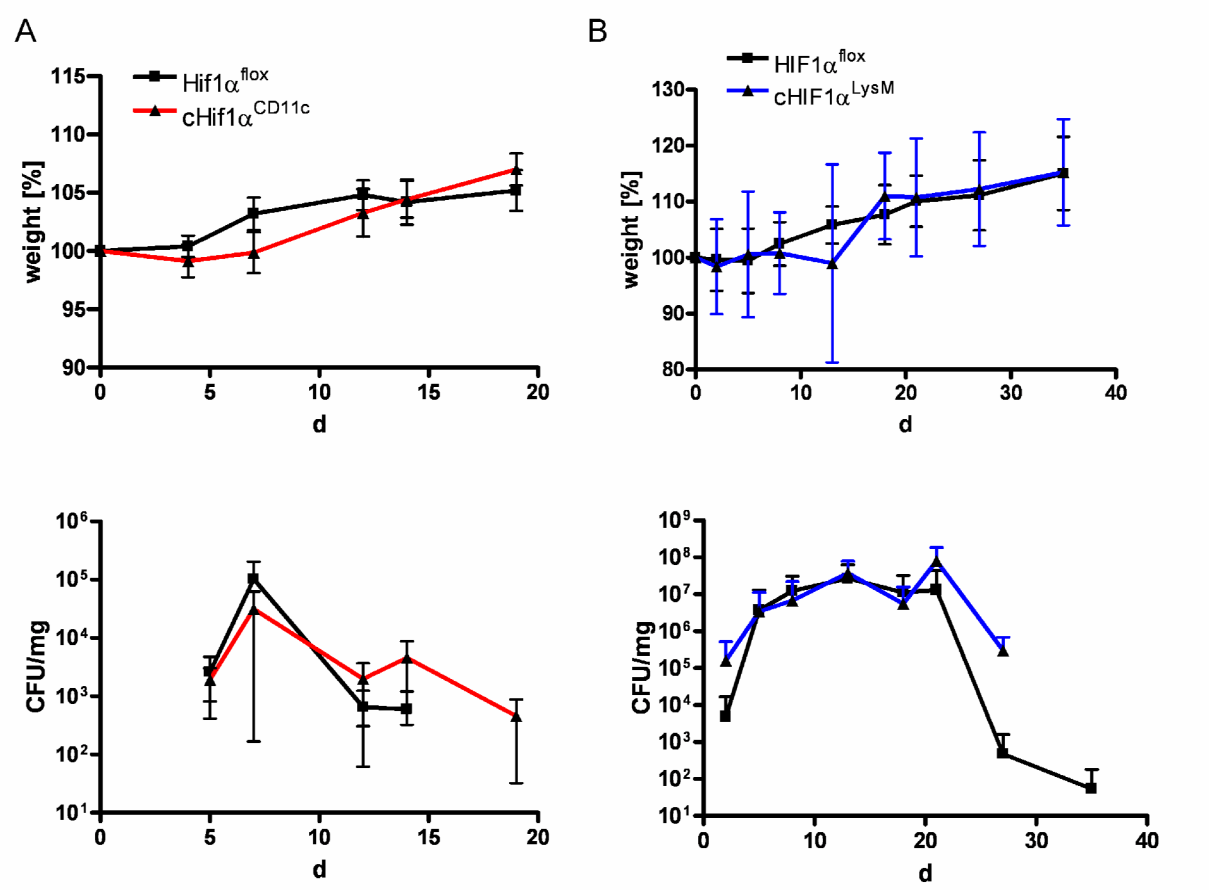

Figure 3.18 ***In vivo infections*** **with** ***Citrobacter rodentium*****. A** HIF1α^{flox} (n = 5) and cHIF1α^{CD11c} (n = 7) mice and **B** HIF1α^{flox} (n = 13) and cHIF1α^{LysM} (n = 5) mice were orally infected with *Citrobacter rodentium* and checked for weight and bacterial burden in stool until clearance of bacteria. Feces were weighed and CFU were adjusted to 1 mg of feces. Results are depicted as mean +/- SEM. Graphs are representative for 3 **(A)** and 1 **(B)** independent experiments.

3.4.9 Infection-associated changes in gene expression

Immune cells have evolved a variety of mechanisms to defend the organism against pathogens. To investigate the defence systems of DC and MΦ, the expression of known HIF1α target genes in normoxic and hypoxic cells, as well as HIF1α-proficient and HIF1α-deficient cells was quantified by qRT-PCR. Additionally, genes playing a central role in key mechanisms of host defence, such as inflammasome activation and autophagy, were analyzed. NLPR3 belongs to the NLR family and is also a central molecule of the NLPR3-inflammasome, which is activated by exogenous stimuli, such as UV, particles and pathogens [39]. *S. aureus* derived α-hemolysin, for example, induces caspase-1 dependent inflammatory secretion of the cytokines IL-1β and IL-18 by activation of NLRP3 [110]. In BMMΦ an increased NLRP3 expression was detected upon LPS stimulation (Figure 3.19A), which had already been reported before [111]. In this study, I could further show that NLRP3 was

somewhat stronger induced in hypoxic BMMΦ compared with normoxic BMMΦ. This effect was independent of HIF1α expression (Figure 3.19A).

IDO has the capacity to limit bacterial growth, since the amino acid tryptophan is essential for replication of most bacteria. Under normoxic conditions, IDO was upregulated after LPS stimulation in a HIF1α-independent manner. Interestingly, HIF1α-deficient BMMΦ revealed an almost complete shutdown of IDO expression under oxygen-deprived conditions (Figure 3.19B), indicating that somehow HIF1α controls upregulation of IDO in hypoxia.

Autophagy is a system of lysosomal self digestion with the purpose of cytoplasmic protein recycling and cell renovation. It is also an innate immune defence mechanism for elimination of intracellular bacteria, such as *L. monocytogenes* [46]. LC3 is an essential molecule involved in the autodigestive process and frequently used as an autophagy marker [47]. In normoxic BMMΦ, LC3 was downregulated upon LPS stimulation, whereas under hypoxic conditions $HIF1\alpha^{flox}$ and $cHIF1\alpha^{LysM}$ BMMΦ showed increased LC3 expression compared with unstimulated normoxic BMMΦ (Figure 3.19C). These data show that autophagy is induced under conditions of low oxygen, whereas HIF1α does not play a role in this process.

Fpr are involved in the mammalian immune defence system, as they are important sensors of formylated peptides derived from bacteria, such as *S. aureus*. Since the activation of Fpr1 leads to the induction of proinflammatory processes like attraction of neutrophils and the release of antimicrobial proteins [112], the expression of Fpr1 in normoxic and hypoxic BMMΦ was addressed. Fpr1 was strongly upregulated after activation of BMMΦ with LPS. Oxygen deprivation even led to an additional increase of Fpr1 expression in BMMΦ, which was independent of HIF1α (Figure 3.19D). In summary, expression analysis of these four key molecules revealed that NLPR3, as part of the inflammasome, LC3, a central molecule in autophagy, and Fpr1 are induced by hypoxia in LPS-stimulated BMMΦ, but independently of HIF1α. IDO, interestingly, was the only gene found to be expressed under the control of HIF1α in hypoxic BMMΦ.

To investigate the role of hypoxia and the function of HIF1α in different innate immune cells, gene expression of anti-infectious proteins was analyzed and compared in BMDC and BMMΦ. The inducible nitric oxide synthase (iNOS) is a highly efficient enzyme, which catalizes the production of NO from the amino acid L-arginine and is expressed in phagocytes, such as MΦ, neutrophils and DC, but also

in endothelial and epithelial cells. NO is an important inflammatory signaling molecule, which regulates production of cytokines and chemokines, but also activates intracellular key signaling proteins like MAPK, JAK, NF-κB, and AP-1. NO is able to elicit inflammatory, as well as immuno-modulatory effects, depending on its concentrations in the cell [113]. Both, BMDC and BMMΦ express high levels of iNOS after LPS stimulation under normoxic, as well as under hypoxic conditions (Figure 3.19E and F). iNOS gene expression in normoxic BMDC was unchanged compared with hypoxic BMDC and no influence of HIF1α-deletion could be detected (Figure 3.19E). Hypoxic BMMΦ showed high variability of iNOS expression levels in different experiments (Figure 3.19F). Therefore no definite conclusion can be drawn about the regulation of iNOS under hypoxic conditions and by HIF1α.

Interestingly, expression analysis of Cramp, which is a known target of HIF1α in neutrophils and was reported to be essential in host defence against GAS [73], revealed that Cramp was differentially regulated by HIF1α in BMDC compared with BMMΦ (Figure 3.19G and H). Specifically, Cramp was downregulated upon LPS stimulation under normoxic conditions in $HIF1\alpha^{flox}$ BMDC compared with unstimulated $HIF1\alpha^{flox}$ BMDC (set to 1), whereas HIF1α-deficient BMDC expressed higher levels of Cramp compared with $HIF1\alpha^{flox}$ BMDC. This effect was seen under normoxic, as well as under hypoxic conditions (Figure 3.19G). In contrast, Cramp transcripts were strongly upregulated in hypoxic BMMΦ, which was, at least in part, dependent on HIF1α (Figure 3.19H). These findings implicate a regulating role for HIF1α in the Cramp expression of MΦ, whereas this antimicrobial peptide appears to be induced by a different mechanism in BMDC.

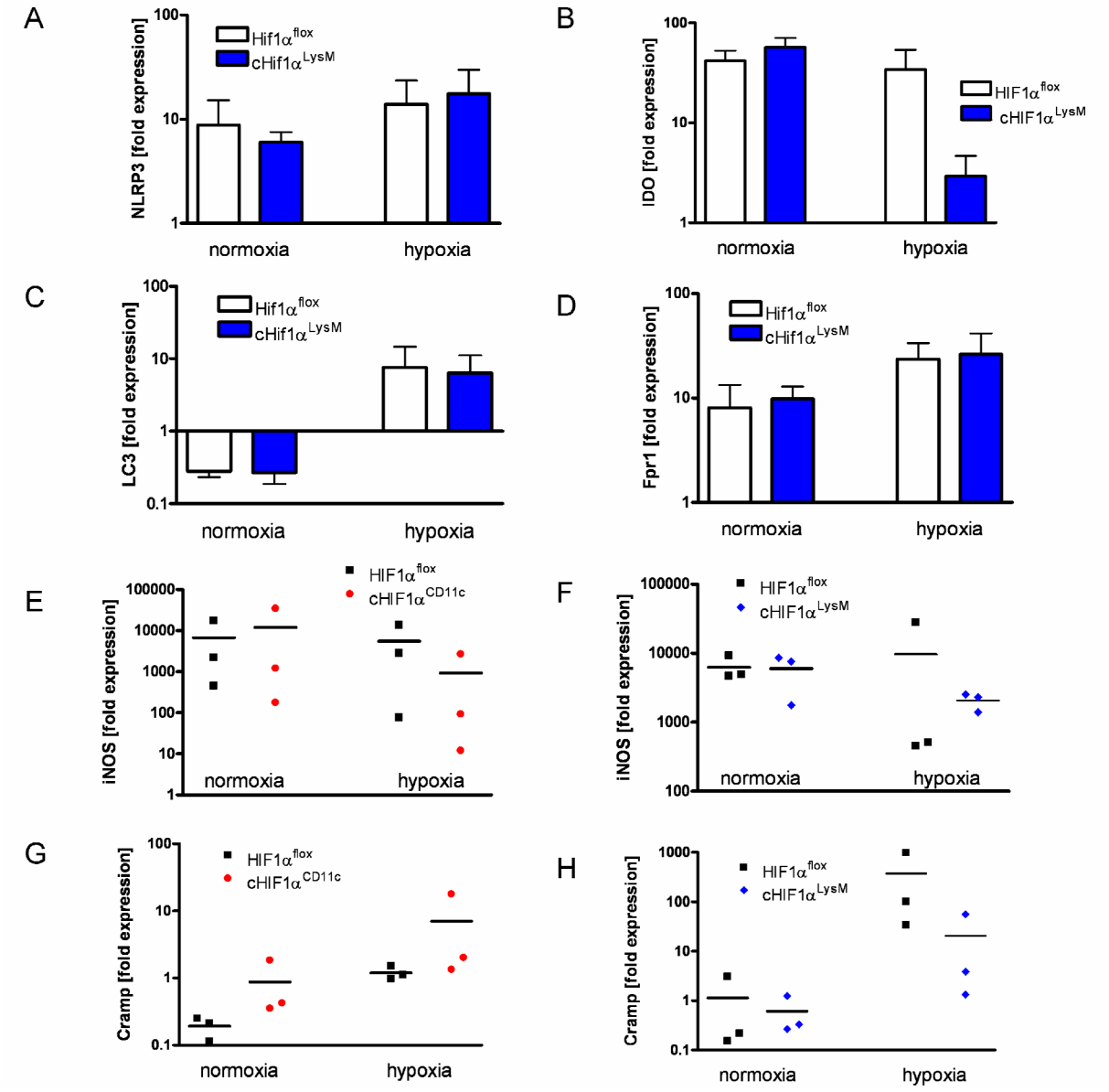

Figure 3.19 Infection-associated changes in gene expression. BMDC of HIF1α^{flox} and cHIF1α^{CD11c} mice and BMMΦ of HIF1α^{flox} and cHIF1α^{LysM} mice were cultured at 21% O_2 or under hypoxic conditions. RNA was isolated 3 h after LPS stimulation and expression of **(A)** NLRP3, **(B)** IDO, **(C)** LC3, **(D)** Fpr1, **(E and F)** iNOS and **(G and H)** Cramp was determined by relative quantification. Expression levels of unstimulated normoxic HIF1α^{flox} cells were set to 1. Results are depicted as mean + SEM of at least 3 independent experiments, (n = 3).

3.5 Expression of HIF2α in BMDC and BMMΦ

As many hypoxia-driven effects in BMDC and BMMΦ occur independently of HIF1α, an obvious candidate to compensate for the HIF1α-deficiency is HIF2α. HIF2α structurally, as well as functionally, resembles HIF1α [114-115]. The distribution of HIF2α throughout the body is not very well characterized. In hypoxic rats, HIF2α was found to be expressed in all organs, although only distinct cell types in these tissues

showed nuclear accumulation of HIF2α [116]. To investigate, if HIF2α is expressed in BMDC and BMMΦ and if HIF2α might regulate the HIF1α-independent hypoxia-driven effects, RT-PCR was conducted to quantify RNA levels of HIF2α. Analysis of HIF2α expression in BMDC and BMMΦ revealed that, surprisingly, in BMDC almost no transcripts of HIF2α were detectable. Only marginal amounts of HIF2α levels were detected in LPS-stimulated cHIF1α^{CD11c} BMDC under normoxic conditions, but not in hypoxia (Figure 3.20 left). In contrast, expression of HIF2α was clearly detectable in BMMΦ. The levels of HIF2α were higher in unstimulated BMMΦ, which was surprising, because HIF1α is known to be induced by LPS stimulation [56]. An increase of HIF2α levels was seen in hypoxic BMMΦ compared with normoxic BMMΦ. Comparing HIF1α-deficient BMMΦ with HIF1α^{flox} BMMΦ, the HIF2α expression was even more prominent in cells with a deletion of HIF1α (Figure 3.20 right). These results show that, at least on transcript levels, HIF2α is differentially expressed in BMDC and BMMΦ. Since HIF2α is increased in HIF1α-deficient BMMΦ, a compensatory effect of HIF2α in this cell type has to be considered.

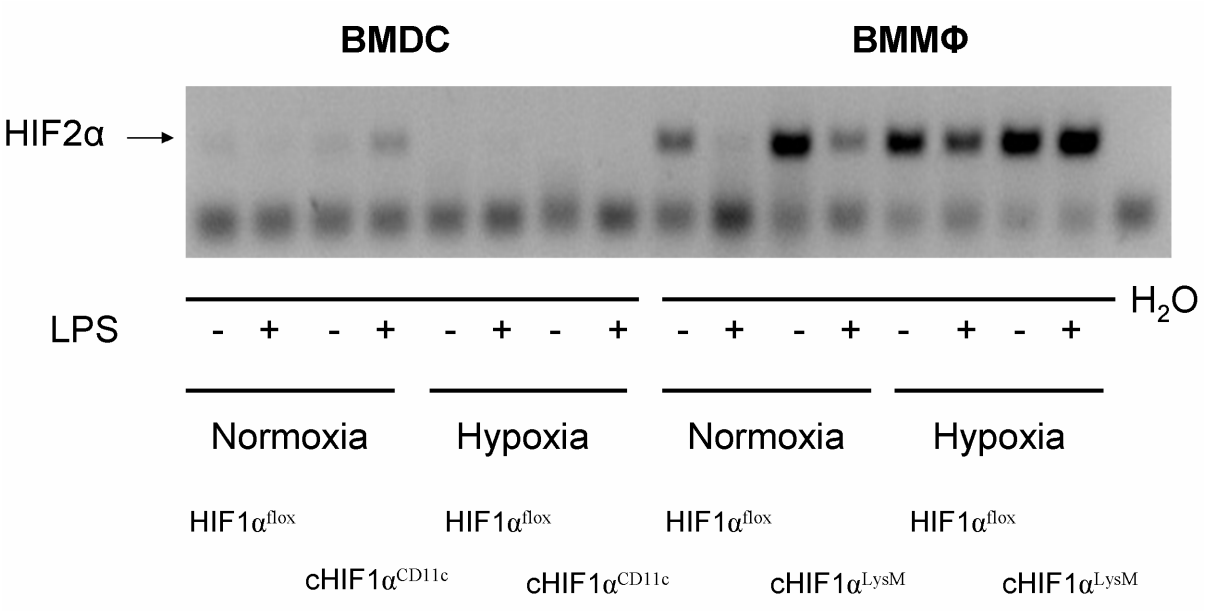

Figure 3.20 Expression of HIF2α in BMDC and BMMΦ. BMDC of HIF1α^{flox} and cHIF1α^{CD11c} mice and BMMΦ of HIF1α^{flox} and cHIF1α^{LysM} mice were cultured at 21% O_2 or under hypoxic conditions. RNA was isolated 3 h after LPS stimulation and expression of HIF2α was determined by RT-PCR and subsequent analysis by gel electrophoresis, (n = 2).

4 DISCUSSION

Oxygen tensions in our body differ not only from those in ambient air, but also from tissue to tissue, depending on blood perfusion and anatomy of the organ. So far, a lot is known about the function of hypoxia during angiogenesis and vascularisation, but the role in innate immunity is not well characterized yet. Immune cells are able to circulate through the body to home to lymphoid organs or to immigrate to the site of infection. As they migrate through different tissues, immune cells frequently are exposed to changing oxygen concentrations and need to adapt rapidly to these conditions. Therefore, it is of special interest to investigate the capacity of innate immune cells to react to alterations in oxygen tension. In this study, the role of hypoxia in differentiation and function of important cell types of the innate immune system, DC and MΦ, was analyzed. Phenotypical and functional changes of both cell types were analyzed *in vitro* and additionally investigated in diverse disease models, such as CHS and bacterial infections. HIF1α is a transcription factor regulating the adaptation of cell metabolism to hypoxia. To analyze the contribution of HIF1α to hypoxia-induced changes in DC and MΦ, conditional knockout mice were used. These mice show a cell type-specific deletion of HIF1α, either in DC or in MΦ. By generation of DC and MΦ from these mice under normoxic and hypoxic conditions, it was possible to identify HIF1α-dependent and HIF1α-independent genes, which were regulated by hypoxia. Additionally, the role of hypoxia and the function of HIF1α were compared between DC and MΦ revealing striking differences in the regulation of hypoxia-induced changes by HIF1α. In the following, I would first like to evaluate the role of hypoxia in the innate immune system and during infection. Later the function of HIF1α in different types of cells and under pathological conditions will be discussed, finally leading to new insights and new hypotheses in the field of hypoxia.

4.1 The impact of hypoxia on DC and MΦ

In this thesis, previously unknown effects of hypoxia on differentiation and functional characteristics of DC and MΦ were discovered. One of the first findings was that generation of BMDC and BMMΦ in hypoxia leads to impaired growth of both cell types (Figure 3.3A and 3.8A). The decreased number of cells generated in hypoxia might be due to the switch from the highly efficient aerobic oxidative phosphorylation

to anaerobic glycolysis, which produces only low amounts of ATP [57]. Apoptotic pathways might also play a role during hypoxic cell differentiation. Phenotypical maturation of BMDC marked by upregulation of the surface molecules MHCII and CD86 (Figure 3.3D) confirmed previous studies showing maturation of immature human monocyte-derived DC within hypoxic environments [91-92, 117], but also of murine BMDC with or without LPS stimulation under hypoxia [118-119]. It appears that hypoxia can act as a danger signal, just like DAMPs or PAMPs. Nevertheless, the inhibition of maturation markers on DC by low oxygen concentrations [120-121] or no influence at all [122] was also reported. These differences could be explained by the fact that cells from different species were analyzed, or by differences in the specific experimental set-up. In conclusion, both findings, inhibition of growth and induction of maturation of hypoxic BMDC, lead to the assumption that hypoxic conditions might induce a shift from a rather proliferating to a differentiating phenotype. This is further supported by the finding that 0.1% oxygen induced cell cycle arrest and granulo-monocytic differentiation of a murine myeloid progenitor cell line [123].

Regarding the functionality of BMDC, a strong influence of low oxygen tensions on cytokine secretion was discovered. Production of the proinflammatory cytokines IL-12p70, IL-6, TNFα and IL-1β, but also of the anti-inflammatory cytokine IL-10 was downregulated in BMDC generated in hypoxia (Figure 3.4). In $HIF1\alpha^{flox}$ BMMΦ, hypoxia did not have an effect on the secretion of IL-12p70, TNFα and IL-23, whereas IL-10 was strongly suppressed in conditions of low oxygen (Figure 3.9), indicating that anti-inflammatory responses of MΦ might be diminished in hypoxia. These findings differ from those, which report an upregulation of IL-10 [117] and an induction of the proinflammatory cytokines TNFα and IL-1β in an oxygen-deprived milieu in human monocyte-derived DC [124]. Murine BMDC, generated under normoxic conditions and exposed to hypoxia for 24 h, showed increased levels of TNF and IL-6 [118]. One group of researchers, however, demonstrated a downregulation of cytokine production of human DC in hypoxia [91].

Surprisingly, the production of IL-22 was induced by hypoxia in BMDC (Figure 3.4A). Hypoxic BMMΦ also revealed upregulation of IL-22 secretion compared with normoxic BMMΦ, although levels of IL-22 were much lower compared with BMDC (Figure 3.9). So far, there is only one report in the literature, in which BMDC were shown to produce IL-22. However, this was seen only after IL-23 stimulation [55].

Interestingly, peritoneal MΦ derived from IL-10-deficient mice produce high levels of IL-22 after LPS stimulation [125], which might be in line with the data shown in this study, that IL-10 is strongly suppressed in hypoxic BMMΦ (Figure 3.9). IL-22 is known to induce anti-microbial peptides and differentiation-associated proteins in keratinocytes and epithelial cells [89]. This cytokine also confers protection for the integrity of the gut epithelium during mucosal inflammation [126]. IL-22-deficient mice were not able to efficiently clear intestinal infections with *Citrobacter rodentium* [55]. The importance of IL-22 in the host defence against bacteria is further illustrated in a model of *Klebsiella pneumoniae* infection, where treatment of mice with a neutralizing antibody to IL-22 caused an increase in bacterial burden [96].

Another prominent effect of hypoxia on BMDC was the upregulation of CCR7 (Figure 3.5A) and accordingly the enhanced capacity for migration, which was observed in two independent assays (Figure 3.6). CCR7 has been reported to be upregulated in lung cancer cells in low oxygen conditions [127], whereas CCR7 was seen to be downregulated on T cells in hypoxia [128]. In contrast to a study reporting an upregulation of CXCR4 in monocytes, MΦ, endothelial cells and cancer cells after stimulation with low oxygen concentrations [129], I observed no effect of hypoxia on the expression of CXCR4 and CCR5 on BMDC (Figure 3.5A). In hypoxic BMMΦ, on the other hand, the expression of both chemokine receptors was decreased (Figure 3.10A). The inhibition of CCR5 in murine MΦ by hypoxia was reported before [130]. Two independent studies showed an upregulation of CCR5 and an impaired upregulation of CCR7 on hypoxic human immature monocyte-derived DC [92, 124]. The hypoxia-induced upregulation of CCR7, seen in this study, went along with an enhanced migration of HIF1α^{flox} BMDC in hypoxia, which was shown in two independent assays, using transwell chambers and an adoptive transfer of *in vitro* generated BMDC (Figure 3.6). These results were not confirmed by other groups; instead it was shown that hypoxia has a suppressive effect on the ability of human monocyte-derived DC to migrate because of an upregulation of tissue inhibitors of matrix metalloproteinases (TIMP) and downregulation of matrix metalloproteinases (MMP) in hypoxic DC [131-132]. These controversial results might be caused by inter-species differences or different experimental procedures. Anyhow, it would be interesting to investigate the expression of tissue inhibitors of matrix metalloproteinases (TIMP) and of matrix metalloproteinases (MMP) in murine BMDC generated under normoxic and under hypoxic conditions.

In this study, an increased secretion of the chemokines CCL17 and CCL22 was detected after LPS stimulation under hypoxic conditions (Figure 3.5B). This probably also contributes to the enhanced capacity of hypoxic HIF1α^{flox} DC to migrate, since it was shown before that CCL17 is required for migration of cutaneous DC [10]. The enhanced production of these chemokines was also found in hypoxic BMMΦ, although these cells produced much lower amounts compared with BMDC (Figure 3.10B). Although it was shown before that especially M2 MΦ are able to produce CCL17 and CCL22 [133], LPS induction of M1 MΦ usually leads to the secretion of CCL2, CCL3, CCL3 and CCL5 [134], which were not tested in this study.

Since certain chemokines and chemokine receptors are increased under hypoxic conditions (Figure 3.5), the reduced cytokine production in hypoxic BMDC apparently is not simply a result of a generally decreased protein translation as a consequence of a disturbed energy metabolism. Taken together, hypoxia differentially influences BMDC and BMMΦ regarding the expression of maturation markers, cytokine secretion and chemokine, as well as chemokine receptor expression. Hypoxic BMDC upregulated their surface maturation markers and downregulated most of the cytokines tested, whereas hypoxia did not influence BMMΦ regarding the expression of surface molecules, as well as the expression of the cytokines IL-12p70, TNFα and IL-23. An important finding in BMDC was the hypoxia-induced increase of CCR7 expression and the enhanced capability to migrate in a hypoxic milieu. On the other hand, similar effects of hypoxia on BMDC and BMMΦ were the growth reduction and the strong induction of chemokine expression. Additionally, IL-22 was upregulated in both innate immune cell types under hypoxic conditions, which is an interesting finding and has so far not been shown before.

4.2 Hypoxia as a hallmark of infection

As low oxygen tensions represent a major feature of local inflammation in the course of bacterial infections, BMDC and BMMΦ differentiated in normoxia and hypoxia were challenged with different types of bacteria again under normoxic and hypoxic conditions. One prominent finding was that both cell types survived better in co-cultures with bacteria in an oxygen-deprived environment compared with a normoxic milieu. BMMΦ showed increased survival in anoxia compared with normoxia, when infected with *S. aureus* (Figure 3.11B upper panel), *L. monocytogenes* (Figure 3.13B

upper panel) or *E. coli* (Figure 3.17B upper panel). Similarly, BMDC showed stronger resistance to GBS (Figure 3.16A upper panel) and to *E. coli* (Figure 3.17A upper panel) in an oxygen-deprived milieu. Here, I addressed the question, if the increased viability of immune cells is due to reduced replication rates of bacteria under anoxic conditions versus normoxic conditions. I found that growth of *S. aureus* and *E. coli* did not differ between anoxic and normally oxygenated conditions. Only *L. monocytogenes*, which usually replicate intracellularly, revealed a tenfold reduced growth under anoxic conditions compared with normoxic conditions. This finding might also account for the increase in viability of anoxic BMMΦ infected with *L. monocytogenes*.

So far, no study has addressed the viability of cells infected with bacteria in hypoxia since most projects focus on the bactericidal capacity of phagocytes.

In the present study, the ability of BMDC and BMMΦ to kill pathogens was also addressed and I could show that anoxia increases the capacity of BMMΦ to kill intracellular *L. monocytogenes* (Figure 3.13B lower panel). I could not find any differences regarding the bacterial burden of BMDC or BMMΦ in an oxygen-deprived environment compared with normoxic conditions, when they were infected with extracellular bacteria, such as *S. aureus* (Figure 3.11 lower panel), GAS (Figure 3.15 lower panel), GBS (Figure 3.16 lower panel) or *E. coli* (Figure 3.17 lower panel). Recently, it was reported that the ability to kill ingested *S. aureus* and *E. coli* is impaired in hypoxic murine BMMΦ [135]. In contrast, several papers showed enhanced killing of the intracellular parasite *Leishmania amazoniensis* in hypoxia, when human DC or MΦ were infected [25, 136]. This goes in line with the finding in this study that less *L. monocytogenes* survived, when hypoxic BMMΦ were infected. In the studies dealing with *Leishmania amazoniensis*, as well as in the experiments I conducted with *L. monocytogenes*, the intracellular lifestyle of both pathogens might be the key to the increased bactericidal capacity of phagocytes in an oxygen-deprived milieu. But not only the killing of intracellular and extracellular bacteria might be affected differentially by hypoxia, also the mechanisms activated to kill pathogens are differentially influenced by conditions of low oxygen. This was shown in human neutrophils, which act differentially under hypoxia, since they show a reduction of *S. aureus* killing due to a defect in the NADPH-oxidase-dependent respiratory burst, but still maintain their capacity to efficiently kill *E. coli*, which is NADPH-oxidase-independent [137]. Similar results were found, when RAW MΦ were infected with

non-pathogenic *E. coli* and bactericidal activity was enhanced by hypoxia [138]. It seems that the capacity to kill bacteria depends on a variety of parameters, such as species, cell type, differentiation and maturation status of the cell and, of course, on the type of bacteria. Bacteria have evolved different mechanisms to attack cells and to escape the host immune system. Similarly, innate immune cells have developed a variety of specialized methods to cope with bacteria and to counteract their actions. Anyhow, it is important to note that oxygen-deprived conditions increase the survival of phagocytes during bacterial infections and enhance the bactericidal functions of BMMΦ against intracellular pathogens, as seen, when infecting BMMΦ with *L. monocytogenes* under anoxic conditions.

To unravel the molecular mechanisms playing a role in host defence under hypoxic conditions, expression of several candidate genes conferring antimicrobial and immuno-modulating functions to BMDC and BMMΦ was investigated. Expression of NLRP3 was enhanced in hypoxic BMMΦ (Figure 3.19A). Activation of the NLRP3-inflammasome by a wide range of bacteria and bacterial products leads to secretion of IL-1β and IL-18, which both have been shown to act protective during several infection models [139]. Since the absence of NLRP3 and AIM2, another molecule involved in formation of the inflammasome, in *L. monocytogenes*-infected MΦ leads to increased replication rates of the bacteria [140], it can be speculated that there is a connection between the increased NLRP3 expression in hypoxia and the decrease of intracellular burden of *L. monocytogenes* in hypoxic BMMΦ, as well as the enhanced viability of hypoxic BMMΦ. Fpr1 was also enhanced in hypoxic BMMΦ (Figure 3.19C). Activation of this receptor leads to enhanced phagocytosis of bacteria and production of ROS [8]. Therefore, the increased expression of Fpr1, at least in part, may explain the enhanced survival of hypoxic BMMΦ in co-cultures with bacteria and the decreased bacterial burden of *L. monocytogenes* under hypoxic conditions, probably by increasing the phagocytotic activity of BMMΦ. LC3, implicated in autophagy, showed a strong upregulation in BMMΦ in an oxygen-low milieu (Figure 3.19D). There are several reports showing that hypoxia enhances autophagy, as described in [141-142], where the importance of this self-digesting mechanism as a nutrient-recycling and ROS-producing process is discussed in context with cancer. Autophagy can decisively influence the outcome of bacterial infections and is accompanied by upregulation of LC3 [46]. The increased expression of LC3 under hypoxic conditions, indicating the induction of autophagy in hypoxic BMMΦ, might

account for the enhanced survival of these cells in oxygen-deprived conditions. Especially, the reduced bacterial burden of intracellular *L. monocytogenes* in hypoxia could be explained by autophagy induction under conditions of low oxygen availability.

In contrast to iNOS, which was unaffected by hypoxia (Figure 3.19 E and F), Cramp, an antimicrobial peptide, was induced in BMDC, as well as in BMMΦ under oxygen-deprived conditions (Figure 3.19 G and H). Cramp was previously shown to be induced by hypoxia [73] and might contribute to the enhanced bactericidal capacity of hypoxic BMMΦ during *L. monocytogenes* infection. In BMDC, upregulation of Cramp was accompanied by an increased capability to kill bacteria. However, these results obtained by qRT-PCR of LPS stimulated cells have to be evaluated critically. LPS induced TLR4 activation reflects only a part of the machinery activated by bacteria. Special microbial products derived from *S. aureus*, *L. monocytogenes*, GAS, GBS or *E. coli* trigger a variety of different signalling pathways.

For technical reasons, in some experiments anoxic conditions were used instead of hypoxia. It has to be considered that concentrations below 1% oxygen might affect BMDC and BMMΦ, as well as the bacteria in a different way than 1% oxygen. The anoxomat cannot completely eliminate all oxygen and a rest of 0.1 -0.2% oxygen is left inside the incubation jars. Other groups have performed experiments in conditions of 0.1 -0.2% oxygen and defined these concentrations as hypoxia [73, 143-144]. In another study, the effects of extremely low oxygen concentration on a murine haematopoietic cell line were investigated. In 0.1% oxygen, these cells showed growth arrest, which was not due to apoptosis rather than to cell cycle arrest [123]. *S. aureus*, *L. monocytogenes* and *E. coli* are facultative anaerobe bacteria, which use oxygen for respiration, if available. In oxygen-deprived environments, they use alternative mechanisms for energy metabolism such as fermentation and nitrate respiration [27-28, 145]. Since aerobic respiration occurs above 0.5% oxygen, anaerobic respiration between 0.1% and 0.5% oxygen, and fermentation occurs below 0.1% oxygen [146], there might be critical differences in the bacterial metabolism, which might differentially influence the experiments either in hypoxia or in anoxia.

In addition to that, is has to be considered that the presence or the absence of oxygen also affects expression of bacterial genes responsible for bacterial pathogenicity [146]. In *S. aureus*, for example, oxygen depletion was found to induce various bacterial virulence factors [28]. This might influence pathogen recognition and the host defence of BMDC and BMMΦ.

In summary, I could show that under hypoxic conditions gene expression of NLRP3, LC3 and Fpr1 is enhanced in BMMΦ and gene expression of Cramp is induced in BMDC and BMMΦ. The upregulation of these genes might contribute to the enhanced cell survival and the increased capacity to kill bacteria under hypoxia.

4.3 Characterization of transgenic Cre-lines for cell-type specific deletion of HIF1α

To unravel the molecular mechanism causing these hypoxia-induced changes, I used several mouse lines, which show cell-type specific ablation of HIF1α either in DC (CD11cCre), in CCL17-positive DC (CCL17Cre) or MΦ (LysMCre). The transcription factor HIF1α is the key regulator of gene expression in an oxygen-deprived milieu. First, HIF1α^{flox} mice were crossed to the CD11cCre line [78]. Analyzing the efficiency of HIF1α-deletion, I could show that more than 90% of the BMDC generated *in vitro* revealed Cre-recombination of the HIF1α gene (Figure 3.2B). However, it was also evident from this study that the Cre-recombinase is also active in a major subset of T cells, as shown clearly in the crosses to HIF1αflox and RA/EG mice in this study (Figure 3.2B and C). In other conditional mutant mice, T cells have also been reported to be affected by the Cre-recombinase expressed under the promoter of CD11c, although to a lesser extent [78, 147-148]. Therefore, phenotypic changes in *in vivo* studies of cHIF1α^{CD11c} mice have to be interpreted critically as they may also result from T cell-dependent effects [68, 70-71].

Additionally, HIF1α^{flox} mice were crossed to the CCL17Cre line to induce deletion of HIF1α only in the CCL17-positive subset of DC. In BMDC generated from the bone marrow of cHIF1α^{CCL17} mice, I could detect a HIF1α-deletion efficiency of 95% (Figure 3.2B). In contrast to cHIF1α^{CD11c} mice this cross did not show deletion in the T cell compartment (Figure 3.2B). In mice from the cHIF1α^{CCL17} line, HIF1α-deletion affects only the CCL17-producing DC subset that is mainly found in barrier organs like skin, lung and gut [79]. These tissues are frequently confronted with hypoxia, in

particular in inflamed areas, where $CCL17^+$ DC represent potent sentinels for incoming pathogens.

As MΦ are important APC acting in areas of low oxygen content and frequent changes of oxygen tension, the HIF1αflox line was crossed to LysMCre mice [80] to specifically delete HIF1α in myeloid cells. A deletion efficiency of 83-98% was reported for mature macrophages and in granulocytes the loxP flanked gene was exised in nearly 100% of the cells [80]. In conclusion, the $cHIF1\alpha^{LysM}$ mouse represents an adequate model to investigate the function of HIF1α in *in vitro* generated BMMΦ, as well as *in vivo* studies. Both mouse lines with specific deletions of HIF1α in DC are suitable for analysis of HIF1α in *in vitro* generated BMDC, since the Cre-recombinase is active in almost 100% of the cells. In *in vivo* models of diseases employing these mice, it has to be considered that in $cHIF1\alpha^{CCL17}$ mice only a subset of peripheral DC is affected by HIF1α-deletion, whereas in $cHIF1\alpha^{CD11c}$ mice, next to DC, a large proportion of T cells is affected by HIF1α-deletion. Depending on the study, this might influence the outcome of the experiments, as deficiency of HIF1α in T cells was shown to strongly change the function [68] and differentiation [69] of T cells.

4.4 The role of HIF1α in hypoxia-induced changes in BMDC

To analyze the HIF1α-dependent and the HIF1α-independent signalling pathways leading to the cellular response to hypoxia, BMDC from $cHIF1\alpha^{CD11c}$ and $cHIF1\alpha^{CCL17}$mice, as well as BMMΦ from $cHIF1\alpha^{LysM}$ mice were analyzed in comparison to $HIF1\alpha^{flox}$ mice as controls and examined for their phenotype and functionality under hypoxic conditions. BMDC with a deletion of HIF1α revealed minimal, but notable deficits in growth, as well as reduced surface expression of CD11c in comparison with $HIF1\alpha^{flox}$ BMDC in hypoxia (Figure 3.3A). This might result from a disturbed energy metabolism in the absence of HIF1α [57], which was also reflected in the reduced production of ATP in hypoxic $cHIF1\alpha^{CD11c}$ BMDC (Figure 3.3B).

As expected, CD73, which is a known target of HIF1α in epithelial cells [88], was induced HIF1α-dependently in conditions of low oxygen (Figure 3.3C).

I could not find an influence of the presence or absence of HIF1α on the hypoxia-induced upregulation of surface maturation markers (Figure 3.3D), although a study

describes an inhibition of BMDC maturation after knockdown of HIF1α with siRNA in hypoxia as well as in normoxia [118]. However, it is difficult to compare both studies, as siRNA was applied to BMDC generated under normoxia prior to the hypoxic incubation of 16 hours [118], whereas in this study the BMDC were already differentiated in hypoxia.

Since hypoxia leads to reduced production of cytokines, the question was addressed, if HIF1α contributes to this functional alteration. As hypoxic HIF1α-deficient BMDC downregulate these cytokines to the same extent as hypoxic HIF1α-proficient BMDC, it can be concluded that the inhibition of the secretion of the respective cytokines is regulated independently of HIF1α expression (Figure 3.4A). Interestingly, IL-22 was strongly induced by hypoxia in HIF1α^{flox} BMDC, but to a lesser extent in hypoxic cHIF1α^{CCL17} BMDC and even lower in hypoxic cHIF1α^{CD11c} BMDC. Therefore, it can be concluded that the secretion of IL-22 by BMDC in an oxygen-deprived milieu is, at least in part, dependent on HIF1α (Figure 3.4A). So far, neither the induction of IL-22 by hypoxia, nor the dependency of the IL-22 expression on HIF1α has been reported before.

Another major finding was that hypoxia enhanced the migration of BMDC, at least in part, due to a HIF1α-dependent upregulation of CCR7 in hypoxia (Figure 3.5A). Additionally, CXCR4 was expressed at lower levels in cHIF1α^{CD11c} BMDC compared with HIF1α^{flox} BMDC in 1% oxygen (Figure 3.5A). Upregulation of CCR7 in hypoxic BMDC could lead to enhanced capacity of these cells to migrate towards CCL19 in chemokine-driven transwell experiments *in vitro*. Additionally, footpad migration assays *in vivo* were carried out (Figure 3.6), showing that the ability of BMDC to migrate *in vivo* was enhanced, when they were generated in hypoxia. By employment of HIF1α-deficient BMDC, I was able to illustrate the importance of the expression of HIF1α for this process. Deletion of HIF1α in BMDC inhibited the hypoxia-induced enhanced migration of BMDC (Figure 3.6). Previously, it was shown in transwell assays with a lung cell line treated with siRNA against HIF1α and HIF2α, that these factors are responsible for induction of CCR7 and migration in an hypoxic milieu [127]. Both HIF1α and HIF2α were demonstrated to be necessary for hypoxia-induced upregulation of CXCR4 in MΦ [149].

In the following scheme the regulation of hypoxia-induced changes in BMDC is summarized (Figure 4.1).

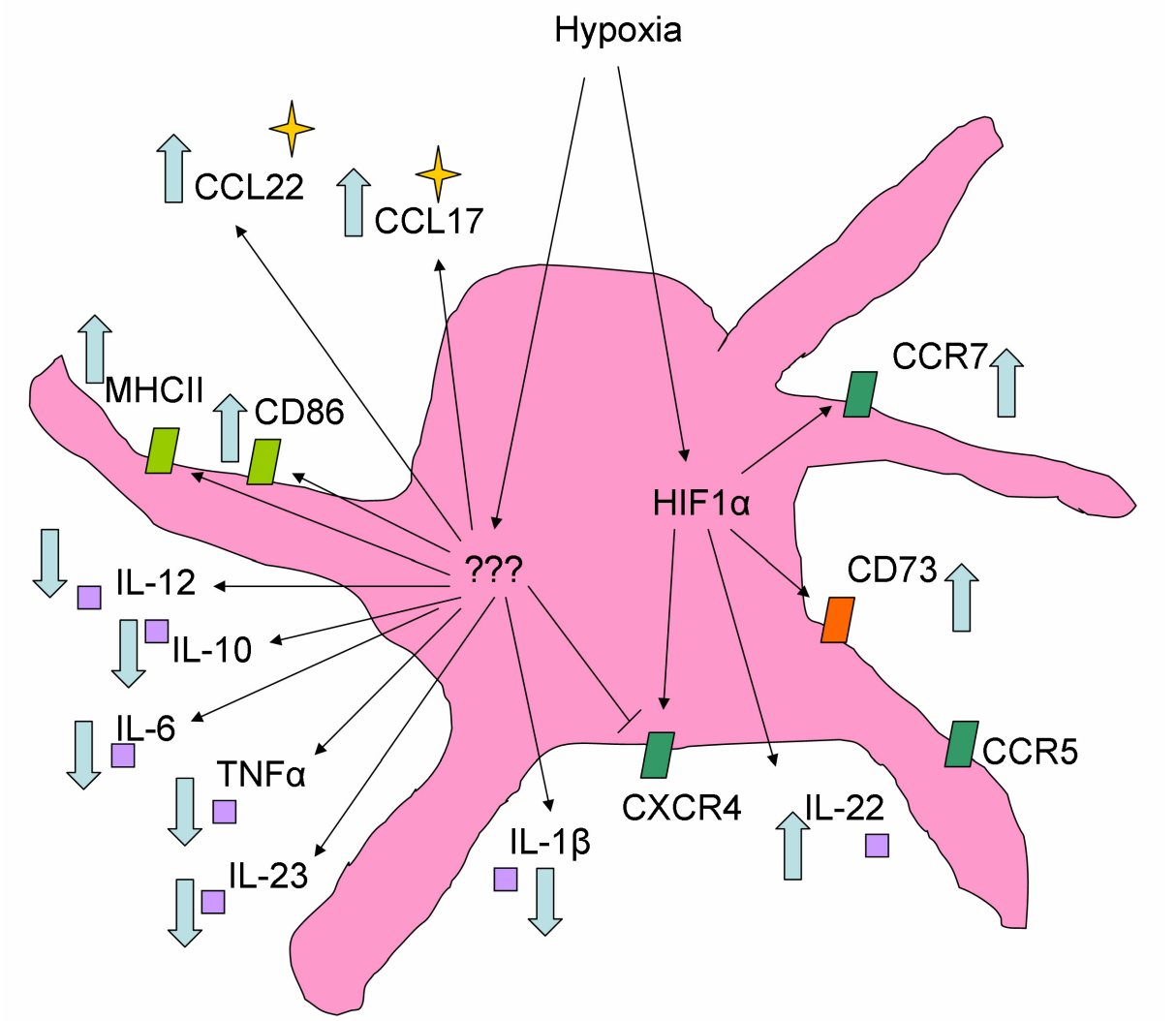

Figure 4.1 Regulation of hypoxia-induced changes in BMDC. Under hypoxic conditions a variety of signalling pathways induce cellular changes by activation (thin arrow) and inhibition (flat arrow head) of gene expression. Hypoxia leads to differential expression of certain chemokines (yellow star), surface maturation markers (light green quadrangle), cytokines (purple square) and chemokine receptors (dark green quadrangle).

It was shown in this study that oxygen-deprived conditions have a major influence on the ability of *in vitro* generated BMDC to migrate dependent on the presence of HIF1α. It was not possible to confirm this effect in *in vivo* models, which depend on direct *in vivo* activation of DC by hypoxia and not, as shown for the migration assay, on injection of *in vitro* generated hypoxic BMDC.

First a CTL assay was carried out, in which migration of DC is required to prime CD8 T cells. The ability of CD8-positive T cells to kill target cells in HIF1α^{flox} mice compared with cHIF1α^{CD11c} and cHIF1α^{CCL17} mice was unchanged (Figure 3.7A). This might be due to the fact, that the subcutaneous OVA/CpG injection did not induce hypoxic conditions in the tissue. It has been reported that even under non-inflammatory conditions the epidermis is hypoxic [150], but OVA/CpG was injected

into the dermis or even deeper lying tissues with better perfusion and therefore better oxygenation. Although CTL in cHIF1α^{CCL17} mice displayed comparable killing rates to HIF1α^{flox} mice, it has to be considered that a substantial proportion of CD8-positive T cells in cHIF1α^{CD11c} mice showed also deletion of HIF1α. Since HIF1α-deficiency in T cells can increase their cytokine production [68] and also results in diminished Th17 differentiation [71], differential behavior of CTL may counteract effects induced by HIF1α-deficient DC in these mice.

Next, a model of CHS was applied using DNFB as contact allergen. CCL17-positive Langerhans cells and dermal DC from HIF1α^{flox}, cHIF1α^{CCL17} and cHIF1α^{CD11c} mice were able to efficiently prime T cells and no difference in ear swelling was seen (Figure 3.7B). The contact sensitizer DNFB induces a strong immune reaction and irritation of the skin, resulting in an immune response, which might lead to hypoxia. Therefore, I expected the skin to be hypoxic after DNFB sensitization. But also in this model, T cells play a major role during the challenge phase, so that HIF1α-deficiency of a large proportion of T cells in cHIF1α^{CD11c} mice might also influence the outcome of the experiments. However, T cells of cHIF1α^{CCL17} mice do not show deletion of HIF1α, but still no defects in induction of the ear swelling of these mice were detected. Since cHIF1α^{CCL17} mice only express the chemokine CCL17 on one allele, and CCL17 is required for DC migration and induction of CHS [10], I would have expected a reduced immune response in these mice.

In the FITC migration assay, Langerhans cells and dermal DC of HIF1α^{flox}, cHIF1α^{CCL17} and cHIF1α^{CD11c} mice migrated equally well to the draining LN (Figure 3.7C). FITC does not induce a strong skin irritation and it can be assumed, that the oxygen concentration in the tissue is not low enough to induce HIF1α. This might be the reason for the absence of effects of the HIF1α-deficiency in DC using this assay.

4.5 The role of HIF1α in hypoxia-induced changes in BMMΦ

Compared with BMDC, BMMΦ were affected in a different way by hypoxia and HIF1α played a differential role in regulating hypoxia-induced changes in these two cell types. Only HIF1α-deficient BMMΦ seemed to be affected by hypoxia, whereas HIF1α^{flox} BMMΦ generated in conditions of low oxygen revealed no changes compared with normoxic BMMΦ. The maturation marker CD86, as well as the MΦ-characteristic surface molecule F4/80, were upregulated in HIF1α-deficient hypoxic

BMMΦ (Figure 3.8C). Increased secretion of IL-12p70, TNFα, IL-23 and, to a lesser extent, IL-22 was restricted to cHIF1α^{LysM} BMMΦ generated in hypoxia. In contrast, IL-10 was strongly inhibited in HIF1α-deficient BMMΦ, even under normoxic conditions (Figure 3.9). High production of IL-12, TNF and IL-23, as well as high expression of CD86 and low secretion of IL-10 are characteristic features of classically activated M1 MΦ [134]. Therefore, it seems that the absence of HIF1α leads to a M1 polarization, whereas the presence of HIF1α somehow suppresses this MΦ activation.

Analysis of chemokine receptor expression under hypoxic conditions showed that CCR5 was upregulated, when HIF1α was absent in hypoxic BMMΦ, whereas the hypoxia-induced downregulation of CXCR4 was not affected by deletion of HIF1α in BMMΦ (Figure 3.10A). This kind of expression pattern has not been observed before. Other studies have demonstrated a dependency on HIF1α of the expression of IL1-β, VEGF and CXCL8, in hypoxic human MΦ [149] or mast cells [151]. I could detect a HIF1α-dependent upregulation of the chemokines CCL17 and CCL22 in BMMΦ in a hypoxic milieu (Figure 3.10B), although compared with BMDC, BMMΦ only produce very low amounts of these chemokines. Interestingly, the expression of these chemokines in hypoxia is depended on HIF1α in BMMΦ, but not in BMDC. The downregulation of CCL17 and CCL22 in hypoxic HIF1α-deficient BMMΦ confirms my hypothesis that HIF1α rather favors an alternatively activated M2 polarization of MΦ, than a classical M1 activation, since high expression of CCL17 and CCL22 is characteristic for M2 MΦ [134]. Against this hypothesis, I found a publication reporting that deletion of HIF1α in TAM enhances the M2 polarization of MΦ, since they reduce secretion of TNFα, IL-6 and iNOS. However, this study was not carried out under hypoxic conditions, instead TAM were co-cultured with tumour spheroids [152].

Surprisingly, the increased maturation was HIF1α-independent in hypoxic BMDC, whereas in hypoxic BMMΦ the increased maturation was induced upon deletion of HIF1α. To explain this exceptional phenotype of hypoxic BMMΦ, I assume, that hypoxia induces activation of BMMΦ independently of HIF1α. Simultaneous expression of HIF1α somehow inhibits this activation in HIF1α-proficient hypoxic BMMΦ. In the following scheme the regulation of hypoxia-induced changes in BMMΦ is summarized (Figure 4.2).

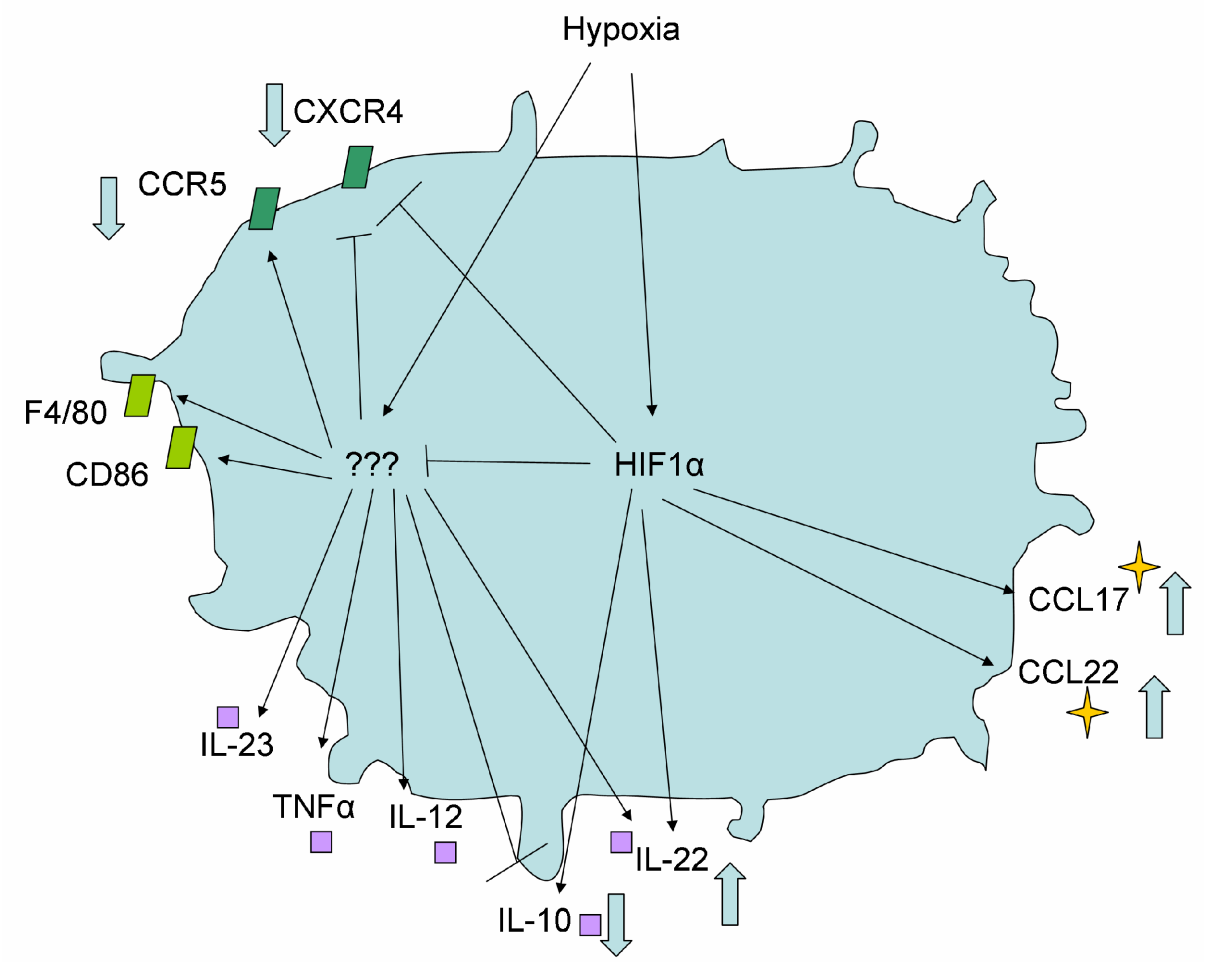

Figure 4.2 Regulation of hypoxia-induced changes in BMMΦ. Under hypoxic conditions a variety of signalling pathways induce cellular changes by activation (thin arrow) and inhibition (flat arrow head) of gene expression. Hypoxia leads to differential expression of chemokines (yellow star), surface markers (light green quadrangle), cytokines (purple square) and chemokine receptors (dark green quadrangle).

4.6 The function of HIF1α during infection

It is known that HIF1α accumulates in different cell-types in response to bacterial stimulation [153]. To find out, if HIF1α affects host defence of innate immune cells, BMMΦ and BMDC were infected *in vitro* with various types of bacteria under normoxic and hypoxic conditions. Further, *in vivo* infection models were applied, in which DC and MΦ presumably need to act under hypoxic conditions. Cell survival and intracellular survival of bacteria was analyzed. HIF1α-deficiency inhibited efficient killing of *E. coli* in BMMΦ generated in a hypoxic milieu (Figure 3.17B lower panel). Furthermore, BMMΦ from cHIF1α^{LysM} mice showed defects in the killing of *L. monocytogenes* in oxygen-deprived conditions (Figure 3.13B lower panel). In infections with *L. monocytogenes in vivo,* however, no difference in bacterial colonization was detected in cHIF1α^{LysM} mice, indicating that the ability of myeloid

cells to kill listeria has not been altered upon deletion of HIF1α. However, an increased accumulation of monocytes and neutrophils was seen in the spleens of cHIF1α^{LysM} mice at day 4 compared to HIF1α^{flox} BMMΦ (Figure 3.14C). As the spleen is one of the main organs, which is colonized by Listeria, it can be assumed, that here monocytes and neutrophils exert bactericidal functions. The increased amount of these HIF1α-deficient myeloid cells in the spleen might be due to changes in expression of chemokines and chemokine receptors, which facilitate the entry of monocytes and neutrophils into the spleen. As seen in *in vitro* experiments, HIF1α-deficient hypoxic BMMΦ show altered expression levels of CCR5, CCL17 and CCL22 (Figure 3.10). The increased frequency of monocytes and neutrophils in the spleen might also be due to functional defects, such as reduced microbicidal capacity caused by HIF1α-deficiency. Therefore, more monocytes and neutrophils might be recruited to the spleen to compensate for the loss of function.

The accumulation of monocytes and neutrophils in spleens of cHIF1α^{LysM} mice was only found at later time points. Therefore, it might be worth to elongate the experiments by reduction of the infection dose to study the influence of the increased frequency of myeloid cells in the spleen on the survival of the mice.

Since intravenous infection of mice with *L. monocytogenes* does not resemble the natural oral route of infection [41], it has to be considered that during oral infection with *L. monocytogenes*, DC and MΦ, as well as HIF1α might play a different role.

Not only hypoxic HIF1α-deficient BMMΦ, but also hypoxic HIF1α-deficient BMDC lost their ability to efficiently kill *E. coli*. However, this was only seen after 1h, but not after 16h co-culturing (Figure 3.17A lower panel). The differences in the bacterial burden between the two time points might be due to induction of genes after different time spans. In reaction to Listeria, for example, human monocyte-derived DC express immediate response genes within the first 2 hours after infection and early response genes 6 hours after infection [154]. HIF1α is stabilized relatively fast in response to hypoxia. Expression of early and late response genes, which encode for antimicrobial proteins, might compensate at later time points for the loss of HIF1α. Additionally, it was reported, that *E. coli* is able to induce apoptosis in RAW MΦ at later time points after infection [155]. This fact might also explain the discrepancy between the results seen after 1 h compared with those after 16 h.

Skin of *S. aureus*-infected cHIF1α^{CD11c} mice displayed increased bacterial loads, which, however, were not statistically significant compared with HIF1α^{flox} mice (Figure

3.12B). In this infection model, the transcription levels of IL-22 in the skin were reduced mildly in cHIF1α^{CD11c} mice (Figure 3.12D), in line with the data, which have shown HIF1α-dependent IL-22 production of hypoxic DC.

Although in this study deletion of HIF1α in MΦ did not affect colonization of *S. aureus* in the skin, it was demonstrated before that induction of HIF1α by the agonist mimosine enhances the bactericidal activity of neutrophils and monocytes during *S. aureus* infection [156]. Others have shown that cHIF1α^{LysM} myeloid cells and cHIF1α^{LysM} mice display major deficits in the killing of diverse types of bacteria, such as GAS, GBS and *Pneumonia aeruginosa* [72-73].

In the third infection model, HIF1α^{flox} mice, cHIF1α^{CD11c} mice and cHIF1α^{LysM} mice were infected with *C. rodentium* and analyzed for bacterial burden in the feces and for changes of body weight. It is known that the gut is a hypoxic tissue even under non-inflammatory conditions and these conditions are further intensified during infections [60]. In addition, it was shown that IL-22 is required for efficient clearance of *C. rodentium* [55]. Nevertheless, no differences in weight loss and bacterial clearance during the course of infection could be detected comparing these mouse strains (Figure 3.21). However, *C. rodentium* utilizes the same mechanism to induce a gastrointestinal infection like the attaching and effacing (A/E) bacterial pathogens, EHEC and EPEC. It is obvious that expression of virulence factors, as well as host defense against these pathogens differ among species. Although deficiency of HIF1α in DC or MΦ did not display any defects in bacterial clearance in this model, HIF1α could be important for host defense against EHEC and EPEC at a different level.

I could show that not only the bactericidal functions of BMMΦ and BMDC generated *in vitro* in hypoxia were affected by HIF1α expression, but also the ability of cells to survive bacterial challenge under oxygen-deprived conditions. BMDC from cHIF1α^{CD11c} mice infected with GAS showed decreased survival rates in hypoxia compared with normoxia (Figure 3.15A upper panel), whereas analysis of HIF1α-deficient BMMΦ revealed a higher viability after infection in an oxygen-deprived environment compared with HIF1α^{flox} BMMΦ (Figure 3.15B upper panel). These results were not statistically significant, but were concordantly found, when infecting hypoxic BMMΦ with *S. aureus* (Figure 3.11B upper panel), *L. monocytogenes* (Figure 3.13B upper panel), GAS (Figure 3.15B upper panel), GBS (Figure 3.16B upper panel) and *E. coli* (Figure 3.17B upper panel). In all cases enhanced viability was found in HIF1α-deficient BMMΦ infected in hypoxia. It can be assumed, that the

enhanced maturation of hypoxic cHIF1α^{LysM} BMMΦ, characterized by upregulated expression of CD86 and CCR5, as well as by increase of cytokine secretion (see above), contributes to the higher resistance to pathogens.

To understand the role of HIF1α in regulation of microbicidal activities and in resistance against pathogens, expression of several infection-associated proteins was analyzed in BMMΦ. Among these, only IDO and Cramp were found to be regulated by HIF1α under hypoxic conditions. Expression of IDO, an anti-inflammatory tryptophan-degrading enzyme, was downregulated in hypoxic HIF1α-deficient BMMΦ (Figure 3.19B). Expression of the anti-microbial peptide Cramp was also inhibited in hypoxic BMMΦ from cHIF1α^{LysM} mice (Figure 3.19H). This confirmed a publication, in which Cramp expression of peritoneal neutrophils was shown to be upregulated by HIF1α [73]. Inhibition of these important effector molecules might explain the defects observed in bacterial killing of hypoxic cHIF1α^{LysM} BMMΦ. Nevertheless, other anti-inflammatory molecules might be involved in host defence of BMDC, since decreased capacity of HIF1α-deficient BMDC to kill *E. coli* under hypoxic conditions did not correlate with Cramp expression.

In none of the three *in vivo* infection models, HIF1α played an obvious role in either DC or MΦ in host defence against pathogens. As these innate immune cells share many characteristics and functional abilities, it might be possible that the defects of HIF1α-deficient DC can be compensated by MΦ, and vice versa. In addition, it is not clear, which oxygen concentrations are found in the different tissues after infection and if HIF1α, is actually stabilized by these conditions. As for the *in vivo* migration studies, the deletion of HIF1α in a substantial proportion of T cells in cHIF1α^{CD11c} mice has also to be taken into account, as changes in T cell differentiation and function could influence the infection models as well [68-69].

However, additionally it has to be considered that results obtained from experiments with mice cannot always easily be applied to humans. For example, a study comparing the *S. aureus* colonization of mice with that of humans has shown that these staphylococci prefer utilization of human hemoglobin to acquire iron, and therefore, mice show less susceptibility to *S. aureus* than humans [157].

Taken together, infection experiments *in vitro* have shown that HIF1α influences the survival of BMDC and BMMΦ, after co-incubation with certain pathogens under hypoxic conditions. Additionally, the capacity to kill bacteria was regulated by HIF1α in conditions of low oxygen, probably by induction of antimicrobial effector molecules.

4.7 Regulation of the cellular response to hypoxia

Several of the phenotypic changes observed in hypoxic BMDC, such as the enhanced maturation (Figure 3.4D) and the altered cytokine production (Figure 3.5), occurred independently of HIF1α expression. Hypoxic BMMΦ upregulated several infection-associated genes, such as NLRP3, LC3 and Fpr1, in a HIF1α-independent manner (Figure 3.19). This indicates that there must be another mechanism besides HIF1α-induced gene transcription, which transmits hypoxia-induced changes. Recently, HIF2α, another member of the family of hypoxia-inducible transcription factors, has been reported to be expressed by MΦ [149, 158-159]. HIF1α and HIF2α are closely related, not only structurally, but also concerning their binding to ARNT and their ability to activate HRE-containing genes [114]. HIF1α is ubiquitously expressed throughout the body, whereas HIF2α is expressed tissue and cell-type specific [115, 160]. HIF1α was demonstrated to be stabilized by Th1 cytokines in M1 polarized MΦ, whereas HIF2α was rather induced by Th2 cytokines in M2 polarized MΦ [158]. Additionally, it was shown that the roles of HIF1α and HIF2α do not overlap, but rather complement each other, as during angiogenesis HIF1α induces the expression of VEGF, whereas HIF2α induces the expression of the VEGF receptor in BMMΦ under hypoxic conditions [159]. In the BMDC used in this study, it was not possible to detect expression of HIF2α mRNA (Figure 3.20) and so far, I could not find any study reporting expression of HIF2α in DC. Interestingly, HIF2α-induction by hypoxia was restricted to BMMΦ (Figure 3.20). In contrast, MΦ, especially TAM and M2 polarized MΦ, have been reported to mainly produce HIF2α [149, 158], which is in line with the results obtained from the quantitative RT-PCR analysis performed here (Figure 3.20).

However, oxygen sensing can also be mediated through several other mechanisms. A recent review, for example, has suggested chromatin as an oxygen sensor, which is able to orchestrate cellular responses to hypoxia, since hypoxia-induced acetylation and methylation of histones can alter the interaction between proteins and DNA. Some enzymes responsible for chromatin remodeling were found to be inducible by HIF1α, whereas the regulation of the most histone modifying proteins remains elusive [161].

In addition, several other signaling pathways interfere with HIF-dependent gene regulation or control hypoxia-induced changes independently of HIFs. The NF-κB pathway [56] and the expression of extracellular signal-regulated kinase (ERK)

enhance the expression and stabilization of HIFs, whereas the inhibition of mTOR by hypoxia and the actions of the endoplasmatic reticulum (ER) in the response to hypoxia were described to be independent of HIF expression (Figure 4.3). One key protein has been described to be Siah2, which can actively degrade PHD3 and thus support stabilization of HIFs (Figure 4.3) [162] .

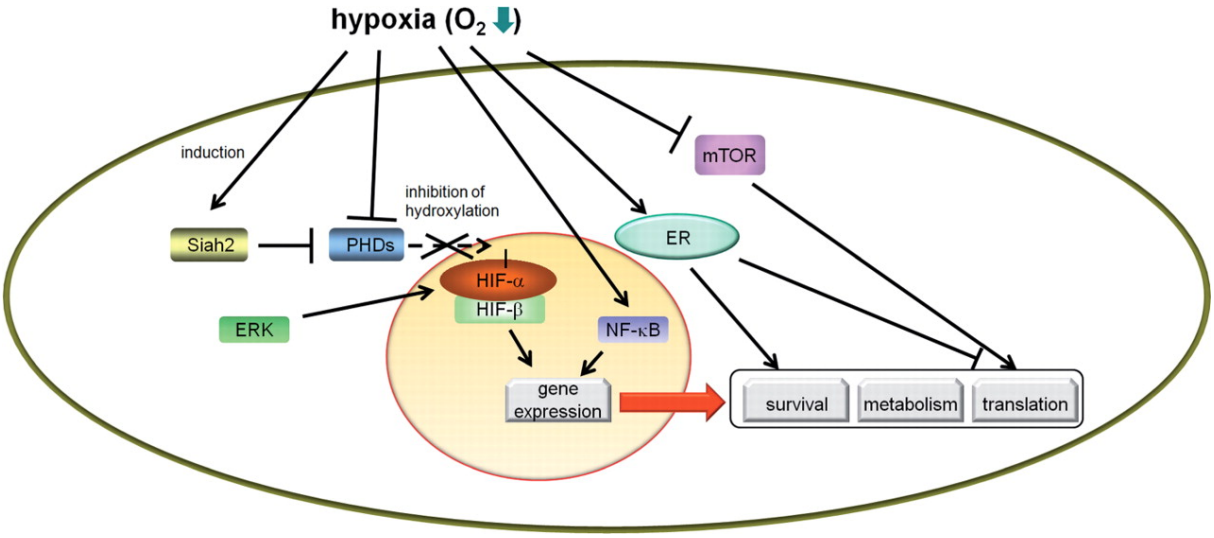

Figure 4.3 Hypoxia-induced pathways. Under hypoxic conditions a variety of signalling pathways are activated to induce cellular changes. Siah2 is expressed through an unknown mechanism and targets PHD3 for degradation, so that hydroxylation of HIFs is suppressed. This leads to HIF stabilization and susequent induction of genes containing HRE sites. ERK also positively regulates HIF by phosphorylation. NF-κB is also induced in an oxygen-deprived environment and is known to activate a ladder of genes. The ER is involved in cell survival and translational regulation under hypoxic stress by activation of the unfolded protein response pathway. mTOR regulates mRNA translation of various genes and is inhibited in conditions of low oxygen to shut down mRNA translation to save cellular energy (taken from Nakayama, 2009 [162]).

There are also several studies, which have analyzed different mechanisms by which HIFs exert their actions. Investigations on HIF-activity have shown that only around 20% of the genes, which positively respond to HIF-stabilization, and hardly any genes, which were downregulated in response to HIFs, bound HIFs at their promoter. The large majority of these genes was regulated indirectly by HIF-dependent induction of secondary transcription factors, or suppression by microRNAs, which themselves were induced by hypoxia or HIFs [163]. Additionally, it was shown that HIF1α can interact with other transcription factors by displacing these from target gene promoters without induction of transcriptional activity and DNA binding, as it was shown for Myc, a basic helix-loop-helix leucine zipper transcription factor [164-165].

To find out how different isoforms of HIF orchestrate the cellular responses to hypoxia, it is necessary to understand their role in different cell types. In this study, I could demonstrate that although MΦ and DC both are phagocytes belonging to the innate immune system, their response to hypoxia differed in many cases and gene regulation by HIF1α in BMDC was different from that of BMMΦ. It was described before that hypoxia, as well as HIF1α affects different immune cells in different ways, which was confirmed in this study by comparison of MΦ and DC. I could illustrate, that hypoxia itself hardly induced any changes regarding the expression of surface markers and cytokine secretion in BMMΦ, whereas the deletion of HIF1α caused remarkable changes in the phenotype and the gene expression of BMMΦ under hypoxic and sometimes even under normoxic conditions. In contrast, BMDC were highly susceptible to conditions of low oxygen regarding their maturation status and cytokine production, as well as chemokine secretion. Interestingly, most of these hypoxia-induced changes were found to be regulated independently of HIF1α, indicating that in DC another hypoxia-sensitive pathway must be active. The hypothesis that HIF2α might compensate for the deletion of HIF1α during hypoxia in BMDC, was disproven by the finding that HIF2α was almost exclusively expressed in BMMΦ, but not in BMDC. This indicates that there are yet unknown mechanisms and pathways, by which low conditions of oxygen can alter the phenotype and the function of BMDC. The stabilization of HIF is still the most investigated and probably the best understood response to hypoxia, which is shared by a wide range of different cells. However, it has to be considered that cell type-specific, as well as tissue-specific mechanisms activated by low oxygen concentrations can alter the HIF-induced gene expression and cellular response.

4.8 Outlook

Responses to hypoxic conditions need to be investigated intensely and carefully with regard to the cell-type experiencing the change from high oxygen concentration to low oxygen concentrations. To discover potential tissues with increased stabilization of HIFs, it is necessary to investigate oxygen tensions in different tissues under normal conditions, as well as under pathological conditions, such as inflammation and cancer. Matching the actual oxygen concentration in a tissue with the expression and stabilization of HIFs, would allow scientists to further define the roles of HIF1α

and HIF2α. An interesting tool to track hypoxia through HIF stabilization is the infection of cells with a recombinant adenovirus, which expresses a red fluorescent protein under the control of HRE [166]. This method would allow the visualization of HIF1α activity and thereby, conclusions on the oxygen concentrations could be drawn.

Although I have found several essential genes to be regulated by HIF1α in hypoxia *in vitro*, it was not possible to define the function of HIF1α in MΦ and DC in *in vivo* bacterial infections with *S. aureus*, *L. monocytogenes* and *C. rodentium*. This might be due to the fact that closely related innate immune cells can compensate for HIF1α-deficiency in DC or MΦ. DC, as well as MΦ, possess the potential to present antigens to adaptive immune cells and both exert microbicidal functions after pathogen recognition and thus induce an immune response. Therefore, it is very likely that these cell types can compensate for each other to a certain extent. To further elucidate the role of HIF1α concerning the effector functions of DC and MΦ during inflammation and infection *in vivo*, it is planned to generate mice with a deficiency of HIF1α in both cell types, DC and MΦ. Thereby, it will be possible to exclude a redundant function of these cell types.

To further elucidate the role of HIF2α in DC and MΦ, a mouse strain with a conditional deletion of both, HIF1α and HIF2α, could bring new insights concerning the functional differences between these two HIFs. Since many of the hypoxia-induced effects were found to be independent of HIF1α in this study, mice with a double-knockout for HIF1α and HIF2α might reveal an importance for HIF2α during these processes.

In the future, I would like to focus on the role of HIF1α in MΦ, especially on the microbicidal functions of these cells under hypoxic conditions. Since I could show, that the killing of different bacteria is differentially affected by conditions of low oxygen, probably due to different virulence factors, I would like to analyze the effects of hypoxia on different bacterial killing mechanisms of phagocytes. Furthermore, the influence of low oxygen concentrations on growth and survival of the bacteria themselves needs to be addressed, since these are also able to sense oxygen and to react to changes in oxygen tension [167]. Taking into account that both, the phagocyte and the microbe, adapt to hypoxia, I hope to get a more precise picture of the interactions of the host immune system with pathogens.

5 SUMMARY

Hypoxia is a key feature of inflammation. The transcription factor Hypoxia-inducible factor (HIF) 1α is responsible for major alterations in gene expression as part of the cellular adaptation to hypoxia. Since dendritic cells (DC) and macrophages (MΦ) are the main antigen presenting cells and need to also act under conditions of extremely low oxygen, the function of HIF1α in these cell types was investigated. Therefore, mice with a specific deficiency for HIF1α in DC and in MΦ were employed and bone marrow (BM)-derived DC and MΦ were generated in normoxic versus hypoxic conditions. BMDC and BMMΦ showed reduced growth in hypoxia. Increased maturation in BMDC was induced by hypoxia independently of HIF1α, whereas in BMMΦ upregulation of the maturation marker CD86 was restricted to HIF1α-deficient cells. In hypoxic BMDC production of the cytokines IL-12, IL-10, IL-23, IL-6, IL-1β and TNFα was inhibited, whereas secretion of IL-22 was strongly enhanced under hypoxic conditions in a HIF1α-dependent manner. BMMΦ showed a remarkably different expression pattern of cytokines than BMDC, with enhanced production of IL-12, TNFα and IL-23 only in hypoxic HIF1α-deficient BMMΦ. Studying BMDC migration markers, an upregulation of CCR7 in a HIF1α-dependent manner in hypoxia was found. Using two independent migration assays, I could observe that this was accompanied by an enhanced migratory capability of hypoxic BMDC, which was less pronounced in HIF1α-deficient BMDC. Production of the chemokines CCL17 and CCL22 by BMDC was increased in conditions of low oxygen independent of HIF1α, in contrast to hypoxic BMMΦ, which showed moderate CCL22 and CCL17 expression under the control of HIF1α.

In addition, the role of HIF1α in DC and MΦ was studied in various infection models. BMDC and BMMΦ were infected with *S. aureus*, *L. monocytogenes*, group A streptococcus (GAS), group B streptococcus (GBS), and *E. coli in vitro* under normoxic and under oxygen-deprived conditions. Independent of the bacterial strain, a better survival of anoxic and hypoxic BMMΦ compared to normoxic BMMΦ was observed in the experiments, which was even more pronounced in HIF1α-deficient BMMΦ. Hypoxic BMDC also revealed enhanced survival rates in response to GAS, GBS and *E. coli* compared to normoxic BMDC. Additionally, I could find a decreased capacity of HIF1α-deficient innate immune cells to kill *E. coli* or intracellular *L. monocytogenes* in hypoxia *in vitro*. This might be explained, at least in BMMΦ, by a

decreased expression of the antimicrobial peptide Cramp and the anti-inflammatory enzyme IDO, which was detected in hypoxic HIF1α-deficient BMMΦ. Despite these findings, no effects of HIF1α-deficiency were seen in an *in vivo* model of a systemic infection with *L. monocytogenes*. Neither in a skin infection model, in which cell-type specific HIF1α-knockout mice were infected with *S. aureus*, nor in an oral infection model with *Citrobacter rodentium*, HIF1α in DC and MΦ was found to be required for efficient host defence against these pathogens *in vivo*.

6 ZUSAMMENFASSUNG

Der Transkriptionsfaktor Hypoxia-Inducible Factor (HIF) 1α ist essentiell für jede Zelle, um sich sauerstoffarmen Bedingungen, wie sie zum Beispiel bei Infektionen und anderen Entzündungen vorherrschen, anzupassen. HIF1α induziert nicht nur die Umstellung des zellulären Metabolismus von aerober oxidativer Phosphorilierung zur anaeroben Glykolyse, sondern reguliert auch Immunantworten in hypoxischem Milieu. Besonders dendritische Zellen (DC) und Makrophagen (MΦ), beides Antigen-präsentierende Zellen des angeborenen Immunsystems, agieren an Orten mit niedrigen Sauerstoffkonzentrationen. Um die Rolle von HIF1α in diesen beiden Zelltypen zu untersuchen, wurden Knockout-Mauslinien generiert, in denen HIF1α DC-spezifisch oder MΦ-spezifisch deletiert ist. DC und MΦ wurden aus Knochenmarks (BM) -Vorläuferzellen dieser Mäuse unter normoxischen, als auch unter hypoxischen Bedingungen differenziert. Für beide Zelltypen konnte ein geringeres Wachstum in Hypoxie beobachtet werden. Hypoxie führte in BMDC zur Aktivierung der Zellen, während der Reifungsmarker CD86 in BMMΦ nur in hypoxischen HIF1α-defizienten BMMΦ verstärkt exprimiert wurde. Passend dazu konnte gezeigt werden, dass nur HIF1α-defiziente BMMΦ die Zytokine IL-12, TNFα und IL-23 verstärkt in einem hypoxischem Milieu sekretieren, während hypoxische BMDC die Zytokine IL-12, IL-10, IL-23, IL-6, IL-1β und TNFα HIF1α-unabhängig inhibieren. Erstaunlicherweise konnte erstmals gezeigt werden, dass BMDC in sauerstoffarmer Atmosphäre IL-22 produzieren, und zwar abhängig von HIF1α.

Eine erhöhte Expression des Chemokinrezeptors CCR7, welcher notwendig zur Auswanderung von DC aus entzündetem Gewebe ist, konnte in hypoxischen HIF1α-profizienten BMDC gefunden werden. Passend dazu konnte in zwei unabhängigen Migrations-Studien gezeigt werden, dass Hypoxie zu einer verstärkten Wanderung von BMDC führt. Dieser Effekt konnte nicht in HIF1α-defizienten BMDC beobachtet werden. Dagegen wurden die Chemokine CCL17 und CCL22 in hypoxischen BMDC HIF1α-unabhängig hochreguliert, während hypoxische BMMΦ zwar eine verstärkte HIF1α-abhängige Sekretion von CCL17 and CCL22, jedoch nur einen Bruchteil dessen, was DC produzieren, aufwiesen.

Zusätzlich wurde auch die Funktion von HIF1α in DC und MΦ in verschiedenen Infektionsmodellen untersucht. BMDC und BMMΦ wurden *in vitro* mit *S. aureus*, *L. monocytogenes*, group A streptococcus (GAS), group B streptococcus (GBS), and *E.*

coli in normoxischen, sowohl als auch in sauerstoffarmem Milieu infiziert. Unabhängig vom Bakterienstamm konnte gezeigt werden, dass mehr BMMΦ in anoxischen und hypoxischen Co-Kulturen überleben als in den normoxischen, welches noch deutlicher ausgeprägt bei den HIF1α-defizienten BMMΦ war. Auch BMDC wiesen eine erhöhte Viabilität in sauerstoffarmem Milieu auf, jedoch nur in Co-Kulturen mit GAS, GBS and *E. coli*. Zusätzlich konnte in BMDC und BMMΦ gezeigt werden, dass HIF1α in hypoxischem Milieu notwendig ist, um *E. coli* oder intrazelluläre *L. monocytogenes in vitro* zu töten, welches zumindest bei hypoxischen HIF1α-defizienten BMMΦ auf eine geringere Expression des antimikrobiellen Peptids Cramp und des anti-inflammatorischen Enzyms IDO zurückzuführen ist. Trotz dieser Ergebnisse konnten in systemischen *in vivo* Infektionen mit *L. monocytogenes* keine Effekte nach Verlust von HIF1α in DC oder MΦ beobachtet werden. Weder in einem *S. aureus* Hautinfektionsmodel, noch nach oraler Infektion mit *Citrobacter rodentium* konnten Unterschiede zwischen Zelltyp-spezifischen HIF1α-knockout Mäusen und wildtyp Mäusen *in vivo* aufgezeigt werden.

7 REFERENCES

1. **Geissmann, F., M.G. Manz, S. Jung, M.H. Sieweke, M. Merad, and K. Ley, *Development of monocytes, macrophages, and dendritic cells.* Science, 2010. 327(5966): p. 656-61.**
2. **Kushwah, R. and J. Hu, *Complexity of dendritic cell subsets and their function in the host immune system.* Immunology, 2011. 133(4): p. 409-19.**
3. **Naik, S.H., *Demystifying the development of dendritic cell subtypes, a little.* Immunol Cell Biol, 2008. 86(5): p. 439-52.**
4. **Stutte, S., B. Jux, C. Esser, and I. Forster, *CD24a expression levels discriminate Langerhans cells from dermal dendritic cells in murine skin and lymph nodes.* J Invest Dermatol, 2008. 128(6): p. 1470-5.**
5. **Banchereau, J., F. Briere, C. Caux, J. Davoust, S. Lebecque, Y.J. Liu, B. Pulendran, and K. Palucka, *Immunobiology of dendritic cells.* Annu Rev Immunol, 2000. 18: p. 767-811.**
6. **Dennehy, K.M. and G.D. Brown, *The role of the beta-glucan receptor Dectin-1 in control of fungal infection.* J Leukoc Biol, 2007. 82(2): p. 253-8.**
7. **Kumagai, Y. and S. Akira, *Identification and functions of pattern-recognition receptors.* J Allergy Clin Immunol, 2010. 125(5): p. 985-92.**
8. **Bardoel, B.W. and J.A. Strijp, *Molecular battle between host and bacterium: recognition in innate immunity.* J Mol Recognit, 2011. 24(6): p. 1077-86.**
9. **Zanoni, I. and F. Granucci, *Regulation of antigen uptake, migration, and lifespan of dendritic cell by Toll-like receptors.* J Mol Med (Berl), 2010. 88(9): p. 873-80.**
10. **Stutte, S., T. Quast, N. Gerbitzki, T. Savinko, N. Novak, J. Reifenberger, B. Homey, W. Kolanus, et al., *Requirement of CCL17 for CCR7- and CXCR4-dependent migration of cutaneous dendritic cells.* Proc Natl Acad Sci U S A, 2010. 107(19): p. 8736-41.**
11. **Randolph, G.J., J. Ochando, and S. Partida-Sanchez, *Migration of dendritic cell subsets and their precursors.* Annu Rev Immunol, 2008. 26: p. 293-316.**
12. **Shortman, K. and Y.J. Liu, *Mouse and human dendritic cell subtypes.* Nat Rev Immunol, 2002. 2(3): p. 151-61.**
13. **Diebold, S.S., *Determination of T-cell fate by dendritic cells.* Immunol Cell Biol, 2008. 86(5): p. 389-97.**
14. **Neefjes, J., M.L. Jongsma, P. Paul, and O. Bakke, *Towards a systems understanding of MHC class I and MHC class II antigen presentation.* Nat Rev Immunol, 2011. 11(12): p. 823-36.**
15. **Belz, G.T., F.R. Carbone, and W.R. Heath, *Cross-presentation of antigens by dendritic cells.* Crit Rev Immunol, 2002. 22(5-6): p. 439-48.**
16. **Kurts, C., B.W. Robinson, and P.A. Knolle, *Cross-priming in health and disease.* Nat Rev Immunol, 2010. 10(6): p. 403-14.**
17. **Mahnke, K., T.S. Johnson, S. Ring, and A.H. Enk, *Tolerogenic dendritic cells and regulatory T cells: a two-way relationship.* J Dermatol Sci, 2007. 46(3): p. 159-67.**
18. **Probst, H.C., K. McCoy, T. Okazaki, T. Honjo, and M. van den Broek, *Resting dendritic cells induce peripheral CD8+ T cell tolerance through PD-1 and CTLA-4.* Nat Immunol, 2005. 6(3): p. 280-6.**
19. **Del Prete, A., P. Zaccagnino, M. Di Paola, M. Saltarella, C. Oliveros Celis, B. Nico, G. Santoro, and M. Lorusso, *Role of mitochondria and reactive oxygen species in dendritic cell differentiation and functions.* Free Radic Biol Med, 2008. 44(7): p. 1443-51.**

20. **Lawrence, T. and G. Natoli, *Transcriptional regulation of macrophage polarization: enabling diversity with identity.* Nat Rev Immunol, 2011. 11(11): p. 750-61.**
21. **Benoit, M., B. Desnues, and J.L. Mege, *Macrophage polarization in bacterial infections.* J Immunol, 2008. 181(6): p. 3733-9.**
22. **Stout, R.D. and J. Suttles, *Functional plasticity of macrophages: reversible adaptation to changing microenvironments.* J Leukoc Biol, 2004. 76(3): p. 509-13.**
23. **Mosser, D.M. and J.P. Edwards, *Exploring the full spectrum of macrophage activation.* Nat Rev Immunol, 2008. 8(12): p. 958-69.**
24. **Roth, A., P. Konig, G. van Zandbergen, M. Klinger, T. Hellwig-Burgel, W. Daubener, M.K. Bohlmann, and J. Rupp, *Hypoxia abrogates antichlamydial properties of IFN-gamma in human fallopian tube cells in vitro and ex vivo.* Proc Natl Acad Sci U S A, 2010. 107(45): p. 19502-7.**
25. **Bosseto, M.C., P.V. Palma, D.T. Covas, and S. Giorgio, *Hypoxia modulates phenotype, inflammatory response, and leishmanial infection of human dendritic cells.* APMIS, 2010. 118(2): p. 108-14.**
26. **Luperchio, S.A. and D.B. Schauer, *Molecular pathogenesis of Citrobacter rodentium and transmissible murine colonic hyperplasia.* Microbes Infect, 2001. 3(4): p. 333-40.**
27. **Lungu, B., S.C. Ricke, and M.G. Johnson, *Growth, survival, proliferation and pathogenesis of Listeria monocytogenes under low oxygen or anaerobic conditions: a review.* Anaerobe, 2009. 15(1-2): p. 7-17.**
28. **Fuchs, S., J. Pane-Farre, C. Kohler, M. Hecker, and S. Engelmann, *Anaerobic gene expression in Staphylococcus aureus.* J Bacteriol, 2007. 189(11): p. 4275-89.**
29. **Cho, J.S., E.M. Pietras, N.C. Garcia, R.I. Ramos, D.M. Farzam, H.R. Monroe, J.E. Magorien, A. Blauvelt, et al., *IL-17 is essential for host defense against cutaneous Staphylococcus aureus infection in mice.* J Clin Invest, 2010. 120(5): p. 1762-73.**
30. **Onunkwo, C.C., B.L. Hahn, and P.G. Sohnle, *Clearance of experimental cutaneous Staphylococcus aureus infections in mice.* Arch Dermatol Res, 2010. 302(5): p. 375-82.**
31. **Schmaler, M., N.J. Jann, F. Ferracin, and R. Landmann, *T and B cells are not required for clearing Staphylococcus aureus in systemic infection despite a strong TLR2-MyD88-dependent T cell activation.* J Immunol, 2011. 186(1): p. 443-52.**
32. **Volz, T., M. Nega, J. Buschmann, S. Kaesler, E. Guenova, A. Peschel, M. Rocken, F. Gotz, et al., *Natural Staphylococcus aureus-derived peptidoglycan fragments activate NOD2 and act as potent costimulators of the innate immune system exclusively in the presence of TLR signals.* FASEB J, 2010. 24(10): p. 4089-102.**
33. **Michelsen, K.S., A. Aicher, M. Mohaupt, T. Hartung, S. Dimmeler, C.J. Kirschning, and R.R. Schumann, *The role of toll-like receptors (TLRs) in bacteria-induced maturation of murine dendritic cells (DCS). Peptidoglycan and lipoteichoic acid are inducers of DC maturation and require TLR2.* J Biol Chem, 2001. 276(28): p. 25680-6.**
34. **Hruz, P., A.S. Zinkernagel, G. Jenikova, G.J. Botwin, J.P. Hugot, M. Karin, V. Nizet, and L. Eckmann, *NOD2 contributes to cutaneous defense against Staphylococcus aureus through alpha-toxin-dependent innate immune activation.* Proc Natl Acad Sci U S A, 2009. 106(31): p. 12873-8.**
35. **Zinkernagel, A.S. and V. Nizet, *Staphylococcus aureus: a blemish on skin immunity.* Cell Host Microbe, 2007. 1(3): p. 161-2.**

36. Brosnahan, A.J. and P.M. Schlievert, *Gram-positive bacterial superantigen outside-in signaling causes toxic shock syndrome.* FEBS J, 2011. 278(23): p. 4649-67.
37. Miller, L.S., E.M. Pietras, L.H. Uricchio, K. Hirano, S. Rao, H. Lin, R.M. O'Connell, Y. Iwakura, et al., *Inflammasome-mediated production of IL-1beta is required for neutrophil recruitment against Staphylococcus aureus in vivo.* J Immunol, 2007. 179(10): p. 6933-42.
38. Gross, O., C.J. Thomas, G. Guarda, and J. Tschopp, *The inflammasome: an integrated view.* Immunol Rev, 2011. 243(1): p. 136-51.
39. van de Veerdonk, F.L., M.G. Netea, C.A. Dinarello, and L.A. Joosten, *Inflammasome activation and IL-1beta and IL-18 processing during infection.* Trends Immunol, 2011. 32(3): p. 110-6.
40. Shimada, T., B.G. Park, A.J. Wolf, C. Brikos, H.S. Goodridge, C.A. Becker, C.N. Reyes, E.A. Miao, et al., *Staphylococcus aureus evades lysozyme-based peptidoglycan digestion that links phagocytosis, inflammasome activation, and IL-1beta secretion.* Cell Host Microbe, 2010. 7(1): p. 38-49.
41. Hamon, M., H. Bierne, and P. Cossart, *Listeria monocytogenes: a multifaceted model.* Nat Rev Microbiol, 2006. 4(6): p. 423-34.
42. Zenewicz, L.A. and H. Shen, *Innate and adaptive immune responses to Listeria monocytogenes: a short overview.* Microbes Infect, 2007. 9(10): p. 1208-15.
43. Lochner, M., K. Kastenmuller, M. Neuenhahn, H. Weighardt, D.H. Busch, W. Reindl, and I. Forster, *Decreased susceptibility of mice to infection with Listeria monocytogenes in the absence of interleukin-18.* Infect Immun, 2008. 76(9): p. 3881-90.
44. Pamer, E.G., *Immune responses to Listeria monocytogenes.* Nat Rev Immunol, 2004. 4(10): p. 812-23.
45. Westcott, M.M., C.J. Henry, J.E. Amis, and E.M. Hiltbold, *Dendritic cells inhibit the progression of Listeria monocytogenes intracellular infection by retaining bacteria in major histocompatibility complex class II-rich phagosomes and by limiting cytosolic growth.* Infect Immun, 2010. 78(7): p. 2956-65.
46. Deretic, V., *Autophagy in immunity and cell-autonomous defense against intracellular microbes.* Immunol Rev, 2011. 240(1): p. 92-104.
47. Birmingham, C.L., D.E. Higgins, and J.H. Brumell, *Avoiding death by autophagy: interactions of Listeria monocytogenes with the macrophage autophagy system.* Autophagy, 2008. 4(3): p. 368-71.
48. Wiles, S., S. Clare, J. Harker, A. Huett, D. Young, G. Dougan, and G. Frankel, *Organ specificity, colonization and clearance dynamics in vivo following oral challenges with the murine pathogen Citrobacter rodentium.* Cell Microbiol, 2004. 6(10): p. 963-72.
49. Miao, E.A., D.P. Mao, N. Yudkovsky, R. Bonneau, C.G. Lorang, S.E. Warren, I.A. Leaf, and A. Aderem, *Innate immune detection of the type III secretion apparatus through the NLRC4 inflammasome.* Proc Natl Acad Sci U S A, 2010. 107(7): p. 3076-80.
50. Mundy, R., T.T. MacDonald, G. Dougan, G. Frankel, and S. Wiles, *Citrobacter rodentium of mice and man.* Cell Microbiol, 2005. 7(12): p. 1697-706.
51. Gibson, D.L., C. Ma, K.S. Bergstrom, J.T. Huang, C. Man, and B.A. Vallance, *MyD88 signalling plays a critical role in host defence by controlling pathogen burden and promoting epithelial cell homeostasis during Citrobacter rodentium-induced colitis.* Cell Microbiol, 2008. 10(3): p. 618-31.

52. **Geddes, K., S.J. Rubino, J.G. Magalhaes, C. Streutker, L. Le Bourhis, J.H. Cho, S.J. Robertson, C.J. Kim, et al., *Identification of an innate T helper type 17 response to intestinal bacterial pathogens.* Nat Med, 2011. 17(7): p. 837-44.**
53. **Bergstrom, K.S., H.P. Sham, M. Zarepour, and B.A. Vallance, *Innate host responses to enteric bacterial pathogens: a balancing act between resistance and tolerance.* Cell Microbiol, 2012. 14(4): p. 475-84.**
54. **Zhang, Y.W., L.S. Ding, and M.D. Lai, *Reg gene family and human diseases.* World J Gastroenterol, 2003. 9(12): p. 2635-41.**
55. **Zheng, Y., P.A. Valdez, D.M. Danilenko, Y. Hu, S.M. Sa, Q. Gong, A.R. Abbas, Z. Modrusan, et al., *Interleukin-22 mediates early host defense against attaching and effacing bacterial pathogens.* Nat Med, 2008. 14(3): p. 282-9.**
56. **Nizet, V. and R.S. Johnson, *Interdependence of hypoxic and innate immune responses.* Nat Rev Immunol, 2009. 9(9): p. 609-17.**
57. **Sitkovsky, M. and D. Lukashev, *Regulation of immune cells by local-tissue oxygen tension: HIF1 alpha and adenosine receptors.* Nat Rev Immunol, 2005. 5(9): p. 712-21.**
58. **Balin, A.K. and L. Pratt, *Oxygen modulates the growth of skin fibroblasts.* In Vitro Cell Dev Biol Anim, 2002. 38(5): p. 305-10.**
59. **Bedogni, B., S.M. Welford, D.S. Cassarino, B.J. Nickoloff, A.J. Giaccia, and M.B. Powell, *The hypoxic microenvironment of the skin contributes to Akt-mediated melanocyte transformation.* Cancer Cell, 2005. 8(6): p. 443-54.**
60. **Taylor, C.T. and S.P. Colgan, *Hypoxia and gastrointestinal disease.* J Mol Med (Berl), 2007. 85(12): p. 1295-300.**
61. **Perez-Perri, J.I., J.M. Acevedo, and P. Wappner, *Epigenetics: new questions on the response to hypoxia.* Int J Mol Sci, 2011. 12(7): p. 4705-21.**
62. **Dunwoodie, S.L., *The role of hypoxia in development of the Mammalian embryo.* Dev Cell, 2009. 17(6): p. 755-73.**
63. **Suda, T., K. Takubo, and G.L. Semenza, *Metabolic regulation of hematopoietic stem cells in the hypoxic niche.* Cell Stem Cell, 2011. 9(4): p. 298-310.**
64. **Keith, B., R.S. Johnson, and M.C. Simon, *HIF1alpha and HIF2alpha: sibling rivalry in hypoxic tumour growth and progression.* Nat Rev Cancer, 2012. 12(1): p. 9-22.**
65. **Huang, S., S. Apasov, M. Koshiba, and M. Sitkovsky, *Role of A2a extracellular adenosine receptor-mediated signaling in adenosine-mediated inhibition of T-cell activation and expansion.* Blood, 1997. 90(4): p. 1600-10.**
66. **Taylor, C.T., *Interdependent roles for hypoxia inducible factor and nuclear factor-kappaB in hypoxic inflammation.* J Physiol, 2008. 586(Pt 17): p. 4055-9.**
67. **Cockman, M.E., N. Masson, D.R. Mole, P. Jaakkola, G.W. Chang, S.C. Clifford, E.R. Maher, C.W. Pugh, et al., *Hypoxia inducible factor-alpha binding and ubiquitylation by the von Hippel-Lindau tumor suppressor protein.* J Biol Chem, 2000. 275(33): p. 25733-41.**
68. **Thiel, M., C.C. Caldwell, S. Kreth, S. Kuboki, P. Chen, P. Smith, A. Ohta, A.B. Lentsch, et al., *Targeted deletion of HIF-1alpha gene in T cells prevents their inhibition in hypoxic inflamed tissues and improves septic mice survival.* PLoS One, 2007. 2(9): p. e853.**
69. **Tsun, A., Z. Chen, and B. Li, *Romance of the three kingdoms: RORgammat allies with HIF1alpha against FoxP3 in regulating T cell metabolism and differentiation.* Protein Cell, 2011. 2(10): p. 778-81.**
70. **Dang, E.V., J. Barbi, H.Y. Yang, D. Jinasena, H. Yu, Y. Zheng, Z. Bordman, J. Fu, et al., *Control of T(H)17/T(reg) balance by hypoxia-inducible factor 1.* Cell, 2011. 146(5): p. 772-84.**

71. **Shi, L.Z., R. Wang, G. Huang, P. Vogel, G. Neale, D.R. Green, and H. Chi, *HIF1alpha-dependent glycolytic pathway orchestrates a metabolic checkpoint for the differentiation of TH17 and Treg cells.* J Exp Med, 2011. 208(7): p. 1367-76.**
72. **Cramer, T., Y. Yamanishi, B.E. Clausen, I. Forster, R. Pawlinski, N. Mackman, V.H. Haase, R. Jaenisch, et al., *HIF-1alpha is essential for myeloid cell-mediated inflammation.* Cell, 2003. 112(5): p. 645-57.**
73. **Peyssonnaux, C., V. Datta, T. Cramer, A. Doedens, E.A. Theodorakis, R.L. Gallo, N. Hurtado-Ziola, V. Nizet, et al., *HIF-1alpha expression regulates the bactericidal capacity of phagocytes.* J Clin Invest, 2005. 115(7): p. 1806-15.**
74. **Rupp, J., J. Gieffers, M. Klinger, G. van Zandbergen, R. Wrase, M. Maass, W. Solbach, J. Deiwick, et al., *Chlamydia pneumoniae directly interferes with HIF-1alpha stabilization in human host cells.* Cell Microbiol, 2007. 9(9): p. 2181-91.**
75. **Kietzmann, T. and A. Gorlach, *Reactive oxygen species in the control of hypoxia-inducible factor-mediated gene expression.* Semin Cell Dev Biol, 2005. 16(4-5): p. 474-86.**
76. **Jung, S.N., W.K. Yang, J. Kim, H.S. Kim, E.J. Kim, H. Yun, H. Park, S.S. Kim, et al., *Reactive oxygen species stabilize hypoxia-inducible factor-1 alpha protein and stimulate transcriptional activity via AMP-activated protein kinase in DU145 human prostate cancer cells.* Carcinogenesis, 2008. 29(4): p. 713-21.**
77. **Sauer, B., *Inducible gene targeting in mice using the Cre/lox system.* Methods, 1998. 14(4): p. 381-92.**
78. **Caton, M.L., M.R. Smith-Raska, and B. Reizis, *Notch-RBP-J signaling controls the homeostasis of CD8- dendritic cells in the spleen.* J Exp Med, 2007. 204(7): p. 1653-64.**
79. **Alferink, J., I. Lieberam, W. Reindl, A. Behrens, S. Weiss, N. Huser, K. Gerauer, R. Ross, et al., *Compartmentalized production of CCL17 in vivo: strong inducibility in peripheral dendritic cells contrasts selective absence from the spleen.* J Exp Med, 2003. 197(5): p. 585-99.**
80. **Clausen, B.E., C. Burkhardt, W. Reith, R. Renkawitz, and I. Forster, *Conditional gene targeting in macrophages and granulocytes using LysMcre mice.* Transgenic Res, 1999. 8(4): p. 265-77.**
81. **Aoshi, T., J.A. Carrero, V. Konjufca, Y. Koide, E.R. Unanue, and M.J. Miller, *The cellular niche of Listeria monocytogenes infection changes rapidly in the spleen.* Eur J Immunol, 2009. 39(2): p. 417-25.**
82. **Gu, H., Y.R. Zou, and K. Rajewsky, *Independent control of immunoglobulin switch recombination at individual switch regions evidenced through Cre-loxP-mediated gene targeting.* Cell, 1993. 73(6): p. 1155-64.**
83. **Lieberam, I., *Analyse Zelltyp-spezifischer Genexpression in dendritischen Zellen*. 1999, University of Cologne.**
84. **Kohler, T., B. Reizis, R.S. Johnson, H. Weighardt, and I. Forster, *Influence of hypoxia-inducible factor 1alpha on dendritic cell differentiation and migration.* Eur J Immunol, 2012. 42(5): p. 1226-36.**
85. **Constien, R., A. Forde, B. Liliensiek, H.J. Grone, P. Nawroth, G. Hammerling, and B. Arnold, *Characterization of a novel EGFP reporter mouse to monitor Cre recombination as demonstrated by a Tie2 Cre mouse line.* Genesis, 2001. 30(1): p. 36-44.**
86. **Karasuyama, H. and F. Melchers, *Establishment of mouse cell lines which constitutively secrete large quantities of interleukin 2, 3, 4 or 5, using modified cDNA expression vectors.* Eur J Immunol, 1988. 18(1): p. 97-104.**
87. **Vinay, D.S., C.H. Kim, B.K. Choi, and B.S. Kwon, *Origins and functional basis of regulatory CD11c+CD8+ T cells.* Eur J Immunol, 2009. 39(6): p. 1552-63.**

88. **Synnestvedt, K., G.T. Furuta, K.M. Comerford, N. Louis, J. Karhausen, H.K. Eltzschig, K.R. Hansen, L.F. Thompson, et al., *Ecto-5'-nucleotidase (CD73) regulation by hypoxia-inducible factor-1 mediates permeability changes in intestinal epithelia.* J Clin Invest, 2002. 110(7): p. 993-1002.**
89. **Wolk, K., E. Witte, K. Witte, K. Warszawska, and R. Sabat, *Biology of interleukin-22.* Semin Immunopathol, 2010. 32(1): p. 17-31.**
90. **Bosco, M.C., M. Puppo, F. Blengio, T. Fraone, P. Cappello, M. Giovarelli, and L. Varesio, *Monocytes and dendritic cells in a hypoxic environment: Spotlights on chemotaxis and migration.* Immunobiology, 2008. 213(9-10): p. 733-49.**
91. **Elia, A.R., P. Cappello, M. Puppo, T. Fraone, C. Vanni, A. Eva, T. Musso, F. Novelli, et al., *Human dendritic cells differentiated in hypoxia down-modulate antigen uptake and change their chemokine expression profile.* J Leukoc Biol, 2008. 84(6): p. 1472-82.**
92. **Ricciardi, A., A.R. Elia, P. Cappello, M. Puppo, C. Vanni, P. Fardin, A. Eva, D. Munroe, et al., *Transcriptome of hypoxic immature dendritic cells: modulation of chemokine/receptor expression.* Mol Cancer Res, 2008. 6(2): p. 175-85.**
93. **Kabashima, K., N. Shiraishi, K. Sugita, T. Mori, A. Onoue, M. Kobayashi, J. Sakabe, R. Yoshiki, et al., *CXCL12-CXCR4 engagement is required for migration of cutaneous dendritic cells.* Am J Pathol, 2007. 171(4): p. 1249-57.**
94. **Semmling, V., V. Lukacs-Kornek, C.A. Thaiss, T. Quast, K. Hochheiser, U. Panzer, J. Rossjohn, P. Perlmutter, et al., *Alternative cross-priming through CCL17-CCR4-mediated attraction of CTLs toward NKT cell-licensed DCs.* Nat Immunol, 2010. 11(4): p. 313-20.**
95. **Gordon, S., J. Hamann, H.H. Lin, and M. Stacey, *F4/80 and the related adhesion-GPCRs.* Eur J Immunol, 2011. 41(9): p. 2472-6.**
96. **Aujla, S.J., Y.R. Chan, M. Zheng, M. Fei, D.J. Askew, D.A. Pociask, T.A. Reinhart, F. McAllister, et al., *IL-22 mediates mucosal host defense against Gram-negative bacterial pneumonia.* Nat Med, 2008. 14(3): p. 275-81.**
97. **Alkhatib, G., *The biology of CCR5 and CXCR4.* Curr Opin HIV AIDS, 2009. 4(2): p. 96-103.**
98. **Hahn, B.L., C.C. Onunkwo, C.J. Watts, and P.G. Sohnle, *Systemic dissemination and cutaneous damage in a mouse model of staphylococcal skin infections.* Microb Pathog, 2009. 47(1): p. 16-23.**
99. **Matsui, K. and A. Nishikawa, *Percutaneous application of peptidoglycan from Staphylococcus aureus induces infiltration of CCR4+ cells into mouse skin.* J Investig Allergol Clin Immunol, 2011. 21(5): p. 354-62.**
100. **Edwards, R.J., G.W. Taylor, M. Ferguson, S. Murray, N. Rendell, A. Wrigley, Z. Bai, J. Boyle, et al., *Specific C-terminal cleavage and inactivation of interleukin-8 by invasive disease isolates of Streptococcus pyogenes.* J Infect Dis, 2005. 192(5): p. 783-90.**
101. **Nyberg, P., M. Rasmussen, and L. Bjorck, *alpha2-Macroglobulin-proteinase complexes protect Streptococcus pyogenes from killing by the antimicrobial peptide LL-37.* J Biol Chem, 2004. 279(51): p. 52820-3.**
102. **Nizet, V., *Understanding how leading bacterial pathogens subvert innate immunity to reveal novel therapeutic targets.* J Allergy Clin Immunol, 2007. 120(1): p. 13-22.**
103. **Liu, G.Y., K.S. Doran, T. Lawrence, N. Turkson, M. Puliti, L. Tissi, and V. Nizet, *Sword and shield: linked group B streptococcal beta-hemolysin/cytolysin and carotenoid pigment function to subvert host phagocyte defense.* Proc Natl Acad Sci U S A, 2004. 101(40): p. 14491-6.**

104. Wilson, C.B. and W.M. Weaver, *Comparative susceptibility of group B streptococci and Staphylococcus aureus to killing by oxygen metabolites.* J Infect Dis, 1985. 152(2): p. 323-9.
105. Mohawk, K.L. and A.D. O'Brien, *Mouse models of Escherichia coli O157:H7 infection and shiga toxin injection.* J Biomed Biotechnol, 2011. 2011: p. 258185.
106. Hirota, S.A., K. Fines, J. Ng, D. Traboulsi, J. Lee, E. Ihara, Y. Li, W.G. Willmore, et al., *Hypoxia-inducible factor signaling provides protection in Clostridium difficile-induced intestinal injury.* Gastroenterology, 2010. 139(1): p. 259-69 e3.
107. Hartmann, H., H.K. Eltzschig, H. Wurz, K. Hantke, A. Rakin, A.S. Yazdi, G. Matteoli, E. Bohn, et al., *Hypoxia-independent activation of HIF-1 by enterobacteriaceae and their siderophores.* Gastroenterology, 2008. 134(3): p. 756-67.
108. Shah, Y.M., S. Ito, K. Morimura, C. Chen, S.H. Yim, V.H. Haase, and F.J. Gonzalez, *Hypoxia-inducible factor augments experimental colitis through an MIF-dependent inflammatory signaling cascade.* Gastroenterology, 2008. 134(7): p. 2036-48, 2048 e1-3.
109. Gibson, D.L., M. Montero, M.J. Ropeleski, K.S. Bergstrom, C. Ma, S. Ghosh, H. Merkens, J. Huang, et al., *Interleukin-11 reduces TLR4-induced colitis in TLR2-deficient mice and restores intestinal STAT3 signaling.* Gastroenterology, 2010. 139(4): p. 1277-88.
110. Craven, R.R., X. Gao, I.C. Allen, D. Gris, J. Bubeck Wardenburg, E. McElvania-Tekippe, J.P. Ting, and J.A. Duncan, *Staphylococcus aureus alpha-hemolysin activates the NLRP3-inflammasome in human and mouse monocytic cells.* PLoS One, 2009. 4(10): p. e7446.
111. Guarda, G., M. Zenger, A.S. Yazdi, K. Schroder, I. Ferrero, P. Menu, A. Tardivel, C. Mattmann, et al., *Differential expression of NLRP3 among hematopoietic cells.* J Immunol, 2011. 186(4): p. 2529-34.
112. Leibig, M., M. Liebeke, D. Mader, M. Lalk, A. Peschel, and F. Gotz, *Pyruvate formate lyase acts as a formate supplier for metabolic processes during anaerobiosis in Staphylococcus aureus.* J Bacteriol, 2011. 193(4): p. 952-62.
113. Kobayashi, Y., *The regulatory role of nitric oxide in proinflammatory cytokine expression during the induction and resolution of inflammation.* J Leukoc Biol, 2010. 88(6): p. 1157-62.
114. Loboda, A., A. Jozkowicz, and J. Dulak, *HIF-1 and HIF-2 transcription factors--similar but not identical.* Mol Cells, 2010. 29(5): p. 435-42.
115. Imtiyaz, H.Z., E.P. Williams, M.M. Hickey, S.A. Patel, A.C. Durham, L.J. Yuan, R. Hammond, P.A. Gimotty, et al., *Hypoxia-inducible factor 2alpha regulates macrophage function in mouse models of acute and tumor inflammation.* J Clin Invest, 2010. 120(8): p. 2699-714.
116. Wiesener, M.S., J.S. Jurgensen, C. Rosenberger, C.K. Scholze, J.H. Horstrup, C. Warnecke, S. Mandriota, I. Bechmann, et al., *Widespread hypoxia-inducible expression of HIF-2alpha in distinct cell populations of different organs.* FASEB J, 2003. 17(2): p. 271-3.
117. Rama, I., B. Bruene, J. Torras, R. Koehl, J.M. Cruzado, O. Bestard, M. Franquesa, N. Lloberas, et al., *Hypoxia stimulus: An adaptive immune response during dendritic cell maturation.* Kidney Int, 2008. 73(7): p. 816-25.
118. Jantsch, J., D. Chakravortty, N. Turza, A.T. Prechtel, B. Buchholz, R.G. Gerlach, M. Volke, J. Glasner, et al., *Hypoxia and hypoxia-inducible factor-1 alpha modulate lipopolysaccharide-induced dendritic cell activation and function.* J Immunol, 2008. 180(7): p. 4697-705.

119. Goth, S.R., R.A. Chu, and I.N. Pessah, *Oxygen tension regulates the in vitro maturation of GM-CSF expanded murine bone marrow dendritic cells by modulating class II MHC expression.* J Immunol Methods, 2006. 308(1-2): p. 179-91.

120. Wang, Q., C. Liu, F. Zhu, F. Liu, P. Zhang, C. Guo, X. Wang, H. Li, et al., *Reoxygenation of hypoxia-differentiated dentritic cells induces Th1 and Th17 cell differentiation.* Mol Immunol, 2010. 47(4): p. 922-31.

121. Yang, M., C. Ma, S. Liu, J. Sun, Q. Shao, W. Gao, Y. Zhang, Z. Li, et al., *Hypoxia skews dendritic cells to a T helper type 2-stimulating phenotype and promotes tumour cell migration by dendritic cell-derived osteopontin.* Immunology, 2009. 128(1 Suppl): p. e237-49.

122. Bosco, M.C., D. Pierobon, F. Blengio, F. Raggi, C. Vanni, M. Gattorno, A. Eva, F. Novelli, et al., *Hypoxia modulates the gene expression profile of immunoregulatory receptors in human mature dendritic cells: identification of TREM-1 as a novel hypoxic marker in vitro and in vivo.* Blood, 2011. 117(9): p. 2625-39.

123. Guitart, A.V., C. Debeissat, F. Hermitte, A. Villacreces, Z. Ivanovic, H. Boeuf, and V. Praloran, *Very low oxygen concentration (0.1%) reveals two FDCP-Mix cell subpopulations that differ by their cell cycling, differentiation and p27KIP1 expression.* Cell Death Differ, 2011. 18(1): p. 174-82.

124. Mancino, A., T. Schioppa, P. Larghi, F. Pasqualini, M. Nebuloni, I.H. Chen, S. Sozzani, J.M. Austyn, et al., *Divergent effects of hypoxia on dendritic cell functions.* Blood, 2008. 112(9): p. 3723-34.

125. Gu, Y., J. Yang, X. Ouyang, W. Liu, H. Li, J. Bromberg, S.H. Chen, L. Mayer, et al., *Interleukin 10 suppresses Th17 cytokines secreted by macrophages and T cells.* Eur J Immunol, 2008. 38(7): p. 1807-13.

126. Zenewicz, L.A. and R.A. Flavell, *IL-22 and inflammation: leukin' through a glass onion.* Eur J Immunol, 2008. 38(12): p. 3265-8.

127. Li, Y., X. Qiu, S. Zhang, Q. Zhang, and E. Wang, *Hypoxia induced CCR7 expression via HIF-1alpha and HIF-2alpha correlates with migration and invasion in lung cancer cells.* Cancer Biol Ther, 2009. 8(4): p. 322-30.

128. Sun, J., Y. Zhang, M. Yang, Q. Xie, Z. Li, Z. Dong, Y. Yang, B. Deng, et al., *Hypoxia induces T-cell apoptosis by inhibiting chemokine C receptor 7 expression: the role of adenosine receptor A(2).* Cell Mol Immunol, 2010. 7(1): p. 77-82.

129. Schioppa, T., B. Uranchimeg, A. Saccani, S.K. Biswas, A. Doni, A. Rapisarda, S. Bernasconi, S. Saccani, et al., *Regulation of the chemokine receptor CXCR4 by hypoxia.* J Exp Med, 2003. 198(9): p. 1391-402.

130. Bosco, M.C., G. Reffo, M. Puppo, and L. Varesio, *Hypoxia inhibits the expression of the CCR5 chemokine receptor in macrophages.* Cell Immunol, 2004. 228(1): p. 1-7.

131. Qu, X., M.X. Yang, B.H. Kong, L. Qi, Q.L. Lam, S. Yan, P. Li, M. Zhang, et al., *Hypoxia inhibits the migratory capacity of human monocyte-derived dendritic cells.* Immunol Cell Biol, 2005. 83(6): p. 668-73.

132. Zhao, W., S. Darmanin, Q. Fu, J. Chen, H. Cui, J. Wang, F. Okada, J. Hamada, et al., *Hypoxia suppresses the production of matrix metalloproteinases and the migration of human monocyte-derived dendritic cells.* Eur J Immunol, 2005. 35(12): p. 3468-77.

133. Kopydlowski, K.M., C.A. Salkowski, M.J. Cody, N. van Rooijen, J. Major, T.A. Hamilton, and S.N. Vogel, *Regulation of macrophage chemokine expression by lipopolysaccharide in vitro and in vivo.* J Immunol, 1999. 163(3): p. 1537-44.

134. **Mantovani, A., A. Sica, S. Sozzani, P. Allavena, A. Vecchi, and M. Locati, *The chemokine system in diverse forms of macrophage activation and polarization.* Trends Immunol, 2004. 25(12): p. 677-86.**
135. **Wiese, M., R.G. Gerlach, I. Popp, J. Matuszak, M. Mahapatro, K. Castiglione, D. Chakravortty, C. Willam, et al., *Hypoxia-mediated impairment of the mitochondrial respiratory chain inhibits the bactericidal activity of macrophages.* Infect Immun, 2012.**
136. **Degrossoli, A. and S. Giorgio, *Functional alterations in macrophages after hypoxia selection.* Exp Biol Med (Maywood), 2007. 232(1): p. 88-95.**
137. **McGovern, N.N., A.S. Cowburn, L. Porter, S.R. Walmsley, C. Summers, A.A. Thompson, S. Anwar, L.C. Willcocks, et al., *Hypoxia selectively inhibits respiratory burst activity and killing of Staphylococcus aureus in human neutrophils.* J Immunol, 2011. 186(1): p. 453-63.**
138. **Anand, R.J., S.C. Gribar, J. Li, J.W. Kohler, M.F. Branca, T. Dubowski, C.P. Sodhi, and D.J. Hackam, *Hypoxia causes an increase in phagocytosis by macrophages in a HIF-1alpha-dependent manner.* J Leukoc Biol, 2007. 82(5): p. 1257-65.**
139. **Sahoo, M., I. Ceballos-Olvera, L. del Barrio, and F. Re, *Role of the inflammasome, IL-1beta, and IL-18 in bacterial infections.* ScientificWorldJournal, 2011. 11: p. 2037-50.**
140. **Kim, S., F. Bauernfeind, A. Ablasser, G. Hartmann, K.A. Fitzgerald, E. Latz, and V. Hornung, *Listeria monocytogenes is sensed by the NLRP3 and AIM2 inflammasome.* Eur J Immunol, 2010. 40(6): p. 1545-51.**
141. **Zhang, H., M. Bosch-Marce, L.A. Shimoda, Y.S. Tan, J.H. Baek, J.B. Wesley, F.J. Gonzalez, and G.L. Semenza, *Mitochondrial autophagy is an HIF-1-dependent adaptive metabolic response to hypoxia.* J Biol Chem, 2008. 283(16): p. 10892-903.**
142. **Schlie, K., J.E. Spowart, L.R. Hughson, K.N. Townsend, and J.J. Lum, *When Cells Suffocate: Autophagy in Cancer and Immune Cells under Low Oxygen.* Int J Cell Biol, 2011. 2011: p. 470597.**
143. **Beyer, S., M.M. Kristensen, K.S. Jensen, J.V. Johansen, and P. Staller, *The histone demethylases JMJD1A and JMJD2B are transcriptional targets of hypoxia-inducible factor HIF.* J Biol Chem, 2008. 283(52): p. 36542-52.**
144. **Burke, B., N. Tang, K.P. Corke, D. Tazzyman, K. Ameri, M. Wells, and C.E. Lewis, *Expression of HIF-1alpha by human macrophages: implications for the use of macrophages in hypoxia-regulated cancer gene therapy.* J Pathol, 2002. 196(2): p. 204-12.**
145. **Jones, S.A., T. Gibson, R.C. Maltby, F.Z. Chowdhury, V. Stewart, P.S. Cohen, and T. Conway, *Anaerobic respiration of Escherichia coli in the mouse intestine.* Infect Immun, 2011. 79(10): p. 4218-26.**
146. **Marteyn, B., F.B. Scorza, P.J. Sansonetti, and C. Tang, *Breathing life into pathogens: the influence of oxygen on bacterial virulence and host responses in the gastrointestinal tract.* Cell Microbiol, 2011. 13(2): p. 171-6.**
147. **Sathaliyawala, T., W.E. O'Gorman, M. Greter, M. Bogunovic, V. Konjufca, Z.E. Hou, G.P. Nolan, M.J. Miller, et al., *Mammalian target of rapamycin controls dendritic cell development downstream of Flt3 ligand signaling.* Immunity, 2010. 33(4): p. 597-606.**
148. **Hou, B., B. Reizis, and A.L. DeFranco, *Toll-like receptors activate innate and adaptive immunity by using dendritic cell-intrinsic and -extrinsic mechanisms.* Immunity, 2008. 29(2): p. 272-82.**

149. Fang, H.Y., R. Hughes, C. Murdoch, S.B. Coffelt, S.K. Biswas, A.L. Harris, R.S. Johnson, H.Z. Imityaz, et al., *Hypoxia-inducible factors 1 and 2 are important transcriptional effectors in primary macrophages experiencing hypoxia.* Blood, 2009. 114(4): p. 844-59.

150. Peyssonnaux, C., A.T. Boutin, A.S. Zinkernagel, V. Datta, V. Nizet, and R.S. Johnson, *Critical role of HIF-1alpha in keratinocyte defense against bacterial infection.* J Invest Dermatol, 2008. 128(8): p. 1964-8.

151. Imtiyaz, H.Z. and M.C. Simon, *Hypoxia-inducible factors as essential regulators of inflammation.* Curr Top Microbiol Immunol, 2010. 345: p. 105-20.

152. Werno, C., H. Menrad, A. Weigert, N. Dehne, S. Goerdt, K. Schledzewski, J. Kzhyshkowska, and B. Brune, *Knockout of HIF-1alpha in tumor-associated macrophages enhances M2 polarization and attenuates their pro-angiogenic responses.* Carcinogenesis, 2010. 31(10): p. 1863-72.

153. Zinkernagel, A.S., R.S. Johnson, and V. Nizet, *Hypoxia inducible factor (HIF) function in innate immunity and infection.* J Mol Med, 2007. 85(12): p. 1339-46.

154. Popov, A., Z. Abdullah, C. Wickenhauser, T. Saric, J. Driesen, F.G. Hanisch, E. Domann, E.L. Raven, et al., *Indoleamine 2,3-dioxygenase-expressing dendritic cells form suppurative granulomas following Listeria monocytogenes infection.* J Clin Invest, 2006. 116(12): p. 3160-70.

155. Hacker, H., C. Furmann, H. Wagner, and G. Hacker, *Caspase-9/-3 activation and apoptosis are induced in mouse macrophages upon ingestion and digestion of Escherichia coli bacteria.* J Immunol, 2002. 169(6): p. 3172-9.

156. Zinkernagel, A.S., C. Peyssonnaux, R.S. Johnson, and V. Nizet, *Pharmacologic augmentation of hypoxia-inducible factor-1alpha with mimosine boosts the bactericidal capacity of phagocytes.* J Infect Dis, 2008. 197(2): p. 214-7.

157. Pishchany, G., A.L. McCoy, V.J. Torres, J.C. Krause, J.E. Crowe, Jr., M.E. Fabry, and E.P. Skaar, *Specificity for human hemoglobin enhances Staphylococcus aureus infection.* Cell Host Microbe, 2010. 8(6): p. 544-50.

158. Takeda, N., E.L. O'Dea, A. Doedens, J.W. Kim, A. Weidemann, C. Stockmann, M. Asagiri, M.C. Simon, et al., *Differential activation and antagonistic function of HIF-{alpha} isoforms in macrophages are essential for NO homeostasis.* Genes Dev, 2010. 24(5): p. 491-501.

159. Eubank, T.D., J.M. Roda, H. Liu, T. O'Neil, and C.B. Marsh, *Opposing roles for HIF-1alpha and HIF-2alpha in the regulation of angiogenesis by mononuclear phagocytes.* Blood, 2011. 117(1): p. 323-32.

160. Hu, C.J., L.Y. Wang, L.A. Chodosh, B. Keith, and M.C. Simon, *Differential roles of hypoxia-inducible factor 1alpha (HIF-1alpha) and HIF-2alpha in hypoxic gene regulation.* Mol Cell Biol, 2003. 23(24): p. 9361-74.

161. Melvin, A. and S. Rocha, *Chromatin as an oxygen sensor and active player in the hypoxia response.* Cell Signal, 2012. 24(1): p. 35-43.

162. Nakayama, K., *Cellular signal transduction of the hypoxia response.* J Biochem, 2009. 146(6): p. 757-65.

163. Mole, D.R., C. Blancher, R.R. Copley, P.J. Pollard, J.M. Gleadle, J. Ragoussis, and P.J. Ratcliffe, *Genome-wide association of hypoxia-inducible factor (HIF)-1alpha and HIF-2alpha DNA binding with expression profiling of hypoxia-inducible transcripts.* J Biol Chem, 2009. 284(25): p. 16767-75.

164. Podar, K. and K.C. Anderson, *A therapeutic role for targeting c-Myc/Hif-1-dependent signaling pathways.* Cell Cycle, 2010. 9(9): p. 1722-8.

165. Koshiji, M., Y. Kageyama, E.A. Pete, I. Horikawa, J.C. Barrett, and L.E. Huang, *HIF-1alpha induces cell cycle arrest by functionally counteracting Myc.* EMBO J, 2004. 23(9): p. 1949-56.

166. Skiles, M.L., S. Sahai, and J.O. Blanchette, *Tracking hypoxic signaling within encapsulated cell aggregates.* J Vis Exp, 2011(58).
167. Green, J., J.C. Crack, A.J. Thomson, and N.E. LeBrun, *Bacterial sensors of oxygen.* Curr Opin Microbiol, 2009. 12(2): p. 145-51.

8 ACKNOWLEDGEMENTS

I would like to thank Prof. Dr. Irmgard Förster for the official supervision of this PhD thesis and for giving me the opportunity to carry out this PhD project in her lab and for her valuable help and support during this time. I would also like to acknowledge all the members in the Förster lab for the help they have given me, especially Heike Weighardt for mentoring. Additionally, I would like to thank all the group members of the AG Pfeffer, AG Däubener, AG Scheu and Albert & Steff from the institute of microbiology at the University of Düsseldorf for interesting cooperations and for nicely adopting me.

9 APPENDIX

Parts of the data shown in this thesis were published:

Influence of hypoxia-inducible factor 1α on dendritic cell differentiation and migration.

Theresa Köhler, Boris Reizis, Randall S. Johnson, Heike Weighardt and Irmgard Förster

Eur J Immunol, 2012. 42(5): p. 1226-36.

10 DECLARATION OF AUTHORSHIP

I hereby declare that I have written this thesis without any help from others and without the use of documents and aids other than those stated above. This work was neither submitted in the present form nor in a likewise form at any institution.

Düsseldorf, 07.05.2012